DNA DAMAGE RESPONSES IN HUMAN PLURIPOTENT STEM CELLS

by

Olga Momčilović

Diploma, University of Belgrade, Serbia, 2001

Submitted to the Graduate Faculty of

Department of Human Genetics

Graduate School of Public Health in partial fulfillment

of the requirements for the degree of

Doctor of Philosophy

University of Pittsburgh

2010

UNIVERSITY OF PITTSBURGH

Graduate School of Public Health

This dissertation was presented

by

Olga Momčilović

It was defended on

June 23, 2010

and approved by

Dissertation Advisor:
Gerald P. Schatten, PhD
Professor
Department of Obstetrics, Gynecology and Reproductive Sciences
School of Medicine
University of Pittsburgh

Committee Member:
Robert E. Ferrell, PhD
Professor
Department of Human Genetics
Graduate School of Public Health
University of Pittsburgh

Committee Member:
Susanne M. Gollin, PhD
Professor
Department of Human Genetics
Graduate School of Public Health
University of Pittsburgh

Committee Member:
Laura J. Niedernhofer, MD, PhD
Associate Professor
Department of Microbiology and Molecular Genetics
School of Medicine
University of Pittsburgh

Gerald P. Schatten, PhD

DNA DAMAGE RESPONSE IN HUMAN PLURIPOTENT STEM CELLS

Olga Momčilović, PhD

University of Pittsburgh, 2010

Pluripotent stem cells have the capability to undergo unlimited self-renewal and differentiation into all somatic cell types. They have acquired specific adjustments in the cell cycle structure that allow them to rapidly proliferate, including cell cycle independent expression of cell cycle regulators and lax G_1 to S phase transition. However, due to the developmental role of embryonic stem cells (ES) it is essential to maintain genomic integrity and prevent acquisition of mutations that would be transmitted to multiple cell lineages. Here we show that several modifications in DNA damage response of ES cells accommodate dynamic cycling and preservation of genetic information. ATM-dependent checkpoint signaling cascade is activated after irradiation of ES cells, and induces G_2/M, but not G_1/S cell cycle arrest. The absence of a G_1/S cell cycle arrest promotes apoptotic response of damaged cells before DNA changes can be fixed in the form of mutation during the S phase, while G_2/M cell cycle arrest allows repair of damaged DNA following replication. Human ES cells express higher level of DNA repair proteins, and rely on homologous recombination to repair double strand breaks. Radiation does not lead to long-term loss of pluripotency, since irradiated ES cells show transient decrease in the level of pluripotency factor transcripts, while protein levels remains stable. One week after irradiation, ES cells retain capacity to differentiate into three germ layers and form teratomas in immunocompromised mice.

Similarly to ES cells, induced pluripotent stem (iPS) cells are poised to proliferate and exhibit extreme sensitivity to DNA damage, lack of G_1/S cell cycle arrest, and express high level of DNA repair genes, suggesting that DNA damage responses are controlled by developmental state of the cell.

Public health significance of this study originates in great promise that human ES and iPS cells hold in cell replacement therapies. Since human ES, and particularly iPS, cells represent potential source of cells for clinical and pharmaceutical applications, the DNA damage response pathways that maintain genomic integrity need to be studied in greater detail.

TABLE OF CONTENTS

LIST OF TABLES

LIST OF FIGURES

LIST OF SCHEMES

PREFACE

"It takes a village to raise a child".

Growing up is difficult, and even though I started working on my PhD project as a young adult, I was really only a baby scientist. Now, I consider myself a teenager, and this growth would not be possible without generous help of my mentors and colleagues. I wish to thank to my advisors and committee members Dr. Ferrell, Dr. Gollin, Dr. Navara, Dr. Niedernhofer, and Dr. Schatten for their patience, support, guidance and trust; you watched over me and helped me make first steps into exciting field of stem cells. To my colleagues and lab mates Sandra, Sofia, Carlos, Diane, Angela, Chas, Dave, Vonya, Carrie, Stacie, as well as past laboratory members Dan, Ahmi, Hina and Jody for putting up with me during my ups and downs, and sharing troubles and thrills of everyday lab life. During my time at Pitt I also had pleasure of collaborating with other researchers, and I wish to thank Dr. Bakkenist, Serah and Jason for their invaluable advice and assistance with ATM project, Dale and Jianhua for help with making sense of chromosomes and performing SCE analysis, Joan and Lynda for running my flow cytometry experiments, as well as Ms. Norbut for help with organization and administrative tasks.

At all times, I had a lot of friends and family members, at home, in Pittsburgh, and many other places supporting me. I am afraid to miss some of my dear friends, and will risk mentioning only my oldest friends Tijana, Dejan, and Sonja. It was wonderful to share with you good and bad, excitement of my first peer reviewed publication, and great to know there is always a shoulder for me to lay down my troubles. And there were moments when I wanted to pull my hair out, but support and guidance of my mentors, friends and family helped me stay, face challenges, and grow up! For this, and so much, more I am deeply grateful.

Finally, none of this would happen without my parents. Not only did they bring me in this world, loved me and protected me from turmoil of our times, but also they ignited the desire for knowledge, stimulated me to study, and encouraged me to pursue this degree. I am only beginning to imagine how much they sacrificed and endured in order to make possible for me to be here. *Nadam se da ću jednog dana opravdati vaše poverenje, i da ćete moći da budete ponosni na mene.*

1.0   INTRODUCTION

[1]Department of Human Genetics, University of Pittsburgh, Pittsburgh, Pennsylvania, USA, [2]Pittsburgh Development Center, Pittsburgh, Pennsylvania, USA, [3]Department of Biology, University of Texas at San Antonio, San Antonio, Texas, USA, [4]Department of Obstetrics and Gynecology, University of Pittsburgh School of Medicine, Pittsburgh, Pennsylvania, USA.

1.1   PUBLIC HEALTH SIGNIFICANCE

Since life-expectancy has greatly increased in the past century owing to medical breakthroughs, more people are expected to live longer and suffer with age-related degenerative diseases, such as Parkinson's or Alzheimer disease, cancer, and other debilitating conditions. Treatments to some of these conditions exist, but too often they come down to costly disease management. Therefore, as prevalence of chronic and age-related diseases increases, so do the accumulating medical bills.

Stem cells offer great promise in extending patients quality of life by offering higher impact medical care. With derivation of patient-specific induced pluripotent stem (iPS) cells, one can imagine endless possibilities regarding patient-customized curative therapies. Induced pluripotent stem cells and embryonic stem (ES) cells could provide us with unlimited source of cells for cell replacement therapies, as well as material for drug development and toxicity studies. Idea that one day it would be possible to replace, for example, β-cells in the pancreas of diabetic patient with β-cells differentiated from patient-specific iPS cells, and hence avoid long waiting and side-effects of heterologous organ transplant is captivating. However, before iPS or ES cells are used in clinical applications, it is essential to understand the risks associated with such therapies. ES and iPS cells have the ability to form tumors comprised of tissues of all three germ layers in immunocompromised mice, and require that safety protocols are put in place to ensure efficient and complete differentiation of ES/iPS cells prior to transplantation into patients. Furthermore, understanding their genomic stability is essential in order to define risks of malignant

transformation of cells derived from ES or iPS cells. By studying DNA damage responses in ES and iPS cells we can gain insight into mechanisms that safeguard genetic information in these cell types.

1.2   EARLY DEVELOPMENT

In sexually reproducing species development of a new organism of begins with fusion of one male and one female gamete. This process is called fertilization and results in a single cell new organism termed zygote. Zygote will during the course of the several days, exact timing is species-specific, undergo cleavage – cell divisions unaccompanied with cell growth, dividing into smaller daughter cells called blastomeres. Until at least four-cell stage all blastomeres are identical and can be segregated so that each can give rise to an embryo and eventually live birth. Sometimes, segregation of the blastomeres occurs spontaneously during pregnancy and results in monozygous twins. Experimentally, splitting of the blastomeres has been accomplished in several mammalian species, including non-human primates. The property of zygote and 4-8 cell stage blastomeres to give rise to the whole organism, embryo proper and supportive extraembryonic tissues, is defined as totipotency.

At the 16-32 cell stage, human embryo undergoes compaction: tight junctions form between outer cells, and gap junctions form between the inner cells. This is the first differentiation event during mammalian development and results in loss of totipotency due to delineation of the outer cells to trophectoderm (TE), and inner cells to inner cell mass (ICM). Trophectoderm cells transport sodium ions, which is followed by water, resulting in the formation of the fluid filled cavity with inner cell mass in one side, and surrounded with trophectoderm. This developmental stage is referred to as blastocyst. Trophectoderm will give rise to the outer layer of placenta, whereas ICM cells will give rise to all cell types of the embryo proper, as well as some extraembryonic tissues. The cells that
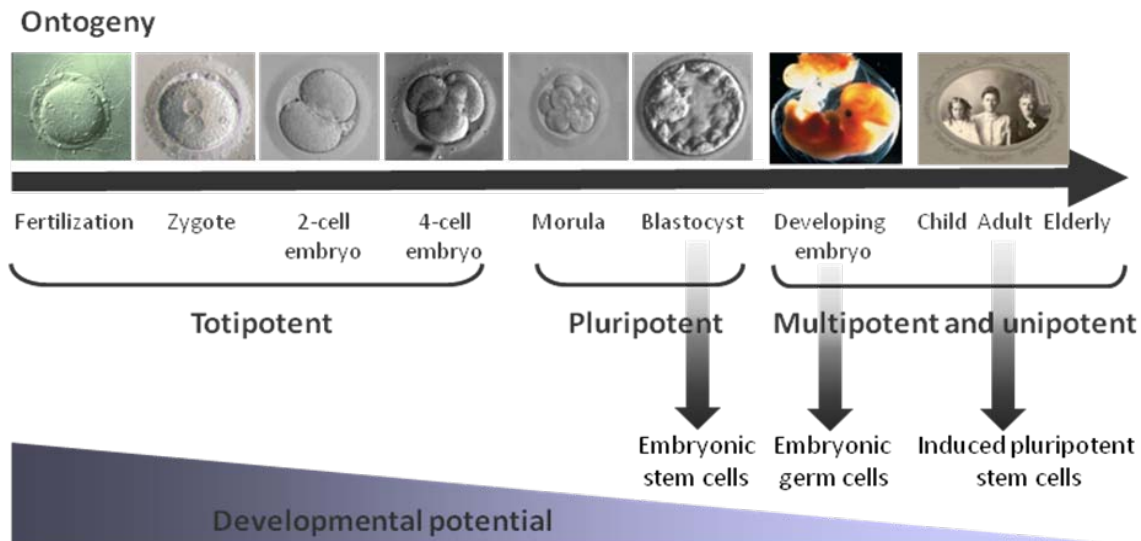
Adopted from: Mitalipov S, Wolf D. Adv Biochem Eng Biotechnol. 2009;114:185-99

Scheme 1: Restiction of developmental potential during ontogeny.

2

form ICM of blastocyst have restricted developmental potential relative to zygote and early blastomeres, and cannot produce the whole organism. Still, ICM cells are capable of differentiating into three primordial germ layers: endoderm, mesoderm, and ectoderm, and can produce 220 cell types of an adult organism, but contribute poorly to extraembryonic structures; hence, they are referred to as pluripotent. The restriction of the developmental potential is common theme during development: as developing organism becomes increasingly complex the "potency" of the cells that make it is gradually restricted. In adult organism stem cells that maintain tissue homeostasis are multipotent – they have the ability to differentiate into a limited number of cell types. Depiction of different stages during ontogeny and accompanying restriction of developmental potential is represented in Scheme 1.

The next step of the development involves blastocyst implantation into uterine wall and further differentiation of the inner cell mass into outer layer called epiblast, or the primary ectoderm, which will eventually give rise to the embryo, and inner layer termed hypoblast, or primitive endoderm that will give rise to extraembryonic endoderm (Larsen, 2001; Mitalipov and Wolf, 2009).

1.3   PLURIPOTENT STEM CELLS

Stem cells are cells with the unique capability to undergo self-renewal and produce more of the same cell type, as well as to differentiate into one or more cell types. In regard to their differentiation potential, or potency, stem cells can be classified as pluripotent and multi/oligopotent. Pluripotent stem cells can differentiate into all cell types of an organism, whereas multipotent stem cells have restricted developmental potential and can differentiate into a limited number of cell types. There are several types of pluripotent stem cells – embryonic carcinoma cells, embryonic stem cells, epiblast stem cells, embryonic germ cells, as well as induced pluripotent stem cells.

In order to understand human embryonic stem cells it is instrumental to put them in context of other pluripotent stem cells, as well as historical perspective in which they were derived.

1.3.1   Embryonic carcinoma cells

Historically the first pluripotent stem cells were derived from teratocarcinomas – malignant tumors originating from the germ cells. Teratocarcinomas are composed of differentiated cells from all three germ layers, as well as undifferentiated pluripotent embryonic carcinoma (EC) cells. Teratocarcinomas can be serially transplanted between mice owing to the presence of pluripotent EC cells. Stable mouse EC cells were derived in 1970s and were shown to be capable of indefinite self-renewal, clonal expansion, and multilineage differentiation (Kahan and Ephrussi, 1970; Kleinsmith and Pierce, 1964). They express proteins that are also expressed in the inner cell mass (ICM) of the blastocyst such as Ssea1 (Gachelin et al., 1977; Knowles et al., 1978) and were perceived as in vitro counterparts of undifferentiated cells of the ICM (Martin, 1980). In spite of their capacity to differentiate in vitro,

mouse EC cells have limited developmental potential in vivo, most likely due to fact they acquire numerous genetic aberrations during teratocarcinoma formation, limiting their use to model early development (Atkin et al., 1974).

Human EC cells were derived several years later (Hogan et al., 1977), but turned out to be very different from mouse EC cells. Human EC cells express different set of cell surface markers (SSEA3 and SSEA4, rather than SSEA1), have high rate of aneuploidy, and limited in vitro differentiation potential (Andrews et al., 1982; Kannagi et al., 1983). Although both mouse and human EC cells have limited value in studying early development, their discovery provided the concept for pluripotent stem cells and cancer stem cells, and paved the road for future studies on these cell types.

1.3.2   Mouse embryonic stem cells

The experiments with intact embryo transfer to extrauterine sites and subsequent teratocarcinoma formation at those sites led to understanding that the intact embryo contains pluripotent stem cell population (Solter et al., 1970; Stevens, 1970). In 1981 mouse embryonic stem (ES) cells were derived from the ICM of pre-implantation embryos (Evans and Kaufman, 1981; Martin, 1981). Similarly to pluripotent EC cells, mouse ES cells undergo unlimited self-renewal, express proteins found in ICM, differentiate into variety of cell types in vitro, and form teratocarcinomas when injected into mice. Unlike EC cells, mouse ES cells maintain stable karyotype in prolonged cell culture and contribute to tissues of all three germ layers and germ cells when injected into recipient mouse embryos. Therefore, mouse ES cells are superior relative to EC cells in studying early development. In addition, ability to form chimeric mice by injection of mouse ES cells into recipient blastocyst provided tool for the production of transgenic animals (Bradley et al., 1984; Evans and Kaufman, 1981; Martin, 1981).

Mouse ES cell derivation and propagation in vitro is supported by the use of mitotically inactivated mouse embryonic fibroblasts (MEF) as feeder cells and leukemia inhibitory factor (Lif) in the growth medium (Evans and Kaufman, 1981; Smith et al., 1988; Williams et al., 1988). Lif acts through gp130 and Lif receptor (Lifr) to activate Janus-associated tyrosine kinases (Jak)/the latent transducer and activator of transcription factor (Stat3). In the presence of serum, activated Stat3 can maintain mouse ES cell self-renewal by itself (Matsuda et al., 1999). The primary target of Lif/Stat3 pathway is Myc and it can promote Lif-independent self-renewal of mouse ES cell (Scheme 2) (Cartwright et al., 2005). Myc is a cellular oncogene that acts as a transcription factor to induce expression of cyclin E and promote G_1 to S transition (Hooker and Hurlin, 2006). Lif signaling pathway can also activate Erk mitogen activated protein kinase (MAPK) (Takahashi-Tezuka et al., 1998), but the effect of Erk activation appears to be negative for self-renewal of mouse ES cells (Scheme 2) (Burdon et al., 1999). Therefore, the balance between Lif promoting and inhibitory effects on mouse ES cells' self-renewal must be finely adjusted to achieve proliferative effect of Lif.

In serum-free conditions Lif alone is not sufficient to maintain self-renewal of mouse ES cells, and additional growth factors, such as bone morphogenic proteins (Bmp) are required (Scheme 2). Bmp signal activation of inhibitor of differentiation (Id) via Smad1/5/8 pathway (Ying et al., 2003). Overexpression of Id proteins can bypass the need for Bmp signaling, further supporting their role in mouse ES cell maintenance. In

addition, Bmp have Smad-independent inhibitory effect on differentiation of mouse ES cells by suppressing p38 Mapk (Qi et al., 2004).

Phosphatidylinositol 3 kinase (Pi3k) signaling pathway is essential for mouse ES cells' self-renewal as well (Scheme 2). Inhibition of Pi3k signaling induces differentiation even in the presence of Lif (Welham et al., 2007), and constitutively active Pi3k downstream target Akt maintains undifferentiated state of mouse and primate ES cells (Watanabe et al., 2006). The positive effect of Pi3k on mouse ES cell proliferation is at least in part due to inhibition of Myc negative regulator, glycogen synthase kinase 3 (Gsk3) (Cartwright et al., 2005; Sato et al., 2004). Pi3k itself is thought to be regulated by Lif directly or indirectly, as well as by other medium components such as insulin/insulin-like growth factor (Igf).

More recently mouse epiblast pluripotent stem cells (EpiSC) have been isolated from the early post-implantation embryos. Although epiblast stem cells share common features with mouse ES cells, such as self-renewal and multilineage differentiation, they exhibit prominent differences. Interestingly, characteristics that distinguish EpiSC from mouse ES cells, including cell culture medium requirements, gene expression pattern and colony morphology, are shared with human ES and iPS cells (Brons et al., 2007; Tesar et al., 2007).
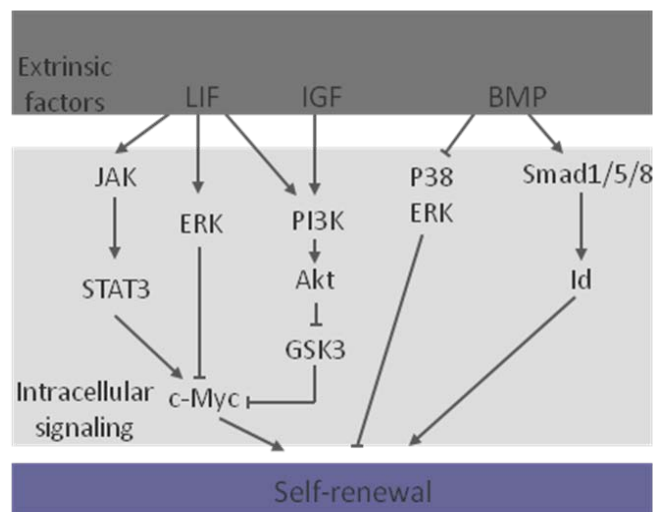
Scheme 2: Extrinsic signaling pathways required for maintenance of mouse embryonic stem cell self-renewal.

1.3.3   Embryonic germ cells

In 1992 mouse embryonic germ (EG) cells were isolated from primordial germ cells (PGC) in vitro (Matsui et al., 1992; Resnick et al., 1992). These cells are morphologically indistinguishable from mouse ES cells and share numerous similarities: express similar pluripotency markers (Oct4 and Ssea1), and contribute to multitude of tissues in chimeric mice, including germ cells (Labosky et al., 1994; Stewart et al., 1994). However, EG cells retain some of the characteristics of the PGC from which they were derived that distinguish them from mouse ES cells. For

example, unlike mouse ES cells, mouse EG cells have global genome demethylation, erased genome imprints and reactivate X chromosome (Labosky et al., 1994; Tada et al., 1997).

1.3.4   Human embryonic stem cells

Even though mouse ES cells became available in the early 1980s, there was substantial delay in derivation of human ES cells. Human ICM were successfully isolated in the early 1990s, but would soon differentiate in vitro under the same culture conditions that supported mouse ES cell derivation (Bongso et al., 1994). Derivation of non-human primate ES cells (Thomson et al., 1995; Thomson et al., 1996) helped define culture conditions for successful derivation of the first human ES cell lines from the surplus in vitro fertilized (IVF) blastocyst stage embryos in 1998 by Thomson and colleagues (Thomson et al., 1998).

Similar to mouse ES cells, human ES cells undergo self-renewal in vitro and maintain stable karyotype for prolong periods of cell culture. Importantly, human ES cells can differentiate into numerous cell types of all three germ layers in vitro, and following injection into immunocompromised mice form teratocarcinomas. However, human ES cells exhibit some prominent differences in comparison to mouse ES cells: human ES cells express cell surface markers SSEA3, SSEA4, TRA-1-60, and TRA-1-81, which are expressed in mouse EpiSC, but are not present in mouse ES cells. Furthermore, the maintenance of self-renewal of human ES cells appears to be regulated by different extrinsic factors. For example, the first attempts to derive human ES cells from human blastocysts using the same conditions as for mouse ES cells, such as presence of LIF and serum in culture medium, failed because isolated human ES cells differentiated (Bongso et al., 1994). The similarities and differences between mouse and human ES cells are summarized in Table 1.
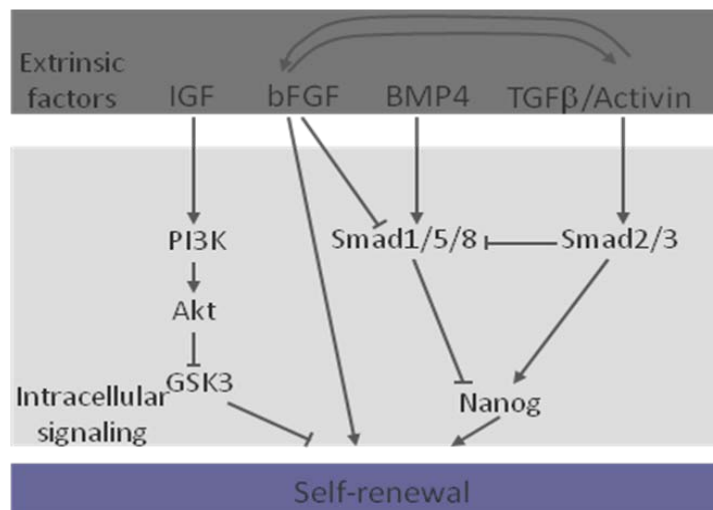
Scheme 3: Extrinsic signaling pathways required for maintenance of self-renewal in human embryonic stem cells.

Undifferentiated state of human ES cells is sustained by the basic fibroblast growth factor (FGF2) (Amit et al., 2000; Xu et al., 2001), TGFB/activin A and PI3K signaling activators, such as IGF, similar to mouse epiblast

stem cells (Brons et al., 2007; Tesar et al., 2007), Scheme 3. In contrast to mouse ES cells, LIF and BMP cause differentiation of human ES cells (Xu et al., 2002). The key extrinsic signaling factors needed for human ES cell self-renewal are represented in Scheme 3.

Table 1: Comparison of characteristics of mouse and human embryonic stem cells.

Properties	Mouse ES cells	Human ES cells
Prolonged propagation in undifferentiated state	✓	✓
Maintain normal karyotype	✓	✓
Pluripotent	✓	✓
Directed differentiation in vitro	✓	✓
Embryoid body formation	✓	✓
Teratoma formation	✓	✓
Chimera formation	✓	Not tested
High nucleus to cytoplasm ratio	✓	✓
Telomerase activity	✓	✓
Alkaline phosphatase activity	✓	✓
OCT4	✓	✓
NANOG	✓	✓
Ssea1	✓	✗
SSEA3	✗	✓
SSEA4	✗	✓
TRA-1-60	✗	✓
TRA-1-81	✗	✓
Lif and Bmp dependent for self-renewal	✓	✗
FGF2 and TGFB dependent for self-renewal	✗	✓
X-chromosome activation	✓	Line dependent
Imprinting	Commonly lost	✓

Basic fibroblast growth factor is thought to act through direct activation of transcriptional factors involved in self-renewal, suppression of BMP signaling, and by stimulating autocrine effects. When grown in the presence of feeder cells, lower concentration of FGF2 (4 ng/ml) is sufficient to maintain human ES cells. However, in feeder-free conditions, either higher concentrations of FGF2 have to be used (100 ng/ml), or BMP signaling inhibitor, such as noggin, has to be supplemented in combination with medium FGF2 concentration (40 ng/ml) (Wang et al., 2005; Xu et al., 2005a; Xu et al., 2005b). Suppression of BMP alone is not sufficient to maintain human ES cells' self-renewal, suggesting that FGF2 has additional functions (Xu et al., 2005b). It has been demonstrated that FGF2 promotes secretion of TGFB ligands and inhibits expression of BMP4 in both feeder and human ES cells (Greber et al., 2007). Activin A, TGFB ligand, stimulates FGF2 secretion creating a positive feedback loop between TGFB/activin A and FGF2 signaling pathways that is responsible for maintenance of human ES cells' self-renewal. It also explains growth factor requirements: at lower FGF2 concentrations it is necessary to supplement medium with TGFB signaling factors, while at higher concentrations of one factor the dependence of human ES cell culture on the other factor is greatly reduced (Ludwig et al., 2006; Vallier et al., 2005; Xiao et al., 2006).

In addition to stimulating FGF2 secretion, TGFB/activin A signals through SMAD2/3 phosphorylation and activation. SMAD2/3 can suppress SMAD1/5 activity, which is involved in BMP signaling, suggesting that

TGFB/activin A negatively regulate BMP signaling in human ES cells (Beattie et al., 2005; James et al., 2005). FGF2 can inhibit nuclear translocation of phospho-SMAD1 thereby assisting TGFB/activin A in suppressing BMP activity (Xu et al., 2005b). More recently, it has been reported that *NANOG* and *POU5F1* are direct transcriptional targets of TGFB/activin A pathway (Babaie et al., 2007), providing a direct link between extrinsic and intrinsic regulators of human ES cells' state.

PI3K signaling pathway may act in human ES cells through suppression of GSK3. Sato and colleagues showed that GSK3 suppression is essential for human ES cell self-renewal short-term (Sato et al., 2004). Furthermore, WNT signaling, which results in inhibition of GSK3B, a target common to PI3K pathway, leads to increased SMAD2/3 phosphorylation and promoted pluripotency of human ES cells (James et al., 2005).

1.4 CORE TRANSCRIPTIONAL FACTORS THAT REGULATE PLURIPOTENCY

Three transcription factors have been demonstrated to be central to the maintenance of ES cells' pluripotency: NANOG, OCT4 and SOX2.

NANOG is a homeodomain protein with specific expression in pre-implantation embryos and ES cells. Mitsui et al. (Mitsui et al., 2003) showed that NANOG actively maintains self-renewal of mouse ES cells and that deletion of the *NANOG* gene results in loss of pluripotency in both ICM and ES cells. *NANOG* disruption in mice resulted in embryos composed of disorganized extraembryonic tissues with no discernable epiblast or extraembryonic ectoderm, and ICMs from *NANOG* null blastocysts failed to proliferate in vitro. *NANOG* downregulation in mouse (Chambers et al., 2003; Mitsui et al., 2003) and human (Hyslop et al., 2005) ES cells resulted in expression of a number of endoderm transcription markers, indicating that *NANOG* disruption specified ES cell fate into extraembryonic endoderm lineages. Furthermore, Chambers et al. (Chambers et al., 2003) showed that forced expression of *NANOG* confers self-renewal on mouse ES cells and suppresses ES differentiation in response to retinoic acid.

POU5F1 (OCT4) is a member of PIT/OCT/UTF (POU) family of transcription factors that is expressed in the ICM, epiblast, primordial germ cells, and unfertilized oocytes (Hansis et al., 2000; Palmieri et al., 1994). It is rapidly down-regulated during retinoic acid-induced differentiation of mouse ES cells (Okamoto et al., 1990). In vivo, OCT4 is absent from trophectoderm, indicating that it acts to prevent differentiation into trophectoderm (Nichols et al., 1998; Niwa et al., 2000; Palmieri et al., 1994). *Pou5f1* knock-out embryos fail to form ICM. Unlike NANOG, whose upregulation prevents differentiation, increased levels of Oct4 lead to differentiation into primitive endoderm and mesoderm in mouse ES cells (Niwa et al., 2000). The pattern of ES cell differentiation following manipulation of *POU5F1* levels is distinct in human ES cells: downregulation of *POU5F1* resulted in increase of endoderm and mesoderm marker expression, whereas upregulation induced markers for endoderm derivatives (Rodriguez et al., 2007). Thus, *POU5F1* must be kept within a critical range of expression in order to maintain pluripotent phenotype in both mouse and human ES cells (Niwa et al., 2000; Rodriguez et al., 2007).

OCT4 binds to SRY-related HMG box family member SOX2 to regulate target genes (Yuan et al., 1995). *Sox2* null embryos die post-implantation, and *Sox2* knock-down mouse ES cells differentiate into multiple lineages (Ivanova et al., 2006). However, *SOX2* overexpression leads to differentiation, suggesting that SOX2 levels must be tightly regulated, similar to OCT4, in order to maintain pluripotency (Fong et al., 2008).

OCT4, SOX2 and NANOG are master regulators of transcriptional network that controls early development and specifies undifferentiated state in both mouse and human ES cells (Chambers et al., 2003; Hart et al., 2004; Mitsui et al., 2003; Nichols et al., 1998). They bind together to the promoters and activate the number of genes that encode transcriptional factors, chromatin remodeling enzymes and micro RNA that maintain self-renewal and pluripotency in ES cells. OCT4, SOX2 and NANOG exert both activating and repressing effects on large groups of genes. The positively regulated genes include: (1) genes for OCT4, SOX2 and NANOG themselves, creating a positive autoregulatory circuit, (2) genes for other transcription factors and components of signaling pathways (such as TGFBand WNT) that promote undifferentiated state and self-renewal in human ES cells, and (3) genes for chromatin remodeling that regulate epigenetic profile of ES cells. In contrast, the group of repressed genes is enriched in transcription factors that are involved in differentiation into ectoderm, mesoderm and endoderm lineages (Boyer et al., 2005). Therefore, these three master transcription factors maintain pluripotency by activating genes essential for self-renewal, while repressing genes involved in differentiation.

In addition to the above described network of transcriptional factors, pattern of epigenetic marks influences the gene expression, and is unique to the cell type and developmental stage. Epigenetic control of gene expression is based on inheritable DNA and histone modifications that alter local chromatin structure and DNA accessibility. ES cells are characterized by generally open chromatin structure that is permissive for gene expression. As ES cells differentiate chromatin becomes gradually more condensed and restrictive. Genes for chromatin remodeling enzymes, such as those involved in DNA methylation and histone modifications are also regulated by OCT4, SOX2 and NANOG (Boyer et al., 2005). Through combination of DNA methylation, activating (histone 3 lysine 4 trimethylation, histone 3 and histone 4 acetylation) and repressing (histone 3 lysine 9 and lysine 27 trimethylation) histone marks, as well as regulation of nucleosome positioning and conformation, remodeling of local chromatin structure adds additional layer to transcriptional control in ES cells and affects balance between self-renewal and differentiation (Fouse et al., 2008; Keenen and de la Serna, 2009). Therefore, in additional to their direct transcriptional control, OCT4, SOX2 and NANOG affect the gene expression profile in ES cells by regulating expression of chromatin remodeling enzymes that define pattern of epigenetic marks.

1.5   NUCLEAR REPROGRAMMING AND INDUCED PLURIPOTENT STEM CELLS

Xenopus laevis somatic nuclear transfer into enucleated eggs and production of fertile animals demonstrated that differentiation process, until then regarded as unidirectional process, can be reversed (Gurdon and Uehlinger, 1966). These experiments established for the first time that genomes of somatic cells contain information needed for

development of entire organism, and that oocytes contain factors that can mediate the reprogramming of differentiated cells into pluripotent cells.

The major advancement in mammalian somatic cell reprogramming was achieved by generation of the first cloned mammal, sheep Dolly (Campbell et al., 1996), by somatic cell nuclear transfer. This process utilizes enucleated oocyte to reprogram transferred somatic cell into totipotent state. All differentiation marks are stripped and such "reprogrammed" nucleus can direct development to live birth. Dolly, as well as clones of other mammalian species, showed that it is possible to reverse differentiation of completely matured adult somatic cells in mammals. This crucial finding was further extended to primates with derivation of cloned ES cells from rhesus macaque blastocysts developed from enucleated oocyte injected with adult skin fibroblasts (Byrne et al., 2007).

The process of nuclear reprogramming using eggs is very inefficient and depends on the availability of oocytes, rendering it highly controversial in humans. In addition, the efficiency of nuclear reprogramming by eggs greatly diminishes as donor cell becomes increasingly differentiated. The previous work with transcription factor induced reprogramming demonstrated that forced expression or deletion of individual lineage specific transcriptional factors could induce lineage conversion in differentiated somatic cells. For example, expression of myogenic transcription factor *MYOD* could convert fibroblasts into muscle cells (Davis et al., 1987), whereas expression of *CEBPA* in mature B cells resulted in their reprogramming into macrophages (Xie et al., 2004). Furthermore, similar principle was found to be true in embryonic cells: overexpression of trophectoderm specifier *Cdx2* in mouse ES cells resulted in their differentiation into trophectoderm (Niwa et al., 2005), whereas expression of endoderm specific transcriptional factors *Gata4* and *Gata6* in ES cells induced formation of primitive endoderm (Fujikura et al., 2002). These experiments provided the rational for the next step in cell reprogramming: to reprogram somatic cells into pluripotent cells by overexpression of transcription factors.

Somatic cells were successfully reprogrammed into pluripotent state first in mouse (Takahashi and Yamanaka, 2006), and then in human (Takahashi et al., 2007; Yu et al., 2007) using defined set of transcriptional factors. The reprogrammed somatic cells are similar to ES cells in morphology, proliferation, expression of ES cell markers, as well as teratoma formation, and are referred to as induced pluripotent stem (iPS) cells. Initial studies required 24 retrovirally carried transgenes that are preferentially expressed in ES cells, but the factors were then reduced to four key transcription factors: *Pou5f1, Sox2, Klf4* and *Myc* (Takahashi and Yamanaka, 2006). At the same time when human iPS cells were produced with these four factors (Takahashi et al., 2007), another group derived human iPS cells with another set of four transcription factors: *NANOG, POU5F1, LIN28* and *SOX2* (Yu et al., 2007). The process of somatic cell reprogramming with defined factors is gradual process and is depicted in Scheme 4. Use of morphological criterion to identify iPS cells frequently leads to isolation of partially reprogrammed cells. These cells exhibit incomplete DNA demethylation and activation of endogenous pluripotency genes, express viral transgenes and lineage genes that are not expressed in the starting population of cells. Inhibition of differentiation pathways greatly improves reprogramming, and facilitates full reprogramming of the partially reprogrammed cells (Mikkelsen et al., 2008). Completely reprogrammed iPS cells have silenced transgenes, express telomerase, reactivate silenced X chromosome, and have gene expression and epigenetic marks similar to ES cells (Mikkelsen et al., 2008; Okita et al., 2007). Functionally, mouse iPS cells form chimeric mice and contribute to the

germ line proving that they are indeed pluripotent (Hanna et al., 2008; Kim et al., 2008). Human iPS cells, however, cannot be tested in this manner, but have been shown to differentiate in multitude of cell types in vitro, and to form teratocarcinomas when injected into immunocompromised mice.
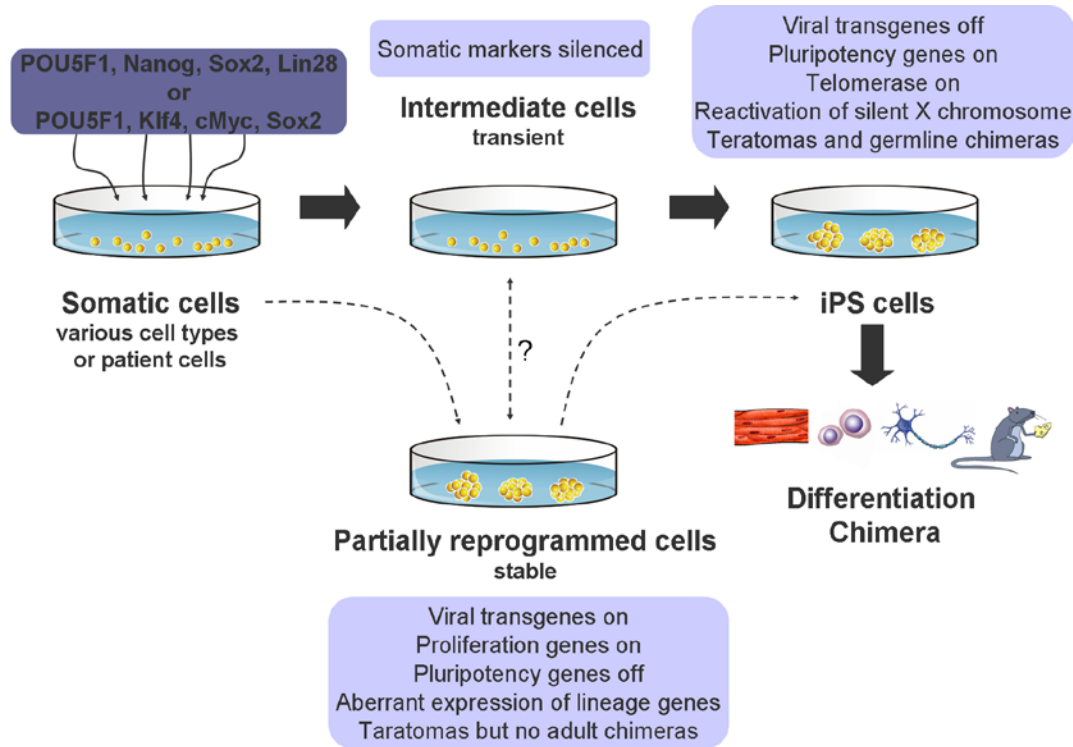
Adopted from Hochedlinger K. and Plath K. (2009) Development, Vol. 136, 509-523

Scheme 4: Steps in somatic cell reprogramming using defined transgenes.

Three of transgenes used in reprogramming cocktail, OCT4, NANOG and SOX2 comprise a vital transcriptional network that maintains ES cells' self-renewal and were already discussed. KLF4 shares many DNA targets with NANOG and its downregulation leads to differentiation. MYC is central for self-renewal in mouse ES cells, as has been already described, but its overexpression in human ES can promote differentiation (Sumi et al., 2007). It is dispensable for somatic cell reprogramming and can be left out from the reprogramming cocktail in mouse and human (Nakagawa et al., 2008). LIN28 blocks processing of micro RNA involved in differentiation, thereby inhibiting micro RNA mediated differentiation (Viswanathan et al., 2008).

Since the first experiments, iPS have been generated from various cell types both in mouse (Aoi et al., 2008; Hanna et al., 2008; Kim et al., 2008) and human (Aasen et al., 2008; Loh et al., 2009), and have been generated from patients with various genetic diseases (Park et al., 2008). Importantly, human iPS cells have been recently derived without viral integration and free from transgene sequences (Yu et al., 2009), making them much safer for prospective clinical applications.

1.6   POTENTIALS AND PROBLEMS WITH USE OF PLURIPOTENT STEM CELLS

1.6.1   Human embryonic stem cells

Differentiation potential of ES cells makes them excellent candidates for source for cell replacement therapies. Human ES cell derived differentiated cells have been used to treat animals with spinal cord injury (Keirstead et al., 2005), retinal disease (Lamba et al., 2009) and Parkinson's disease (Yang et al., 2008). The US Food and Drug Administration (FDA) allowed the first clinical trials for use of human ES cells for therapy of spinal cord injury in January 2009. In addition to potentially treating numerous diseases, ES cells can be used to model human diseases. This approach is particularly valuable when affected tissues cannot be obtained from human subjects – such as in case of Alzheimer's patients. ES cells might prove very useful for drug discovery – coupled with modeling of human diseases in vitro, one can imagine that such tissues can be used to test novel molecules as potential therapeutics. Finally, human ES cells are currently indispensable as the only model for understanding of the early human development.

In spite of their tremendous potential, human ES cells pose serious problems. Although embryos used for human ES cell derivation are most often surplus IVF embryos that would not be used for reproduction, for many people use of human ES cells for clinical purposes presents itself with serious ethical concern: in the very nature of derivation of ES cells lays destruction of the human embryos. The question comes to whether one is going to use these cells for own benefit, at the expense of an embryo? There is a limited number of available human ES cell lines, and they are genetically different than prospective patients; hence any potential replacement therapy carries an inherent risk of tissue rejection. In addition, the existing human ES cells have been derived using the animal products, raising the possibility of xeno-contamination in prospective therapies. Undifferentiated ES cells have strong potential to form malignant tumors in vivo recipients. Therefore, stringent safety protocols must be devised to prevent malignant transformation of incompletely differentiated cells.

1.6.2   Human induced pluripotent stem cells

Induced pluripotent cells are promising source for cell replacement therapies as they have wide developmental potential, similar to ES cells. Furthermore, because iPS cells are derived from reprogrammed somatic cells, the process of derivation does not involve embryo destruction, and accompanying ethical issues. Induced pluripotent stem cells can be derived from each patient individually, therefore eliminating the risk of rejection of genetically (and hence, immunologically) distinct cells/tissue. In addition, iPS technology enables production of ES cell-like cells from patients with complex genetic diseases which could be then used for understanding of disease pathology and drug screening. Indeed, patient-specific iPS cells have been derived from patients with diabetes (Park et al., 2008), Parkinson's disease (Soldner et al., 2009), amyotrophic lateral sclerosis (ALS) (Dimos et al., 2008), and

spinal muscular dystrophy (SMD) (Ebert et al., 2009). Cells differentiated from iPS cells were shown to alleviate symptoms of Parkinson's disease and sickle cell anemia in mouse (Hanna et al., 2007; Wernig et al., 2008).

Similar to ES cells, iPS cells carry certain concerns that include risk of tumor formation following transplantation of incompletely differentiated stem cells, particularly because current protocols rely on use of oncogenic sequences for reprogramming. Although transgenes are silenced during the course of somatic cell reprogramming, there is still a risk of transgene reactivation, especially in case of powerful, oncogenes such as *MYC*. Indeed, Okita et al. (Okita et al., 2007) study demonstrated that 50% of chimeric mice generated from iPS developed tumors. Furthermore, leaky transgene expression may also render iPS resistant to differentiation and maturation, further increasing the risk of tumorigenesis. Some studies show that iPS cells are not identical to ES cells, at least in terms of epigenetic modifications. Finally, it is not known whether obtained iPS are fully reprogrammed, or to which extent they are, suggesting there is a significant heterogeneity even within the same line. Taken together these concerns greatly affect their usefulness, as well as safety.

1.7   CELL CYCLE REGULATION

1.7.1   Somatic cells

The basic function of the cell cycle is to ensure accurate duplication of genetic information and equal segregation of copied DNA between two daughter cells. DNA replication occurs during the S phase of the cell cycle, after which copied DNA molecules are separated during the mitosis (M phase) into two daughter cells. S and M phases are separated by the growth phases, G_1 and G_2, during which cell prepares itself for the DNA duplication and cell division. Progression through the cell cycle is tightly regulated by both extrinsic and intrinsic factors. Deregulation of the cell cycle control may have serious consequences and is part of the malignant transformation.

G_1 phase of the cell cycle is the time between exit from the mitosis and the next round of DNA replication. During this period cells are particularly sensitive to the intracellular and extracellular signals and decide their fate – whether they will go into the S phase, pause in G_1, senesce or become quiescent.   In case that the environment is favorable and signals for division are present, cell will traverse through the restriction point – a point in G_1 phase after which cell is committed to replicate DNA, even if the extracellular signals that stimulate cell division are removed afterwards. Such extracellular signals that stimulate cell division are referred to as mitogens. They act to remove brake systems that inhibit the progression to the S phase.

At the molecular level, the passage through the restriction point and G_1 to S transition is regulated by concerted series of protein phosphorylations and dephosphorylations, as well as timed expression of cell cycle regulators. It is driven by cyclin dependent kinases (CDK), which are kept inactive in the absence of proliferation signals. Their activity is dependent upon presence of the binding partners, cyclins, whose levels oscillate throughout the cell cycle and are tightly regulated (Scheme 5). However, cyclin binding is not sufficient and cdk activation

involves removal of inhibitory phosphate groups by CDC25 phosphatases, as well as phosphorylation at the activating sites by cyclin activating kinase (CAK). Finally, CDK activity can be blocked by binding of CDK inhibitory proteins belonging to INK4 family (CDKN2B, CDKN2A, CDKN2C, CDKN2D) and CIP/KIP family (p21 and CDKN1B) that directly inhibit CDK activity.
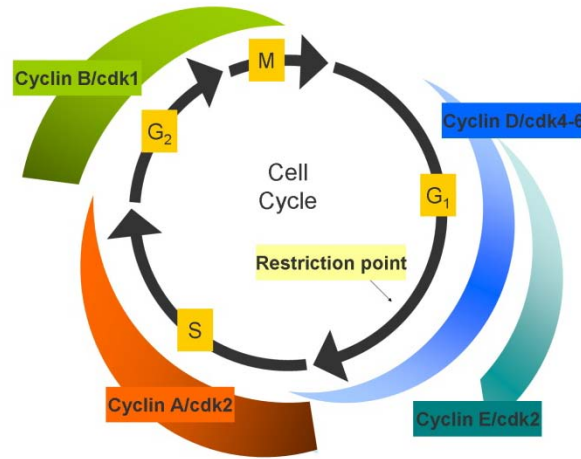
Adopted from www-rcf.usc.edu/~forsburg/cclecture.html

Scheme 5: Oscillation of cyclin protein level and cyclin/cdk activity throughout the cell cycle (Forsburg, 2000).

Mitogens act through cell surface receptors to activate mitogen activated protein (MAP) kinase cascade resulting in increased levels of MYC transcription factor (Scheme 6). MYC promotes expression of D cyclins which bind to and activate CDK4 and CDK6, triggering the phosphorylation of retinoblastoma (RB) family members (p105, p107 and p130). RB proteins are negative regulators of cell proliferation because they bind to and sequester E2F transcriptional factors that are required for the entry into the S phase. RB phosphorylation by cyclin D/CDK4 and cyclin D/CDK6 results in its partial inhibition and E2F release, followed by expression of E2F target genes, such as cyclin E, cyclin A, H2A, PCNA, as well as E2F, creating an amplifying loop. Cyclin E binds to CDK2 which further phosphorylates RB, resulting in its complete inactivation, and passage through the R point. Besides the kinase dependent function in inactivating RB, cyclin D/CDK4 and cyclin D/CDK6 assist in cyclin E/CDK2 activation by titrating away their inhibitors. As cyclin E/CDK2 activity peaks in late G_1, mitogen-dependent cyclin D/CDK4 and cyclin D/CDK6 activity is no longer necessary.

G_2 phase of the cell cycle is the period between the exit from the S phase and entry into mitosis. Transition from the G_2 to mitosis is dependent on the activity of CDK1, and is controlled by the availability of its binding partner, cyclin B, as well as posttranslational modifications of CDK1. CDK1 and cyclin B together form the maturation promoting factor (MPF) (Yamashita et al., 1992), which phosphorylates numerous substrates. The MPF targets include lamins whose phosphorylation leads to nuclear envelope breakdown (Peter et al., 1991), condensins that control chromosome condensation (Kimura et al., 1998), as well as microtubule associated proteins and motor proteins that are involved in centrosome separation and mitotic spindle formation (Blangy et al., 1995).
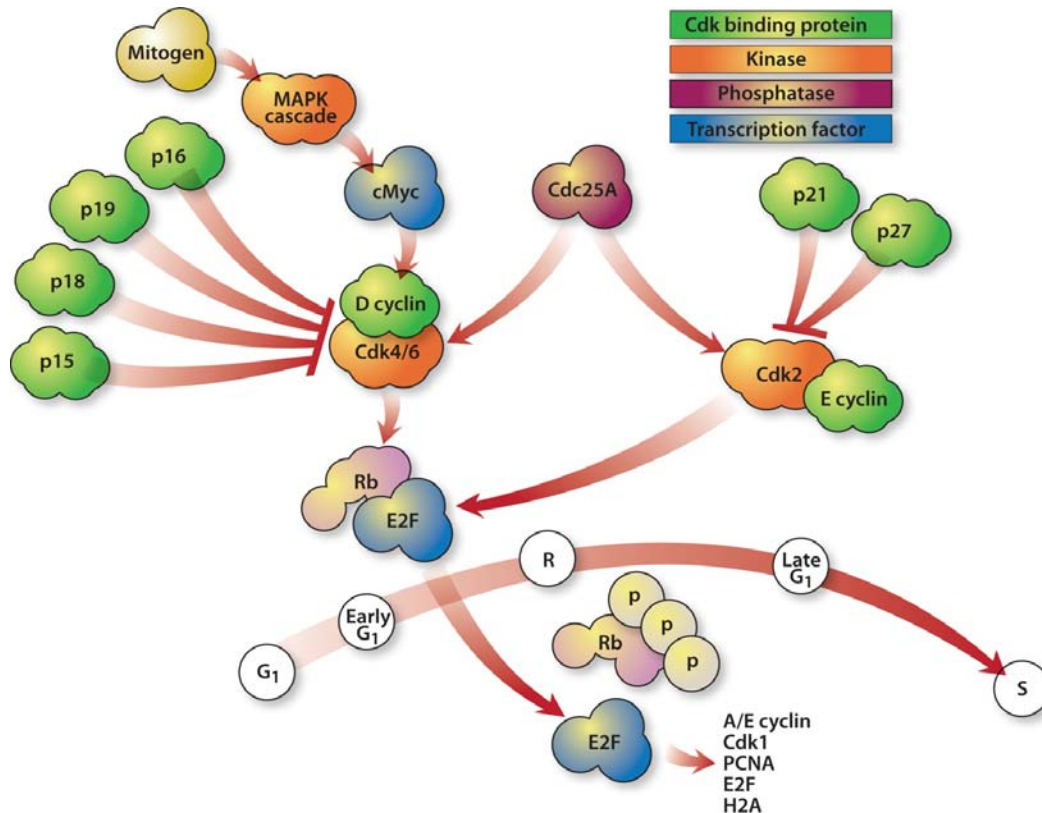
Scheme 6: Regulation of transition from G_1 to S phase of the cell cycle.

Level of cyclin B is set by balancing its gene transcription with protein degradation and peaks in late G_2 and early mitosis (Scheme 5). *CCNB* gene expression is activated by transcription factors that are under control of S phase specific cyclin A/CDK2 complex in order to ensure its timely expression (Chae et al., 2004; Dynlacht et al., 1994; Ziebold et al., 1997). Cyclin B is rapidly degraded by anaphase promoting complex (APC), an E3 ubiquitin ligase that targets cyclin B for proteosomal degradation in the early mitosis (Acquaviva and Pines, 2006). CDK1 is activated once the cyclin B protein level reaches certain threshold, but full activation is achieved by posttranslational modifications of CDK1. Fine tuning of cdk1 function is regulated by opposing effects of CDC25 phosphatase and WEE1/MYT1 kinases. WEE1 and MYT1 place inhibitory phosphate groups on tyrosine 14 and tyrosine 15 in CDK1 (Booher et al., 1997; Liu et al., 1997). These negative marks are removed by CDC25 phosphatases. In addition, CDK1 has to be phosphorylated at threonine 161 by CAK for its full activation (Scheme 7) (Atherton-Fessler et al., 1993; Gould and Nurse, 1989; Tassan et al., 1994).

Once activated, cyclin B/CDK1 can phosphorylate and thereby inactivate WEE1 and MYT1, further promoting its own activation (Watanabe et al., 2005; Watanabe et al., 2004). It can also help activate CDC25 through phosphorylation, further enhancing the amplification of MPF signaling (Hoffmann et al., 1993).

There is a parallel regulatory pathway of onset of mitosis that relies on activation of Polo like kinase (PLK) 1. PLK1 is a positive regulator of mitotic entry and is involved in centrosomes maturation, formation of bipolar spindle, chromosome segregation, as well as cyclin B/CDK1 activation (Alexandru et al., 2001; Yarm, 2002). PLK1 is activated by aurora A/BORA phosphorylation at threonine 210 (Seki et al., 2008). PLK1 phosphorylates CDC25C at seine 198 resulting in CDC25C activation (Roshak et al., 2000; Toyoshima-Morimoto et al., 2002), while phosphorylation of negative regulators of mitotic entry Wee1 and Myt1 leads to their inactivation (Inoue and Sagata, 2005; Nakajima et al., 2003) (Scheme 7). PLK1 can also directly phosphorylate cyclin B (Toyoshima-Morimoto et al., 2001). Activated cyclin B/cdk1 phosphorylate BORA, which enhances aurora A/BORA binding to and activation of PLK1 (Chan et al., 2008; Hutterer et al., 2006), ultimately leading to further stimulation of cyclin B/CDK1 activity and mitotic entry.
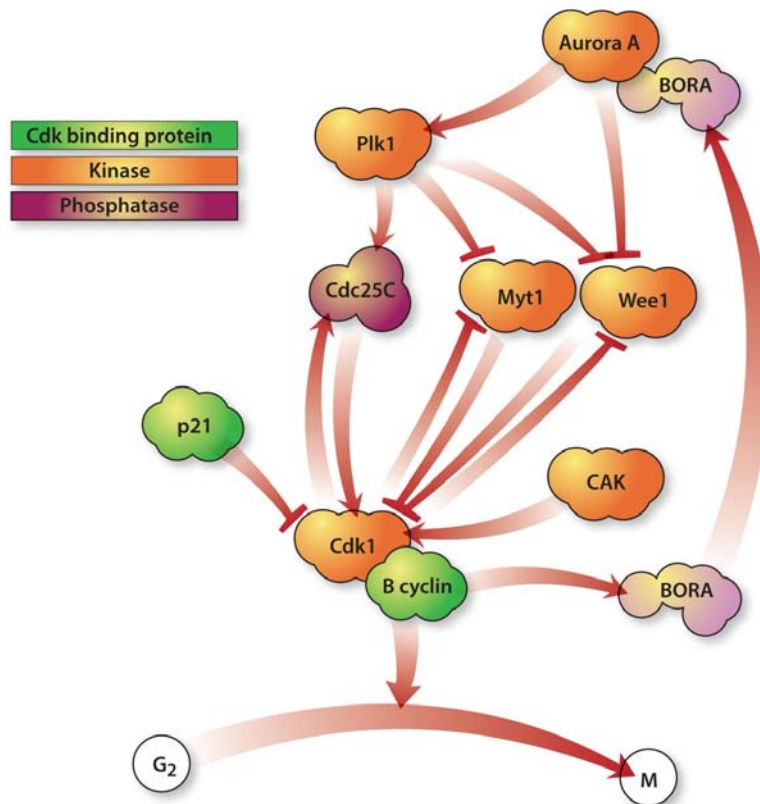
Scheme 7: Regulation of transition from G_2 to mitosis.

1.7.2 Mouse embryonic stem cells

ES cell self-renewal is maintained at least in part by promotion of cellular proliferation. It is not surprising then that ES cells have specific adjustments to the cell cycle regulation that allow them to rapidly proliferate.

Mouse ES cells are characterized by very short cell cycle (11 – 16 hours), predominantly because of the short G_1 phase that accounts for about 15% of the cell cycle time (2 hours) (Savatier et al., 1994). The cyclin

E/Cdk2 activity in mouse ES cells is high and cell cycle independent (unlike in somatic cells where it peaks at the G_1 to S transition, Scheme 5), and cyclin A/Cdk2 is constitutively active. Retinoblastoma tumor suppressor (Rb) is held inactive by hyperphosphorylation throughout the cell cycle, leading to constitutive E2f activation, and non-phasic transcription of E2f target genes (Stead et al., 2002). The D-type cyclin expression is very low, whereas Cdk4 kinase activity is almost undetectable, providing evidence that mitogen-induced cyclin D/Cdk4 or cyclin D/Cdk6 activity do not have a role in regulating Rb/E2f and subsequently cyclin E/Cdk2 activity (Savatier et al., 1994; Savatier et al., 1996). The only cell cycle regulators expressed in cell cycle dependent manner are cyclin B and Cdk1, which are expressed at the G_2 to mitosis transition (Stead et al., 2002). These findings are consistent with the observation that restriction point is bypassed in mouse ES cells, resulting in facilitated G_1 to S transition and proliferation. Following differentiation, restriction point is acquired; Rb/E2f and cyclin E come under mitogen-dependent activity of cyclin D/Cdk4 or cyclin D/Cdk6 complexes and become cell cycle regulated (Savatier et al., 1996; White et al., 2005).

Lif/Stat3/Myc pathway has major role in maintaining mouse ES cell self-renewal by promoting proliferation: Myc is a major target of Lif/Stat3 pathway and is powerful inducer of cyclin E expression, stimulating G_1 to S transition. Therefore, there is a link between regulation of self-renewal and cell cycle control in mouse ES cells. The benefit of having shorter G_1 phase in not only in achieving rapid proliferation, but also in avoiding differentiation signals that are active during early G_1 in other cell types.

1.7.3   Non-human primate embryonic stem cells

Non-human primate ES cells have slightly longer cell cycle duration than mouse ES cells: 12 – 21 hours, with median cell cycle duration of 15 hours. Over 50 % of cells are found in the S phase, and the expression of cyclin E and cyclin A is high. Following differentiation, the fraction of cells in the S phase, as well as the level of cyclin E and cyclin A, is decreased. Similar to the observations in the mouse ES cells, cyclin E expression and RB hyperphosphorylation are independent of the cell cycle stage, but unlike mouse ES cells, cyclin A exhibits transient expression in cell cycle. In addition, non-human primate ES cells do not require serum in the medium, and MAPK activity does not affect the growth rate (Fluckiger et al., 2006).

1.7.4   Human embryonic stem cells

Human ES cells' cell cycle is abbreviated similar to mouse and non-human primate ES cells, with median cell cycle duration of 15.8 hours. Shortening of the G_1 phase is responsible for abbreviated cell cycle in human ES cells. G_1 phase accounts for about 19% of the cell cycle, corresponding to 2.5-3 hours. Vast majority of cells are in the S phase that lasts about 8 hours. In healthy human ES cell cultures all cells are positive for proliferation marker KI-67, demonstrating the absence of quiescent cells (Becker et al., 2006). Unlike in mouse ES cells, in human ES cells most of the cell cycle regulators including cyclins D2, E and A exhibit phase-specific expression (Neganova et al.,

2009); the comparison of expression of key cell cycle controllers between mouse and human ES cells is summarized in Table 2. Becker and colleagues demonstrated that the expression of CDK4 is higher than that of CDK6 in human ES cells, and that cyclin D2 expression is elevated in human ES cells in comparison to somatic cells. Furthermore, the expression of CDK inhibitors CDKN1A, CDKN1B and CDKN1C is barely detectable. Thus, in comparison to mouse ES cells, human ES cells exhibit more prominent control of the cell cycle progression, particularly through G_1 phase. Nevertheless, human ES cells still exhibit shortened G_1 phase and rapid proliferation, and results suggest that this is result of elevated cyclin D2/CDK4 activity (Becker et al., 2006).

As already mentioned, self-renewal is supported by rapid proliferation. Since self-renewal is under control of NANOG, OCT4, and SOX2 transcription factors, it is reasonable to speculate that there is a link between transcriptional network that controls self-renewal and regulation of proliferation. Indeed, NANOG has been found to accelerate G_1 to S transition, as well as S phase progression in human ES cells through direct transcriptional activation of *CDK6* and *CDC25A* gene expression. Overexpression of *NANOG* suppresses the spontaneous differentiation and promotes human ES cells' expansion, without affecting the apoptosis (Zhang et al., 2009).

Table 2: Comparison of expression and activity of cell cycle controllers in mouse and human embryonic stem cells.

	Mouse ES cells	Human ES cells
Cyclin D	Very low	High in G_1
CDK4	Almost undetectable	High activity in G_1
CDK6	High	G_1
Cyclin E/CDK2	Constitutively active	$G_1 - S$
CDC25A		G_1
Cyclin A/CDK2	Constitutively active	$S - G_2$
E2F	Constitutively active	Cell cycle dependent?
Cyclin B/CDK1	Cell cycle dependent – G_2	Cell cycle dependent – G_2
CDKN1A	Undetectable	Very low
RB	Cell cycle independent, hyperphosphorylated	Cell cycle dependent

Link between cell cycle duration and differentiation has been established in cancer cells, somatic cells, and adult stem cells. As already described, cells in the G_1 are particularly responsive to intracellular and extracellular signals based on which they decide their fate. Therefore, it appears the G_1 stage of the cell cycle is a period during which ES cells are most sensitive to differentiation, and the shortening of the G_1 phase contributes to self-renewal. Indeed, it has been demonstrated that pharmacological activation of TTP53 followed by increased expression of CDKN1A leads to accumulation of cells in G_1 phase of the cell cycle followed by human ES cell differentiation (Maimets et al., 2008).

1.8   DNA DAMAGE CHECKPOINT ACTIVATION

1.8.1   Somatic cells

Ionizing radiation induces a variety of DNA lesions (Goodhead, 1989; Hutchinson, 1985; Ward, 1988), including double and single strand breaks, as well as base damage, and, thus, evokes various cellular responses to DNA damage. Double strand breaks (DSB) are particularly toxic for the cell and are more difficult to repair as they cause the loss of integrity of both DNA strands (Karagiannis and El-Osta, 2004). Ionizing radiation-induced DNA damage activates checkpoint machinery in somatic cells and arrests the cell cycle allowing time for DNA repair to occur prior to proceeding to the next stage of the cell cycle.

The upstream checkpoint components, including damage sensors and transducers, are shared by the G_1/S, intra-S and G_2/M checkpoints. Two phosphoinositide 3-kinase like-kinase (PIKK) family members, ataxia telangiectasia mutated (ATM) and ataxia telangiectasia and RAD3 related (ATR) protein kinases are central to initiation of DNA damage and replication checkpoints in response to various genotoxic stresses (Abraham, 2001). Activated ATM and ATR kinases phosphorylate numerous protein targets and transduce signals generated by DNA damage sensors to cell cycle stage specific effector proteins. ATM exists as an inactive dimer that is autophosphorylated at serine 1981 in response to DNA double strand breaks (Bakkenist and Kastan, 2003). Activated ATM monomers localize primarily at DSB, where they phosphorylate many substrates, including TTP53 (Banin et al., 1998; Canman et al., 1998), CHEK2 (Matsuoka et al., 2000; Melchionna et al., 2000), H2AX (Lukas et al., 2004), NBS1 (Gatei et al., 2000; Lim et al., 2000; Wu et al., 2000; Zhao et al., 2000), BRCA1 (Cortez et al., 1999; Li et al., 2000).

Checkpoint signal generated by ATM and ATR is transmitted to checkpoint kinases, CHEK1 and CHEK2 that associate with DSB transiently and are released into the nucleus to transmit the signal throughout the nucleus (Lukas et al., 2003). Although the ATR-CHEK1 pathway is predominantly activated in response to UV treatment (Guo et al., 2000), and ATM-CHEK2 is predominant in response to ionizing radiation (Melchionna et al., 2000), there is significant crosstalk between these two pathways, particularly as they share multiple targets (Shiloh, 2001; Zhou and Elledge, 2000). Both CHEK1 and CHEK2 down-regulate CDC25 phosphatases (Falck et al., 2001; Furnari et al., 1999; Mailand et al., 2000) and activate TTP53 through phosphorylation (Hirao et al., 2000; Shieh et al., 2000).

The tumor suppressor TTP53 plays a major role in multiple cellular processes occurring in response to DNA damage, including cell cycle arrest, apoptosis, and senescence. It is constitutively expressed, but rapidly degraded due to MDM2 ubiquitination and targeting for proteasome degradation (Chehab et al., 1999). ATM, ATR, CHEK2 and CHEK1, among other kinases, phosphorylate TTP53. ATM (Banin et al., 1998; Canman et al., 1998) and ATR (Tibbetts et al., 1999) phosphorylate TTP53 at serine 15 which impairs MDM2 binding and enhances TTP53 accumulation and functional activation in response to DNA damage (Tibbetts et al., 1999). CHEK2 and CHEK1 phosphorylate TTP53 at serine 20 (Hirao et al., 2000; Shieh et al., 2000) promoting its tetramerization, stability and activity (Hirao et al., 2000). Activated TTP53 promotes transcription of its target genes, such as

CDKN1A (p21) (el-Deiry et al., 1993), *GADD45* and *SFN* (14-3-3-σ) (Hermeking et al., 1997), which play a role in the cell cycle arrest and other cellular responses to DNA damage summarized in Table 3.

Table 3: Tumor suppressor TP53 transcriptional target genes activated in response to DNA damage.

DNA repair	Cell cycle arrest	Apoptosis	Feedback regulation
CDKN1A	CDKN1A	PUMA	MDM2
GADD45	SFN (14-3-3-σ)	NOXA	PIRH2
p48 XP	GADD45	BAX	COP1
	CDC25C	TP53-AIP	CCNG
	Reprimo	PIG3	
		FAS/APO1	
		KILLER/DR5	

Cell cycle progression is driven by temporal activation of cyclin/CDK complexes, making them logical targets of the checkpoint response. The ionizing radiation induced DNA damage signaling and checkpoint activation is summarized in Scheme 8.
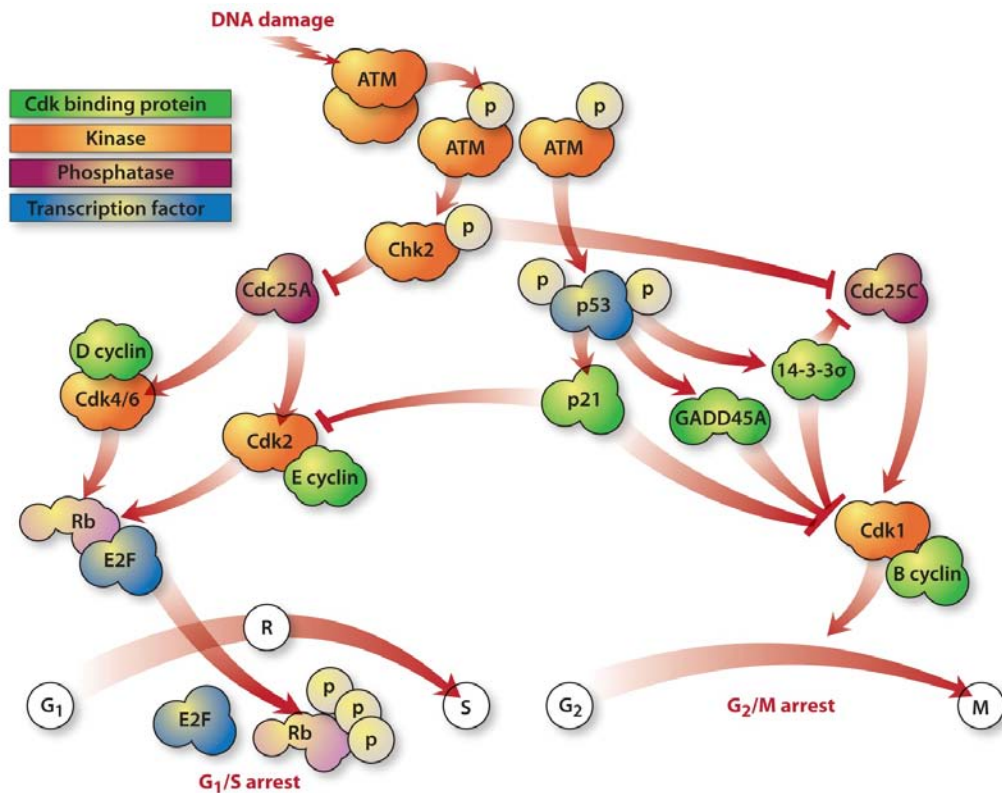
Scheme 8: Ionizing radiation induced checkpoint signaling.

The main targets of the G_1/S cell checkpoint are cyclin/CDK complexes that drive transition from G_1 to the S phase of the cell cycle (Sherr, 1994). Following ATM and CHEK2 activation, CDC25A phosphatase becomes phosphorylated and degraded (Arata et al., 2000; Mailand et al., 2000), rendering CDK2 inactive. This event results in rapid initiation of the G_1/S arrest because cyclin E/CDK2 complex is not activated and cannot phosphorylate RB and promote E2F release (Arata et al., 2000). The G_1/S arrest is sustained by TTP53 dependent *CDKN1A* expression and inactivation of CDK2 (Harper et al., 1993; Nyberg et al., 2002). Therefore, ATM and CHEK2

dependent TTP53 activation is not required for cell cycle arrest initiation, but is required for the maintenance of this arrest.

The main target of the G_2/M cell cycle arrest is cyclin B/CDK1 complex that is essential for mitotic entry. This complex is kept inactive by CDK1 phosphorylation at inactivating sites (tyrosine 14 and 15), and depends on CDC25 phosphatases to remove these inhibitory phosphate groups. CDC25C is phosphorylated by CHEK2 at serine 216 which creates a binding site for an adaptor protein, SFN, resulting in nuclear exclusion and degradation of CDC25C-serine 216 (Furnari et al., 1999; Peng et al., 1997). In addition, SFN affects nuclear localization of cyclin B/CDK1 (Giono and Manfredi, 2006). Cyclin B/CDK1 complex has also been reported to be inhibited by CDKN1A and GADD45, aiding the maintenance of G_2/M arrest (Bunz et al., 1998; Zhan et al., 1999). Therefore, at least three TTP53 dependent genes, *CDKN1A, SFN* and *GADD45*, are involved in initiation and maintenance of G_2/M cell cycle arrest.

1.8.2   Embryonic stem cells

Both mouse (Aladjem et al., 1998; Hong and Stambrook, 2004) and non-human primate (Fluckiger et al., 2006) ES cells have been reported to lack a functional DNA damage induced G_1/S cell cycle arrest, and to be hypersensitive to DNA damaging agents, responding with high levels of apoptosis (Aladjem et al., 1998; Hong and Stambrook, 2004; Qin et al., 2007) and differentiation (Lin et al., 2005; Qin et al., 2007). Furthermore, mouse ES cells may exhibit uncharacteristic localization and expression of checkpoint control proteins. The DNA damage signaling factor Chek2 has been reported to localize aberrantly to the centrosomes in mouse ES cells and failed to translocate to the nucleus following irradiation (Hong and Stambrook, 2004). Additionally, conflicting reports of TTP53 localization and activity have been described in mouse ES cells in response to DNA damage. Aladjem et al. (Aladjem et al., 1998) reported that mouse ES cells do not activate TTP53-dependent DNA damage responses and undergo TTP53-independent apoptosis in response to ionizing radiation. These authors and others have reported that TTP53 was inefficiently translocated to the nucleus after DNA damage in these cells (Aladjem et al., 1998; Chuykin et al., 2008; Hong and Stambrook, 2004). In contrast, others have reported that treatment with DNA damaging agents results in TTP53 induced differentiation of mouse (Lin et al., 2005) and human (Qin et al., 2007) ES cells by suppressing *NANOG* expression through direct binding to the *NANOG* promoter, implying that TTP53 does successfully translocate to the nucleus after DNA damage.

Wang and colleagues (Wang et al., 2009), examined S and G_2/M checkpoint function in human embryonic carcinoma (EC) cells. Human EC cells exhibited an S phase delay in response to irradiation, which has not been detected in mouse, primate or human embryonic stem cells. Embryonic stem cells of different species all show tremendous sensitivity to DNA damage and undergo extensive cell death within hours of DNA damage. However, human EC cells displayed higher survival following irradiation when compared to their differentiated counterparts. It is interesting to note these several differences between ES and EC cells given their numerous similarities and it will be illuminating to examine these two cell types further to better understand their similarities and differences.

1.9   DOUBLE STRAND BREAK REPAIR

Double strands break are regarded as highly toxic for the cell because even one DSB can be potentially lethal (Rich et al., 2000). Pathological DSB are generated by both exogenous agents (ionizing radiation, radiomimetic drugs, or topoisomerase poisons), as well as endogenous sources (reactive oxygen species (ROS) formed during metabolism, stalled replication forks, incorrect resolution during metabolic processing of DNA). There are also physiological (intentional) DSB created during meiotic recombination or V(D)J recombination that would be as toxic as pathological DSB if not removed. However, the predominant cause of DSB in proliferating cells is errors in DNA replication. Given the toxicity of DSB for the cell, several repair pathways exist to remove them. The two main pathways are non-homologous end joining (NHEJ) and homologous recombination (HR).

Double strand breaks occur in various forms, such as blunt ends, 5' and/or 3' overhangs, and gaps, and may contain non-ligatable groups such as 3'-phosphate or 3'-phosphoglycolate groups, requiring processing before ligation (Friedberg Errol C, 2006). NHEJ is an error-prone process that requires processing of DNA ends which may lead to loss of genetic information (Lees-Miller and Meek, 2003; Lieber et al., 2003). Since it does not require the presence of the sister chromatid in the cell, it is present in all phases of the cell cycle, but is predominant during G_1 and early S phases (Lee et al., 1997; Takata et al., 1998). HR, however, depends on the presence of the sister chromatid and consequently is predominant in the late S and in G_2 phases of the cell cycle when the duplicated chromatids are present (Haber, 2000; Rothkamm et al., 2003).

The choice of the pathway depends on several factors, such as kinetics of repair, cell cycle stage, or cell type. NHEJ and HR have rather different kinetics, with NHEJ being responsible for the fast mode of repair. HR depends on the presence of sister chromatid in the cell. Consecutively, HR dominates in late S and G_2, whereas NHEJ is preferred in G_1 and early S (Takata et al., 1998). Finally, the ability of particular cell type to tolerate mutations greatly affects the choice of DSB repair pathway. Somatic cells may be more tolerant to inaccurate repair system such as NHEJ, which may be highly unbeneficial for the germ cells (during certain stages of spermatogenesis KU70/80 is not expressed).

1.9.1   Non-homologous end joining

Non-homologous end joining is error-prone because it involves processing of DNA ends which might lead to loss of nucleotides on both sides of the break (Mahaney et al., 2009). Since it does not require template, it is a predominant way to repair DSB prior to S phase and is a major repair pathway in vertebrates (Branzei and Foiani, 2008; Rothkamm et al., 2003). In addition, it has physiological role and is essential for V(D)J recombination in immunoglobulin genes; hence, mutations in genes that encode NHEJ proteins lead to severe combined immunodeficiency phenotype (SCID) and increased radiosensitivity.

The first step of NHEJ is recognition of and binding to DNA ends by XRCC6 (KU70)/XRCC5 (KU80) heterodimer (KU70/80) which occurs within seconds of break formation. KU70/80 represents the most abundant

end-binding factor in eukaryotes. The complex can accommodate variety of end structures, such as blunt ends, 5' and 3' overhangs, or covalently closed hairpins, in sequence-independent manner. KU70/80 is essential for recruitment of other NHEJ proteins to the DSB in vivo (Mahajan et al., 2002; Mari et al., 2006; Uematsu et al., 2007; Yano et al., 2008). DNA dependent protein kinase catalytic subunit (PRKDC) is a member of PIKK family (together with ATM and ATR), and is the first to be recruited to DSB by KU70/80 (Uematsu et al., 2007). DNA structure is important factor for DNA-PK activation, with DSB being the most effective activators irrespective of DNA sequence. Without DNA, KU70/80 and PRKDC interaction is not strong (Gottlieb and Jackson, 1993; Suwa et al., 1994). Together PRKDC and KU70/80 form DNA-PK complex which tethers the ends and protects them from nuclease attack. Among the DNA-PK targets are NHEJ proteins such as XRCC6, XRCC5 (Douglas et al., 2005), XRCC4 (Yu et al., 2003), DCLRE1C (ARTEMIS) (Ma et al., 2005a), and ligase IV (Wang et al., 2004), but their phosphorylation does not appear to be required for NHEJ in vivo. The best candidate for DNA-PK appears to be PRKDC which is autophosphorylated at numerous sites. This event appears to have role in regulating PRKDC enzymatic function and dissociation of phosphorylated PRKDC from DNA bound KU70/80 (Chan and Lees-Miller, 1996; Ding et al., 2003; Merkle et al., 2002). The next step in NHEJ is processing of DNA ends. Irradiation induced DSB often contain non-ligatable end groups and/or other DNA lesions and can be very complex requiring end processing. As mentioned earlier, NHEJ operates in the absence of the sister chromatid or regions of microhomology that could serve as template, and can lead to loss of genetic information (Budman and Chu, 2005). The main candidate for end processing is ARTEMIS. ARTEMIS is a 5'→3' exonuclease that in the presence of PRKDC and ATP attains endonuclease activity toward double strand DNA to single strand DNA transitions and DNA hairpins (Ma et al., 2002; Ma et al., 2005b). ARTEMIS can process DNA ends until they are compatible (removal of 5' and trimming of 3' overhangs), so at least for some NHEJ events polymerase may not be necessary. However, because radiation induced breaks can be very complex and require further processing leading to formation of DNA gaps, the following steps may include extension by terminal deoxyribonucleotidetransferase (DNTT) (Chappell et al., 2002; Karimi-Busheri et al., 2007), or polymerase λ or μ (Bertocci et al., 2006; Davis et al., 2008; Paull, 2005). Lastly, KU70/80 recruits and loads XRCC4-ligase IV functional complex that ligates DNA termini (Grawunder et al., 1997; Grawunder et al., 1998; Mari et al., 2006).

1.9.2   Homologous recombination

Homologous recombination serves several biological functions such as crossover generation during meiosis, telomerase maintenance, preservation of stalled replication forks, as well as DSB repair (San Filippo et al., 2008). There are several distinct mechanisms of HR that participate in the abovementioned processes (Table 4), but I will focus on double strand break repair and synthesis dependent strand annealing, as these two pathways are typically associated with DSB repair.

Table 4: Homologous recombination pathways (San Filippo et al., 2008)**.**

Pathway	Biological role	Products
Double strand break repair (DSBR)	Meiotic recombination Double strand break repair	Crossovers and noncrossovers
Synthesis dependent strand annealing (SDSA)	Double strand break repair Meiotic recombination	Only noncrossovers
Single strand annealing (SSA)	Repair of breaks within repetitive sequences	Deletion of one direct repeat and nucleotide sequence between repeats
Break induced replication (BIR)	Repair when there is only one DSB end – telomere elongation, replication fork restart	Accurate repair if sister chromatid or homologous chromosome are used, non-reciprocal translocation if repeat sequence on non-homologous chromosomes is used

Homologous recombination DSB repair is critically dependent on the presence of the extensive regions of homology and repairs DSB using the information present on the undamaged sister chromatid. Use of homologous chromosome as a template (such as in G_1 when sister chromatid is not present) can lead to loss-of heterozygosity, which can be even more deleterious than error-prone NHEJ; thus, HR mediated DSB repair occurs when an identical DNA molecule is present in the cell (late S and G_2 phase)(San Filippo et al., 2008).

The first step of HR repair is conversion of broken DNA ends into HR substrates, which involves degradation of 5' ends leaving 3' overhang several hundred bases long (Scheme 9). The candidate for exonucleolytic cleavage is the MRE11/RAD50/NBS1 (MRN) complex (Paull and Gellert, 1998; Paull and Gellert, 1999). The MRN complex has been shown to participate in virtually all aspects of DNA end metabolism – DSB detection (Mirzoeva and Petrini, 2001), DSB processing (Lewis et al., 2004), HR and meiosis (Bressan et al., 1999), telomere maintenance (Boulton and Jackson, 1998; Kironmai and Muniyappa, 1997), and cell cycle checkpoint activation (Carney et al., 1998; Zhao et al., 2000). Upon resection, single-stranded DNA (ssDNA) ends are bound by replication protein A (RPA), which assists in removal of secondary structures that would inhibit the following steps. However, precoating of ssDNA with RPA prevents binding of the RAD51 recombinase. The loading of RAD51 is supported by RAD52, a DNA-binding protein that facilitates interaction of RAD51 with ssDNA in the presence of RPA, and counteracts an otherwise inhibitory effect of RPA (Sung, 1997). RAD51 binding to DNA induces extensive stretching and unwinding of B-DNA leading to presynaptic filament formation that assists homologous strand pairing (Sung and Robberson, 1995). Next, during synapsis, heteroduplex DNA is formed between invading strand coated with RAD51 and template DNA molecule by homologous pairing leading to strand displacement. At this stage RAD52 promotes the annealing of complementary ssDNA strands. Once heteoduplex is formed it can be extended by branch migration. RPA coats displaced strand preventing re-annealing and thus accelerate branch migration. Branch migration is inefficient with RAD51 alone, but is greatly approved by the cofactors, such as RPA and RAD52 (Baumann et al., 1996; Baumann and West, 1999; Benson et al., 1998; Gupta et al., 1997; Sung and Robberson, 1995; Van Dyck et al., 1998). The 3' end of the invading strand primes DNA synthesis using the sister chromatid as a template. Capture of the second DSB end leads to formation of an intermediate with two Holliday junctions (cruciform DNA structure formed by crossing of the invading strand and displaced strand). Finally, the Holliday junctions are resolved by specialized endonucleases giving rise to crossover or noncrossover depending on whether all four strands are cut (Scheme 9: two dark and two light blue arrows;

crossover) or the invading and displaced strand (light blue arrows; noncrossover) (Sugawara et al., 2003; Szostak et al., 1983; Wolner et al., 2003).
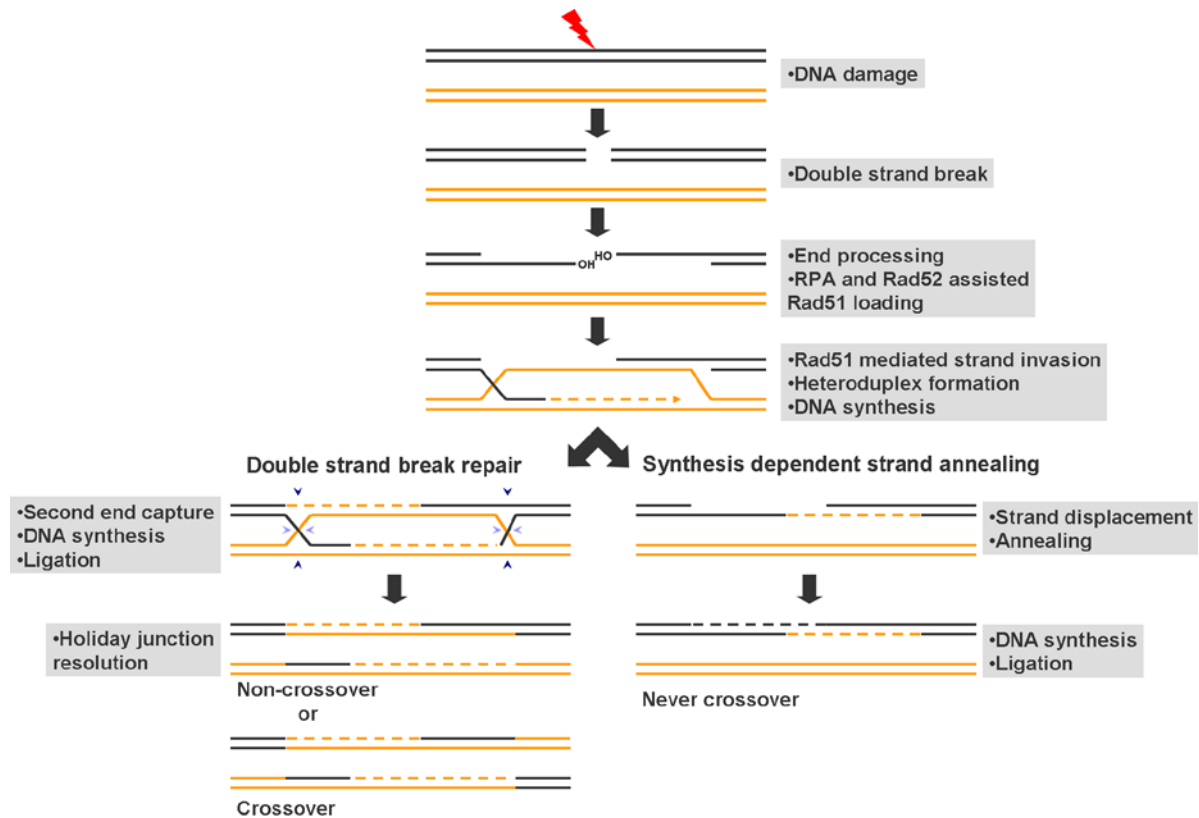
Scheme 9: Double strand break repair by homologous recombination.

Unlike meiotic HR, homologous recombination DSB repair rarely leads to formation of crossovers and hence another model, synthesis dependent strand annealing, was proposed to account for data on mitotic HR (Ferguson and Holloman, 1996; Nassif et al., 1994; Strathern et al., 1982). In this model, following strand invasion and repair DNA synthesis, second DSB end is not captured, and an intermediate with two Holiday junctions is not formed. Instead, the branch migration proceeds until complete displacement of the invading strand is achieved, so that it anneals with the second resected DSB end. Now, the DNA synthesis fills in the gap on the second resected DSB end, whereas the displaced strand reanneals with its complimentary strand forming intact template DNA molecule.

HR may be enhanced when NHEJ is defective, suggesting that KU70/80 binding to DNA ends may interfere with HR (Fukushima et al., 2001; Pierce et al., 2001), and some even suggest that in mammalian cells KU70/80 and RAD52 compete for binding to broken DNA ends. However, experiments with XRCC4/ligase IV mutants demonstrated that in the absence of functional NHEJ homologous recombination is stimulated, suggesting that 1) NHEJ might be the primary pathway for DSB repair, and 2) that if NHEJ fails, HR might take over (Delacote et al., 2002; Frank-Vaillant and Marcand, 2002).

1.9.3   Embryonic stem cells

It has been suggested that mouse ES cells rely mainly on HR to fix DSB because they spend most of their cell cycle time in S phase of the cell cycle when the sister chromatid is present, as well as in order to prevent accumulation and subsequent propagation of genetic changes. In support of this hypothesis, *Rad51* knock out mouse embryos exhibit profound radiosensitivity and die early in development due to decreased proliferation and massive chromosome loss (Tsuzuki et al., 1996). *Rad51* null ES cells cannot be isolated from knock out mouse embryos, nor generated in vitro (Lim and Hasty, 1996). A *T*TP53 null background only partially improves the phenotype of *Rad51* deficient mouse embryos, as double knock-outs exhibit extended development, but still die once accumulated DNA damage interferes with normal cellular function and mitosis (Lim and Hasty, 1996). Similarly, complete loss of *Rad50, Nbs1* and *Mre11* is early embryonic lethal, suggesting that the MRN complex is required for normal cellular function, proliferation, and growth. *Mre11* knock out ES cells cannot be obtained (Xiao and Weaver, 1997), *Nbs1* deficient ICM fail to proliferate and die in vitro (Zhu et al., 2001), whereas early *Rad50* null mouse ES cells are hypersensitive to ionizing radiation and cannot be propagated in cell culture (Luo et al., 1999), indicating that mutations in these genes are toxic at the cellular level.

   Rad52 knock-out mice are viable and show no impaired viability, fertility, or immune system deficiency. Mouse *Rad52* nullizygous ES cells do not show signs of radiosensitivity, and exhibit 30-40% reduction in homologous recombination, unlike yeast mutant RAD52⁻ cells which are not viable (Rijkers et al., 1998). This suggests that there are functionally related genes in mammalian cells that can compensate the absence of *RAD52*. *Rad54* inactivation in mouse ES cells leads to decreased homologous recombination and increased radiosensitivity, but *Rad54* null mice are viable and fertile (Essers et al., 1997), suggesting that Rad54 is not essential for normal mouse development.

   Mice missing any of the genes involved in NHEJ are viable, or die only late in embryonic development. Nullizygous *Lig4* and *Xrcc4* mice are late embryonic lethal due to massive TTP53 dependent neuronal apoptosis, arrested lymphogenesis, and other cellular defects (Barnes et al., 1998; Frank et al., 2000; Li et al., 1995). In this case a *T*TP53 null background rescues embryonic lethality, but not lymphocyte development or radiosensitivity. *Xrcc6* or *Xrcc5* inactivation in mice results in growth retardation, profound immunodeficiency, as well as marked radiosensitivity and inability to perform end-joining at the cellular level (Gao et al., 1998; Gu et al., 1997; Jin et al., 1998; Nussenzweig et al., 1997). Mice lacking *Prkdc* are immunodeficient, but do not exhibit growth retardation (Gao et al., 1998).

   Mouse ES cells that lack *Prkdc* do not exhibit increased radiosensitivity or sensitivity to etoposide treatment, unlike *Prkdc* knock out fibroblasts (Gao et al., 1998; Jin et al., 1998), suggesting that NHEJ is not a predominant DSB repair pathway in ES cells. In addition, wild type mouse ES cells express low levels of *Prkdc*, corresponding to lower activity of DNA-PK in these cells in comparison to mouse embryonic fibroblasts (MEF). Furthermore, mouse ES cells express a 20 fold higher level of Rad51 in comparison to MEF, and about the same level of Xrcc4 (Tichy and Stambrook, 2008).

Important insight into role of homologous recombination and non-homologous end joining came from studies by Banuelos et al. (Banuelos et al., 2008) in wild type and *Atm, H2ax*, and *Prkdc* mutant mouse ES cells. *H2ax* knockout mice exhibit similarities to *Atm* null mice, including radiosensitivity, growth retardation, and chromosomal abnormalities (Celeste et al., 2002; Xu et al., 1996). Mouse ES cells that lack H2ax are highly sensitive to ionizing radiation and radiomimetic drug treatments, show increased spontaneous and irradiation induced chromosomal abnormalities, and a subtle reduction in size of Rad51 foci following ionizing radiation exposure (Bassing et al., 2002). Mouse ES cells defective in *Atm* or *H2ax* exhibit faster DSB repair in comparison to wild type mouse ES cells, decreased survival, and inability to form foci of phosphorylated Atm (although Atm is autophosphorylated). In addition, cells that do not have Atm or H2ax express higher level of Prkdc than wild type mouse ES cells. Inhibition of DNA-PK activity resulted in reduced DSB rejoining in *H2ax* knock-out, but not wild type mouse ES cells, suggesting that DNA-PK has an important role in DSB repair in *H2ax* deficient mouse ES cells. However, in wild type mouse ES cells Prkdc activity still contributes to their survival following irradiation, because inhibition of Prkdc with its specific inhibitor NU7026 reduces survival of wild type and *H2ax* mutant mouse ES cells. Taken together, it appears that DNA-PK dependent DNA repair is not the main pathway for repair of DSB, but still contributes to survival of mouse ES cells following DNA damage. In instances when homologous recombination is impaired, mouse ES cells can redirect DSB repair toward NHEJ.

Both mouse (Saretzki et al., 2004) and human (Maynard et al., 2008) ES cells exhibit increased capacity for DNA damage removal following various genotoxic treatments, including DSB removal after ionizing radiation in comparison to differentiated cells. During differentiation of mouse (Saretzki et al., 2004) and human (Saretzki et al., 2008) ES cells expression of antioxidant and DNA repair genes is reduced, while the frequency of γ-H2AX positive cells increases. Wild type human ES cells express higher level of PRKDC and XRCC6 relative to mouse ES cells and more similar level to differentiated human cells (Banuelos et al., 2008). Interestingly, there is a general difference between mouse and human somatic cells in their dependence on NHEJ. For example, DNA-PK activity (Finnie et al., 1995) and XRCC6 expression (Anderson and Lees-Miller, 1992) are higher in human relative to mouse somatic cells, and XRCC5 is an essential protein in human, but not mouse cells (Li et al., 2002). In addition, human ES cells rejoin DSB faster than mouse ES cells (Banuelos et al., 2008) suggesting there might be difference between mouse and human ES cells' choice or repair pathway.

2.0   MATERIAL AND METHODS

2.1   CELL CULTURE AND DRUG TREATMENTS

2.1.1   Human ES cell culture on feeder cells

Human ES cell lines WA07 and WA09 (WiCell^{TM}, Madison, WI) were cultured in human ES cell medium containing 80% knock-out Dulbecco's Modified Eagle Medium (DMEM), 20% knock-out serum replacer, 1% non-essential amino acids, 1% penicillin/streptomycin (100U/100 µg/ml), 2 mM l-glutamine and 4 ng/ml basic fibroblast growth factor (FGF2; all from Invitrogen, Carlsbad, CA) on mitomycin C-treated mouse embryonic fibroblasts (MEF; Millipore Corporation, Billerica, MA). Cells were passaged manually every seven days and medium was changed every 48 hours. Cells were routinely tested for normal karyotype as previously described (Navara et al., 2007).

2.1.2   Human ES cell culture on Matrigel^{TM}

For flow cytometry experiments human ES cells were plated on BD Matrigel™ human ES cell qualified Matrix (BD Bioscience, Bedford, MA), grown in human ES medium conditioned with feeder cells for 24 hours, and supplemented with an additional 4 ng/ml FGF2. For sister chromatid exchange assay and gene expression studies human ES cells were plated on Matrigel™ and grown in mTeSR^{TM}1 medium (StemCell Technologies, Vancouver, BC, Canada) supplemented with 1% penicillin/streptomycin (100U/100 µg/ml).

2.1.3   Human induced pluripotent stem cell culture

Human iPS(IMR-90)-1 cells were obtained from WiCell^{TM} and amniotic epithelim (AE) iPS cell line was derived in our laboratory buy transduction of AE primary cells with lentiviral vector carrying OCT4, SOX2, KLF4 and MYC. Both iPS cell lines were grown on BD Matrigel™ human ES cell qualified Matrix in mTeSR^{TM}1 medium supplemented with 1% penicillin/streptomycin (100U/100 µg/ml). Medium was changed every 24 hours and cells were passaged every 5 – 6 days using 1 mg/ml dispase (StemCell Technologies).

2.1.4   IMR-90 cell culture

IMR-90 human diploid fibroblast strain was obtained from American Type Culture Collection (ATCC; Manassas, VA). IMR-90 fibroblasts were derived from the 16 week old female fetus. Cells were grown in Eagle's Minimum Essential Medium (ATCC), supplemented with 10% fetal bovine serum (Invitrogen) and 1% penicillin/streptomycin (100U/100 μg/ml), and passaged every 5 – 6 days using TrypLE^{TM} (Invitrogen). Medium was removed, cells washed once with phosphate buffered saline (PBS) to remove any traces of serum, and TrypLE^{TM} was added for five minutes at 37°C. TrypLE^{TM} was neutralized with serum containing cell growth medium, and cells were transferred to a new flask

2.1.5   Teratoma fibroblast cell culture

WA07 derived teratoma fibroblasts (H7TF) were isolated from a teratoma obtained from mice injected with WA07p69 cells. Following tumor growth, teratoma was isolated and tissue enzymatically dissociated into single cell suspension. Teratoma fibroblasts were grown in Dulbecco's Modified Eagle Medium (DMEM), 10% fetal bovine serum, 1% non-essential amino acids, 1% penicillin/streptomycin (100U/100 μg/ml), 2 mM l-glutamine (all from Invitrogen), and passaged every 4 – 5 days using TrypLE^{TM} as described for IMR-90 cells (**2.1.4**).

2.2   DRUG TREATMENTS

2.2.1   KU55933 treatment

For ATM inhibition studies, cells were treated with 10 μM, 50 μM, or 100 μM KU55933 (generously provided by Graeme Smith, Astra Zeneca), or vehicle dimethyl sulfoxide (DMSO; Sigma, St. Louis, MO) one hour prior to γ-radiation treatment.

2.2.2   BrdU and camptothecin treatment

For sister chromatid exchange studies, human ES cells were grown on Matrigel™ as previously described. Four days after plating 10 μM 5-bromo-2'-deoxy-uridine (BrdU; Roche Applied Science, Mannheim, Germany) was added to the human ES cell medium. Following twenty four hours incubation, BrdU containing medium was aspirated, cells washed three times with phosphate-buffered saline (PBS; Invitrogen), and medium containing 100 nM camptothecin (Sigma) was added. One hour following addition of camptothecin, cells were washed three times

with PBS and incubated for 15 hours in fresh medium. In order to arrest mitotic cells 120 ng/ml colcemid (Invitrogen) was added to the medium for 90 minutes. Following colcemid treatment, cells were harvested for cytogenetic preparation (**2.5**).

2.3   IRRADIATION

Human ES cells were irradiated four to seven days after passaging with two grays of γ-radiation using a Gammacell® 1000 Elite cesium[137] irradiator (Nordion, Ottawa, Canada). Immediately after irradiation cells were returned to the incubator for recovery until the appropriate time point.

2.4   IMMUNOCYTOCHEMISTRY AND CONFOCAL MICROSCOPY

For immunocytochemistry human ES cells were grown on Thermanox® plastic coverslips (NUNC[TM], Rochester, NY) on MEF feeder cells, fixed in 2% formaldehyde, and permeabilized in 0.1% Triton X-100 in tris-buffered saline (TBS; both Sigma). Incubation with the primary antibodies listed in Table 5 was carried out in a humidified chamber at 37°C for 45 minutes. Primary antibodies were detected using species-specific fluorescently labeled secondary antibodies (Invitrogen) at 37°C for 45 minutes. DNA was visualized by addition of 1 μM Toto-3 (Invitrogen). Coverslips were mounted onto glass slides with Vectashield anti-fade mounting medium containing DAPI (Vector Laboratories, Burlingame, CA). Slides were examined using a Leica TCS-SP2 laser scanning confocal microscope (Leica Microsystems GmbH, Wetzlar, Germany). The appropriate species-specific secondary antibody controls were obtained in the same manner, but incubation with primary antibodies was omitted. Co-localization of immunocytochemical probes was determined using ImageJ software (Rasband, 1997-2008). For the analysis of mitotic figure morphology the following criterion was used: mitotic figures that displayed misaligned chromosomes in metaphase, lagging chromosomes in anaphase, or multipolar spindles were regarded as aberrant. Prophase cells were considered as non-informative, and were not categorized as either normal or aberrant. Examples of normal and aberrant mitotic figures are shown in the Figure 10D.

Table 5: List of primary antibodies used for immunocytochemistry.

Antigen	Manufacturer (catalogue number)	Dilution
OCT4	Santa Cruz Biotechnology, Inc., Santa Cruz, CA (sc-5279)	1:100
NANOG	R&D Systems, Inc., Minneapolis, MN (AF1997)	1:50
SSEA4	Developmental Studies Hybridoma Bank, The University of Iowa, IA (clone MC-813)	1:5
ATM-serine 1981	Epitomics, Burlingame, CA (EP1981)	1:100
CHEK2-threonine 68	Cell Signaling Technology, Danvers, MA (2661)	1:100
TTP53-serine 15	Cell Signaling Technology, Danvers, MA (9284)	1:100
TTP53-serine15	Cell Signaling Technology, Danvers, MA (9286)	1:100
Histone H3-serine 10	Cell Signaling Technology, Danvers, MA (9701)	1:100
γ-H2AX	Upstate, Lake Placid, NY (05-636)	1:200
RAD51	EMD4Biosciences, Gibbstown, NJ (PC130)	1:200
β-tubulin	Developmental Studies Hybridoma Bank, The University of Iowa, IA (E7)	1:5

2.5   CELL HARVESTING

Human ES cells grown on feeders were manually scraped and transferred to a clean tube. Human ES and iPS cells grown on Matrigel™ were harvested with accutase (Chemicon International, Temecula, CA). Medium was removed, cells washed with PBS once, and treated with accutase for two minutes at 37°C. Detached cells were transferred to a clean tube; dish was rinsed with PBS and scraped with cell scraper to detach any remaining cells. Human fibroblasts (IMR-90 and WA07p69 teratoma fibroblasts) were collected using TrypLE™ (2.1.4).

2.6   RNA EXTRACTION, REVERSE TRANSCRIPTION, TAQMAN® LOW DENSITY ARRAYS, PCR ARRAYS

2.6.1   RNA extraction and DNA clean-up

Collected cells were pelleted by centrifugation, and lysed with 1ml of TRIzol ® Reagent (Invitrogen). The lysate was homogenized and 0.2ml of chloroform (Sigma) was added. Phase separation was achieved by centrifugation at 2500xg for five minutes, and aqueous phase was transferred into clean tube. RNA was precipitated with 0.6ml isopropyl alcohol (Sigma) overnight at -20°C. Following centrifugation at 16,000xg for 30 minutes at 4°C on the next day, RNA pellet was washed with 70% ethanol (Sigma), air dried and redissolved in RNase-free water. Purified RNA was subjected to DNA clean up with the DNA-*free*™ kit (Ambion, Austin, TX). One tenth of the sample volume of the DNase I buffer and two microliters of rDNase I were added to the samples, mixed gently and incubated at 37°C for 30 minutes. The DNase reaction was stopped by addition of one tenth of the total volume of DNase I inactivation reagent, and samples were incubated for two minutes at room temperature. Samples were

centrifuged at 9500xg and clear supernatant containing purified RNA transferred to clean tube. Concentration and quality of the samples were determined by UV spectrophotometry using Eppendorf Biophotometer (Hamburg, Germany). RNA samples of $A_{260/280}$ in range of 1.8 – 2.0 were used for further experimentation.

2.6.2 Reverse transcription and TaqMan® Low Density Arrays

Complementary DNA was produced using High Capacity cDNA RT kit (Applied Biosystems, Foster City, CA). Two micrograms of total RNA were used per reverse transcription reaction which composition is represented in Table 6.

Table 6: Reverse transcription reaction mixture.

Component	Volume/ Reaction [µl]
10X RT buffer	2.0
25X dNTP mix (100 mM)	0.8
10X RT random primers	2.0
MultiScribe™ reverse transcriptase	1.0
RNase inhibitor	1.0
2µg RNA	concentration dependent
Nuclease free water	up to 20µl final reaction volume

Reverse transcription was carried out in thermal cycler with the following conditions: $25^{o}C$ for 10 minutes, $37^{o}C$ for 120 minutes, and $85^{o}C$ for five seconds. The TaqMan® Human Stem Cell Pluripotency Array (Applied Biosystems) was used following manufacturer's instructions. Briefly, 10µl of cDNA reaction product was mixed with 40µl of nuclease free water and 50µl of 2X TaqMan® Universal PCR Master Mix (Applied Biosystems). The mixture was loaded into array with preloaded TaqMan® gene expression assays, and quantitative PCR reaction carried out on Applied Biosystems 7900HT system under following conditions: $50^{o}C$ for two minutes, $95^{o}C$ for 10 minutes, and 40 cycles of $95^{o}C$ followed by $60^{o}C$ for one minute. Data for *NANOG, POU5F1* and *CD9* expression were analyzed using SDS 2.2.2. software (Applied Biosystems). Expression fold changes were calculated using the $-\Delta\Delta Ct$ method and normalized using *ACTB* as the endogenous control.

2.6.3 Reverse transcription and PCR Arrays

Complementary DNA was produced using RT^2 First Strand Kit (SA Biosciences, Frederick, MD). First step was to perform genomic DNA elimination reaction followed by first strand cDNA synthesis reaction following manufacturer's directions. One microgram of total RNA was mixed with 5X genomic DNA elimination buffer, and nuclease free water was added to adjust final volume to 10µl. The genomic DNA elimination mixture was incubated at $42^{o}C$ for five minutes and transferred to ice for at least one minute. The composition of the subsequent reverse transcription reaction is represented in Table 7. The first strand synthesis reaction was carried out at $42^{o}C$ for 15 minutes and immediately stopped by heating to $95^{o}C$ for five minutes. Finally, 91µl of nuclease free water were added to each cDNA synthesis reaction.

Table 7: Reverse transcription reaction mixture.

Component	Volume/ Reaction [µl]
5X RT buffer 3	4
Primer and external control mix	1
RT enzyme mix 3	2
Genomic DNA elimination mixture	10
Nuclease free water	3

DNA Damage Signaling Pathway PCR array (SA Biosciences) was used according to manufacturer's directions. The quantitative PCR reaction mixture is represented in Table 8. The PCR was carried out using the following program on Applied Biosystems 7900HT system: 10 minutes at $95^{o}C$ to activate HotStart DNA polymerase, followed by 40 cycles of $95^{o}C$ for 15 seconds and $60^{o}C$ for one minute.

Table 8: Quantitative PCR reaction mixture.

Component	Volume/ Reaction [µl]
2X SABioscienced RT^2 qPCR Master Mix	2000
Diluted reverse transcription reaction product	102
Nuclease free water	1898

The PCR array contains predispensed primer sets that in addition to 84 DNA damage signaling pathway genes include five housekeeping genes for normalization of PCR array data, one genomic DNA contamination control, three reverse transcription controls, and three PCR positive controls. Data were analyzed using SDS 2.2.2. software and expression fold changes were calculated using the -ΔΔCt method and normalized using ACTB as the endogenous control.

2.7   WESTERN BLOT

Human ES cells grown on feeders, human ES and iPS cells grown on Matrigel™, and IMR-90 and WA07p69 teratoma fibroblasts were harvested as described in 2.5. Collected cells were pelleted by centrifugation, washed once in PBS, and lysed in RIPA buffer supplemented with 1 mM phenylmethylsulphonyl fluoride (PMSF; both Sigma) and 2X Halt™ phosphatase inhibitor cocktail (Pierce, Rockford, IL). The protein concentration was determined using bicinchoninic acid (BCA) assay (Bio-RAD Laboratories, Inc., Hercules, CA) and 5µg of protein were loaded per well. Proteins were separated by SDS-polyacrylamide gel electrophoresis using 4-15% or 4-20% Ready Gel Tris-HCl gels (Bio-RAD Laboratories) at 200 V constant, 120 mA in 25 mM tris, 192 mM Glycine, and 0.1% (w/v) SDS pH 8.3 running buffer, followed by transfer to BioTrace™ PVDF membrane (Pall Life Sciences, East Hills, NY) at 100 V, 350 mA in 25 mM tris, 192 mM glycine, and 20% (v/v) methanol for one hour. Proteins with higher molecular weight (ATM) were separated using 3-8% NuPAGE® Tris-Acetate® gels (Invitrogen) at 150 V constant, 110 mA in Novex® tris-acetate SDS running buffer (Invitrogen), followed by overnight transfer at 30 V, 90 mA in 25 mM tris, 192 mM glycine, and 20% (v/v) methanol. The membrane was blocked in TBS with 5% milk and 0.1% Tween-20 (all from Sigma) for one hour at room temperature. Membranes were incubated with the primary antibodies listed in Table 9 diluted in the blocking solution at 4°C overnight. The next day three washes in

the blocking solution were done and primary antibodies were detected using horse radish peroxidase (HRP)-conjugated species-specific secondary antibodies (Invitrogen) diluted in blocking buffer and incubated for one hour at room temperature. Following three washes in TBS with 0.1% Tween-20, detection of bound antibodies was performed with ECL Advance™ Western Blotting Detection kit (Amersham Biosciences, Piscataway NJ). Chemiluminescent signals were recorded using Hyperfilm™ (Amersham Biosciences).

Table 9: List of primary antibodies used for Western blot analysis.

Antigen	Manufacturer (catalogue number)	Dilution
OCT4	Santa Cruz Biotechnology, Inc., Santa Cruz, CA (sc-5279)	1:1000
NANOG	Kamiya Biomedical Company, Seattle, WA (PC-102)	1:500
Cleaved Caspase-3	Cell Signaling Technology, Danvers, MA (9661)	1:500
ATM	Sigma, St. Louis, MO (MAT3-4G10/8)	1:10,000
ATM-serine 1981	Epitomics, Burlingame, CA (EP1890Y)	1:1000
CHEK2	Thermo Fisher Scientific, Fremont, CA (MS-1515)	1:500
CHEK2-threonine 68	Cell Signaling Technology, Danvers, MA (2661)	1:500
TTP53	Santa Cruz Biotechnology, Inc., Santa Cruz, CA (sc-6243)	1:500
TTP53-serine 15	Cell Signaling Technology, Danvers, MA (9284)	1:500
TTP53-serine20	Cell Signaling Technology, Danvers, MA (9287)	1:500
NBS1	Epitomics, Burlingame, CA (Y112)	1:500
NBS1-serine343	Cell Signaling Technology, Danvers, MA (3001)	1:500
RAD50	GeneTex, Inc., Irvine, CA (GTX70228)	1:500
MRE11	Novus Biologicals, Inc, Littleton, CO (NB100-473)	1:500
RAD51	Thermo Fisher Scientific, Fremont, CA (MS-988)	1:200
RAD52	GeneTex, Inc., Irvine, CA (GTX70301)	1:500
Ligase IV	GeneTex, Inc., Irvine, CA (GTX30740)	1:800
XRCC4	GeneTex, Inc., Irvine, CA (GTX70293)	1:750
RB-serine 780	Cell Signaling Technology, Danvers, MA (9307)	1:750
RB-serine 795	Cell Signaling Technology, Danvers, MA (9301)	1:750
RB-serine 897/811	Cell Signaling Technology, Danvers, MA (9308)	1:750
CDKN1A	Cell Signaling Technology, Danvers, MA (2946)	1:200
α-tubulin	Sigma, St. Louis, MO (T 5168)	1:10,000

2.8   FLOW CYTOMETRIC ANALYSIS

2.8.1   Analysis of cell cycle distribution

Cell cycle analysis by flow cytometry was performed using propidium iodide (PI; BD Biosciences Pharmingen, San Diego, CA). Human ES cells grown on Matrigel™ were harvested using accutase as described in **2.5**, pelleted and washed in PBS. Five hundred thousand cells were resuspended in 1ml of PBS, fixed by addition of ice-cold 70% ethanol drop wise, and placed at -20°C overnight. Following fixation, cells were washed with PBS, and centrifuged at 200xg for five minutes. The cell pellet was resuspended in PBS solution containing PI (5 μg/10^6 cells) and RNase (Sigma; 10 mg/ml), and incubated in the dark at room temperature for 30 minutes. Cells were examined using a Becton Dickinson FACSVantage DiVa (BD, Franklin Lakes, NJ), and DNA-PI-A histograms were analyzed using

ModFit (Verity Software House, Topsham, ME). Results were gated to exclude cellular debris, sub G_0 population, and doublets.

2.8.2   EdU pulse chase incorporation

Human ES cells grown on Matrigel™-coated plates were labeled with 10 μM 5-ethynyl-2'-deoxyuridine (EdU; Invitrogen) for 30 minutes (pulse) before replacing with fresh medium. Human ES cells were immediately collected (non-irradiated control cells), or irradiated with two grays, and left to recover for 4, 8, 16 and 24 hours post irradiation (chase). Cells were harvested with accutase as described in **2.5**. Cell fixation, permeabilization and EdU detection were performed following manufacturer's instructions for Click-iT™ EdU flow cytometry kit (Invitrogen). Following harvesting, five hundred thousand human ES cells were washed in 1% bovine serum albumin (BSA, Sigma) in PBS and centrifuged at 200xg for five minutes. Supernatant was discarded, cell pellet resuspended in 300μl of 4% paraformaldehyde in PBS, and incubated in dark at room temperature for 15 minutes. Following centrifugation and wash in 1% BSA in PBS, cell pellet was resuspended in 1X saponin solution containing 1% BSA in PBS and incubated in dark at room temperature for 15 minutes. Human ES cells were pelleted and stained with 500μl of the reaction cocktail whose composition is presented in Table 10, in dark at room temperature for 30 minutes.

Table 10: Click-iT reaction cocktail composition.

Component	Volume/ Reaction [μl]
1X Click-iT™ reaction buffer	438
100 mM $CuSO_4$	10
10X Click-iT™ reaction buffer additive	5
Alexa Fluor® 647 azide (dye)	2.5
Water	44.5

After staining, 1% BSA in PBS was added to the reaction mixture to wash away the excess of unbound dye, and cells were centrifuged at 200xg for five minutes. The cell pellet was resuspended in PBS solution containing PI (5 μg/10^6 cells) and RNase (10 mg/ml), and incubated at room temperature in the dark for 30 minutes. Appropriate compensation tubes were used to set up the flow cytometer – unstained cells, cells stained with PI only (no dye), cells stained with dye only (no PI), as well as cells that were not incubated with EdU and were stained with both PI and dye. Human ES cells were analyzed using a Becton Dickinson FACSVantage DiVa. Dot plots representing EdU-647 fluorescence against DNA content were analyzed using BD FACSDiva software 6.1.1. (BD Biosciences, San Jose, CA).

2.8.3   Annexin V labeling

Human ES cells were grown on Matrigel™ and harvested by manual scraping in PBS eight hours after exposure to two grays of γ-irradiation. Staining with Annexin V and PI was performed according to manufacturer's instructions

for Annexin V-FITC Apoptosis Detection Kit I (BD Pharmingen). Briefly, harvested cells were centrifuged at 200xg for five minutes and washed twice with cold PBS, and then resuspended in 1X binding buffer at a concentration of one million cells per one milliliter. To one hundred thousand cells 5μl of PI and 5μl of Annexin V-FITC were added, and cells were incubated at room temperature for 15 minutes. At the end of incubation period, 400μl of 1X binding buffer were added to the staining reaction and cells were analyzed immediately using a Becton Dickinson FACSVantage DiVa. Appropriate compensation tubes were used to set up the instrument – unstained cells, cells stained with PI only (no Annexin V-FITC), and cells stained with Annexin V-FITC only (no PI). Dot plots representing PI fluorescence against Annexin V-FITC fluorescence were analyzed using BD FACSDiva software 6.1.1.

2.9   SISTER CHROMATID EXCHANGES

Human ES cells were harvested using accutase and pelleted as described earlier **2.5**. Medium was aspirated and one milliliter of prewarmed 0.75 mM KCl (Sigma) added drop wise while gently tapping the tube. Additional four milliliters of prewarmed hypotonic KCl solution was added and cells were allowed to swell in water bath at 37°C for 20 – 30 minutes. Ten drops of cold fixative (one part of acetic acid and three parts of methanol; all Sigma) were used as prefix, and cells were incubated for five minutes at room temperature. Following centrifugation, supernatant was discarded and fresh cold fixative added for 30 minutes. This step was repeated two more times, for total of three fixation steps. Following last fixation step, cells were dropped onto slides and left to dry and age for at least one day before staining.

Aged slides were rehydrated in PBS and stained in 50 μg/ml Hoechst 33258 (Invitrogen) in dark for 15 minutes. Following a wash in PBS, slides were placed in 2X SSC (0.3 M sodium chloride and 30 mM tri-sodium citrate dihydrate, pH 7.0; Invitrogen) on a 55°C hotplate and exposed to UV at a distance less than 10cm for 15 minutes. Slides were rinsed in PBS and stained in 4% Giemsa for 10 – 15 minutes. Metaphase spreads were visualized using light microscopy and number of chromosomes and sister chromatid exchanges (SCE) counted. Twenty-five metaphase spreads were analyzed per condition. Results are presented as a number of SCE per chromosome per cell.

2.10   STATISTICAL ANALYSIS

Means and SEMs were calculated, and statistical significance for categorical data was determined by χ^2 test. The significance was determined at $p<0.05$. P–values for SA Biosciences PCR arrays were calculated using web-based analysis software available at http://sabiosciences.com/pcrarraydataanalysis.php. Each cell line was run at least three

times. The p-values were calculated based on two-tail Student's t-test with equal variance and statistical significance was determined at $p<0.05$.

3.0   HUMAN EMBRYONIC STEM CELLS EXHIBIT ATM DEPENDENT G$_2$/M CELL CYCLE ARREST

This chapter was published as a research article in Stem Cells:

3.1   ABSTRACT

Human embryonic stem (ES) cells are highly sensitive to environmental insults including DNA damaging agents, responding with high levels of apoptosis. In order to understand the response of human ES cells to DNA damage, we investigated the function of the ataxia telangiectasia mutated (ATM) DNA damage signaling pathway in response to γ-irradiation. Here we demonstrate for the first time in human ES cells that ATM kinase is phosphorylated and properly localized to the sites of DNA double strand breaks within 15 minutes of irradiation. Activation of ATM kinase resulted in phosphorylation of its downstream targets: CHEK2, TP53 and NBS1. In contrast to murine ES cells, CHEK2 and TTP53 were localized to the nucleus of irradiated human ES cells. We further show that irradiation resulted in a temporary arrest of the cell cycle at the G$_2$, but not G$_1$ phase. Human ES cells resumed cycling approximately 16 hours post irradiation, but had a four fold higher incidence of aberrant mitotic figures compared to non-irradiated cells. Finally, we demonstrate an essential role of ATM in establishing G$_2$/M arrest, since inhibition with the ATM specific inhibitor KU55933 resulted in abolishment of G$_2$/M arrest, evidenced by an increase in the number of cycling cells two hours after irradiation. In summary, these results indicate that human ES cells activate the DNA damage checkpoint, resulting in an ATM dependent G$_2$/M arrest. However, these cells reenter the cell cycle with prominent mitotic spindle defects.

3.2 INTRODUCTION

Since all organisms are continually exposed to environmental and metabolic factors that cause DNA damage, eukaryotic cells have developed elaborate cell cycle checkpoint control and DNA repair mechanisms that act in an orchestrated manner to arrest the cell cycle until the damage is repaired (Jackson, 2002; Khanna and Jackson, 2001). Failure to do so can have detrimental consequences – transmission of genetic defects to the daughter cell or cell death. If DNA damage cannot be repaired, cells containing DNA damage may undergo apoptosis, removing their damaged DNA from the pool of cycling cells (Jackson, 2001; Jackson, 2002; Norbury and Hickson, 2001; Rich et al., 2000).

Ionizing radiation induces a variety of DNA lesions in exposed cells (Goodhead, 1989; Hutchinson, 1985; Ward, 1988), of which DNA double strand breaks (DSB) are particularly toxic because they are more difficult to repair due to the loss of integrity of both DNA strands (Karagiannis and El-Osta, 2004). In somatic cells, ionizing radiation induced DNA damage signaling is initiated by the DSB sensor ataxia telangiextasia mutated (ATM) kinase (Lavin et al., 2005). ATM is a member of the phosphatydilinositol 3'-kinase (PI3K)-related kinase family, but it phosphorylates protein rather than lipid substrates. In the presence of DSB ATM becomes activated and phosphorylates numerous downstream targets, including CHEK2 and TTP53, which act as signal transducers and effectors that initiate cell cycle arrest and apoptosis in G_1, S and G_2 phases of the cell cycle (Niida and Nakanishi, 2006).

While DNA damage responses have been extensively studied in somatic cells in vitro, the limiting nature of the available tissues and the ethical concerns in studying early human development in vivo have precluded studying DNA damage responses during very early human development. The successful isolation of human ES cells from blastocyst embryos by Thomson et al. (Thomson et al., 1998) enables these pluripotent, immortal cells to be used to study the corresponding developmental stages in vitro.

It has been reported that both mouse and non-human primate ES cells have developed modifications of checkpoint response that allow them to escape G_1/S arrest and to arrest in G_2/M instead (Aladjem et al., 1998; Fluckiger et al., 2006; Hong and Stambrook, 2004). In mouse ES cells two main pathways that become activated after DNA damage and lead to G_1/S checkpoint activation in somatic cells, namely ATM-CHEK2-CDC25A and ATM-TTP53-CDKN1A, are compromised (Hong and Stambrook, 2004). Mouse ES cells mis-localize and fail to activate CHEK2, do not express CDKN1A, and respond to DNA damage with high levels of apoptosis (Aladjem et al. 1998; Hong and Stambrook 2004; Chuykin et al. 2008). In addition, conflicting reports of TP53 localization and activity have been described in mouse ES cells in response to DNA damage. It has been demonstrated that mouse ES cells do not activate TP53-dependent DNA damage responses, undergo TP53-independent apoptosis in response to ionizing radiation, and do not translocate TP53 to the nucleus after DNA damage (Aladjem et al., 1998; Hong and Stambrook, 2004). Other report however, has stated that after irradiation TP53 induces differentiation of mouse ES cells by suppressing NANOG expression through direct binding to the *NANOG* promoter (Lin et al., 2005), implying that TP53 is successfully translocated to the nucleus.

In this study we examined the events in the ATM kinase dependent checkpoint signaling pathway and cell cycle arrest in human ES cells following exposure to two grays of γ-radiation. We demonstrated phosphorylation and localization of ATM at the sites of DNA DSB, as well as phosphorylation and nuclear localization of ATM downstream targets, CHEK2 and TP53, similar to that in irradiated human somatic cells. We further showed that irradiated human ES cells arrest in G_2/M, but not in the G_1/S phase of the cell cycle. We used the ATM-specific inhibitor KU55933 to evaluate the role of ATM in effecting this G_2/M arrest. Checkpoint signaling in irradiated human ES cells was inhibited using KU55933, but only at concentrations ten fold higher than that necessary to inhibit ATM function in somatic cells. Inhibition of ATM function compromised G_2/M arrest in human ES cells, and irradiated cells proceeded to mitosis in the presence of KU55933.

3.3   RESULTS

3.3.1   Pluripotency and radiosensitivity in human embryonic stem cells

Both mouse and human ES cells have been reported to reduce the expression of NANOG and differentiate in response to DNA damage (Lin et al., 2005; Qin et al., 2007). In order to confirm the populations of cells that we were studying were pluripotent human ES cells, we followed the expression of the pluripotency transcription factors *NANOG* and *POU5F1* by quantitative PCR (Figure **1**A), Western blot (Figure **1**B, 1C) and immunocytochemistry (Figure **1**D, E) for 24 hours following two grays irradiation. Additionally, we examined the cell surface markers CD9 (Figure **1**A), and SSEA4 (Figure **1**F). We observed that the mRNA levels for *CD9, NANOG* and *POU5F1* decreased relative to non-irradiated cells six hours following irradiation, similar to what has been described in mouse and human ES cells previously (Lin et al., 2005; Qin et al., 2007) (Figure **1**A). However, when we continued to follow human ES cells at later time points, the mRNA levels returned to those values observed in non-irradiated cells by 24 hours post irradiation. We did not detect a similar decrease in the protein level of NANOG and OCT4 (Figure **1**B). In accordance with the Western blot results, OCT4 (Figure **1**C), NANOG (Figure **1**D), and SSEA4 (Figure **1**E) were detected in human ES cells prior to and following irradiation by immunocytochemistry. Additionally, we exposed human ES cells to one gray of ionizing radiation, and left them to recover for one, two, four and six days post irradiation. At the given time points we collected floating cells and adherent cells separately, and analyzed expression of NANOG and OCT4 by Western blot (Figure **1**C). We discovered there was no change in the expression of NANOG and OCT4 in the adherent cells during one week recovery following one gray of radiation. However, in the population of floating cells, the expression of NANOG and OCT4 was completely lost. Furthermore, when we irradiated human ES cells with one Gy, left them to recover for six days, and inject them into immunocompromised mice, teratomas composed of three germ layers were formed (Figure 2).

Following exposure to five grays of ionizing radiation, large holes began appearing in the colonies within six hours (Figure **1**D, Figure 3A, right). To determine if this was cell death, as previously reported for ES cells

(Aladjem et al., 1998; Hong and Stambrook, 2004; Qin et al., 2007), or a detachment of cells from the substrate, we performed a Western blot for cleaved caspase-3 (Figure 3B) and flow cytometry for Annexin V and propidium iodide (PI; Figure 3C) following exposure to two grays of γ-radiation. Cleaved caspase-3 began appearing in the samples four hours after irradiation and continued to increase for at least 24 hours. A marked increase in percentage of cells positive for Annexin V and doubly positive for propidium iodide was observed eight hours following irradiation. This finding confirms that the observed loss of cells was due to cell death, most likely via apoptosis. We also noted a change in size of the cells. We believe this is not due to differentiation, as demonstrated by maintenance of pluripotency markers, but rather the result of human ES cells expanding into space freed by the cell death.
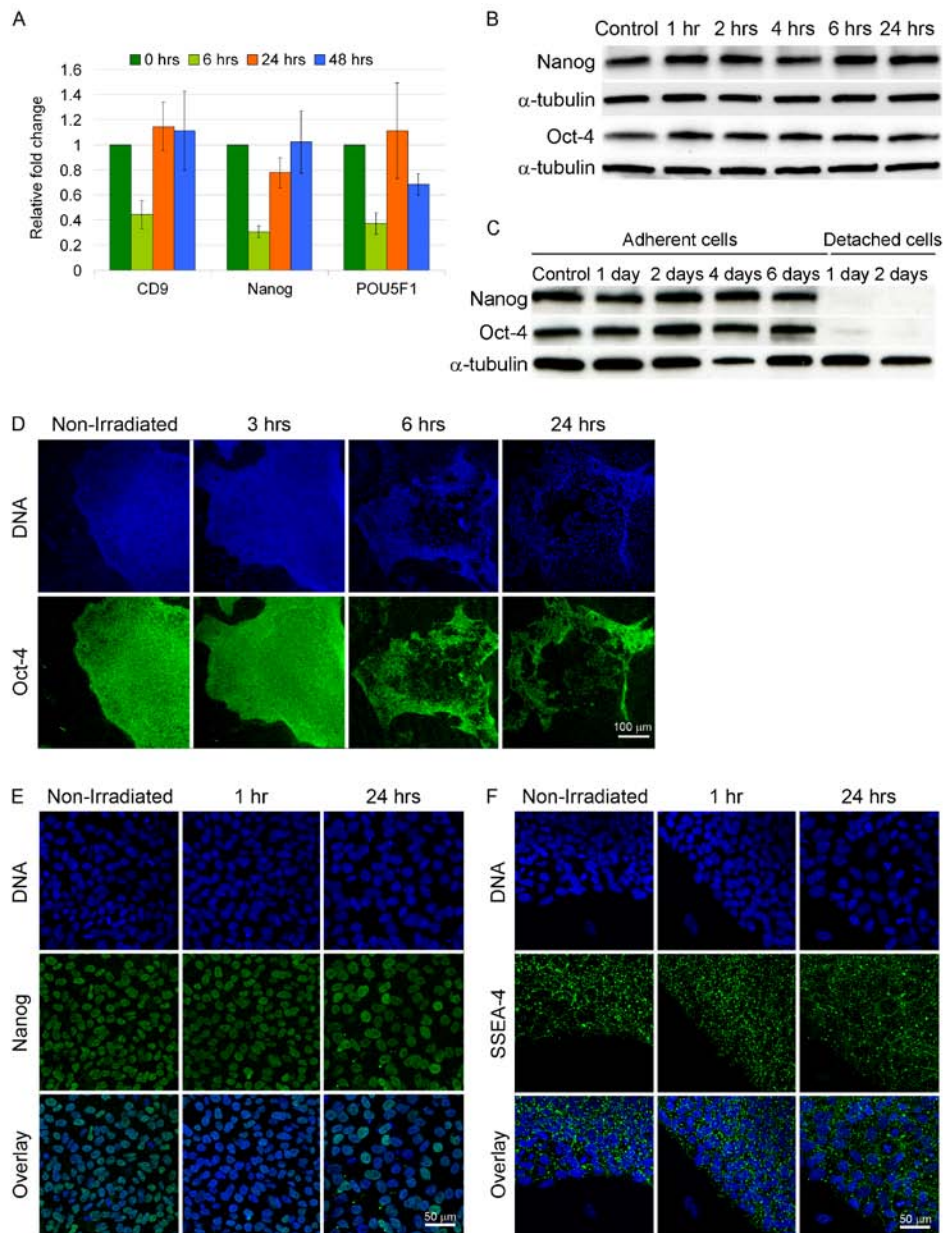
Figure 1: Pluripotency of irradiated human embryonic stem cells.
(A): Human ES cells were irradiated, or left untreated, and allowed to recover for the indicated time periods prior to collection. Total RNA was isolated and the expression of pluripotency markers *CD9, NANOG* and *POU5F1* analyzed by TaqMan® human stem cell pluripotency array. The mRNA fold changes were calculated using the -ΔΔCt method and normalized using *ACTB* as endogenous control. The results in non-irradiated cells were normalized to one, and the value in irradiated cells was calculated in respect to this. (B): Western blot analysis of NANOG and OCT4 protein levels following the irradiation of human ES cells. (C): Protein level of NANOG and OCT4 in human ES cells that were irradiated with one gray of γ-irradiation and left to recover for the indicated periods of time. Whole cell lysates of adherent and floating cells were collected separately and analyzed by Western blot. α-tubulin served as the loading control. Confocal microscopy for (D): OCT4, (E): NANOG, and (F): SSEA4 in human ES cells at indicated time points after irradiation. Bar = 100μm (D), 50μm (E, F).
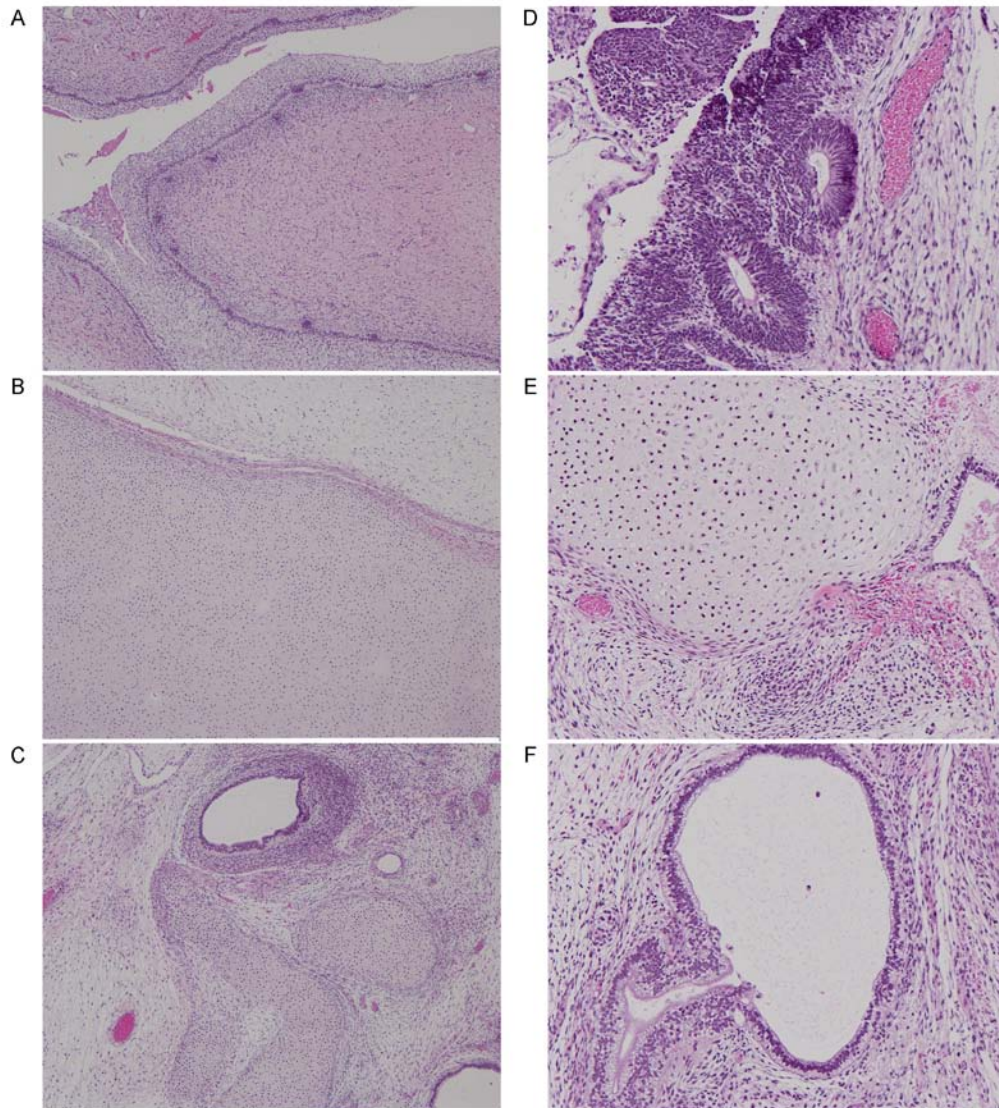
Figure 2: Pluripoterncy of irradiated human embryonic stem (ES) cells.
One week after irradiation with one Gy human ES cells were injected into mice and three months later teratomas comprised of ectoderm (A, D), mesoderm (B, E), and endoderm (C, F) developed. (A): developing skin with sensory patches, (B) developing cartilage, (C) developing gastro-intestinal tissue, with examples of cartilage, (D): developing neuronal rossetes with surrounding blood vessels. (E): maturing cartilage with surrounding periosteum, (F): maturing gastro-intestinal epithelium.
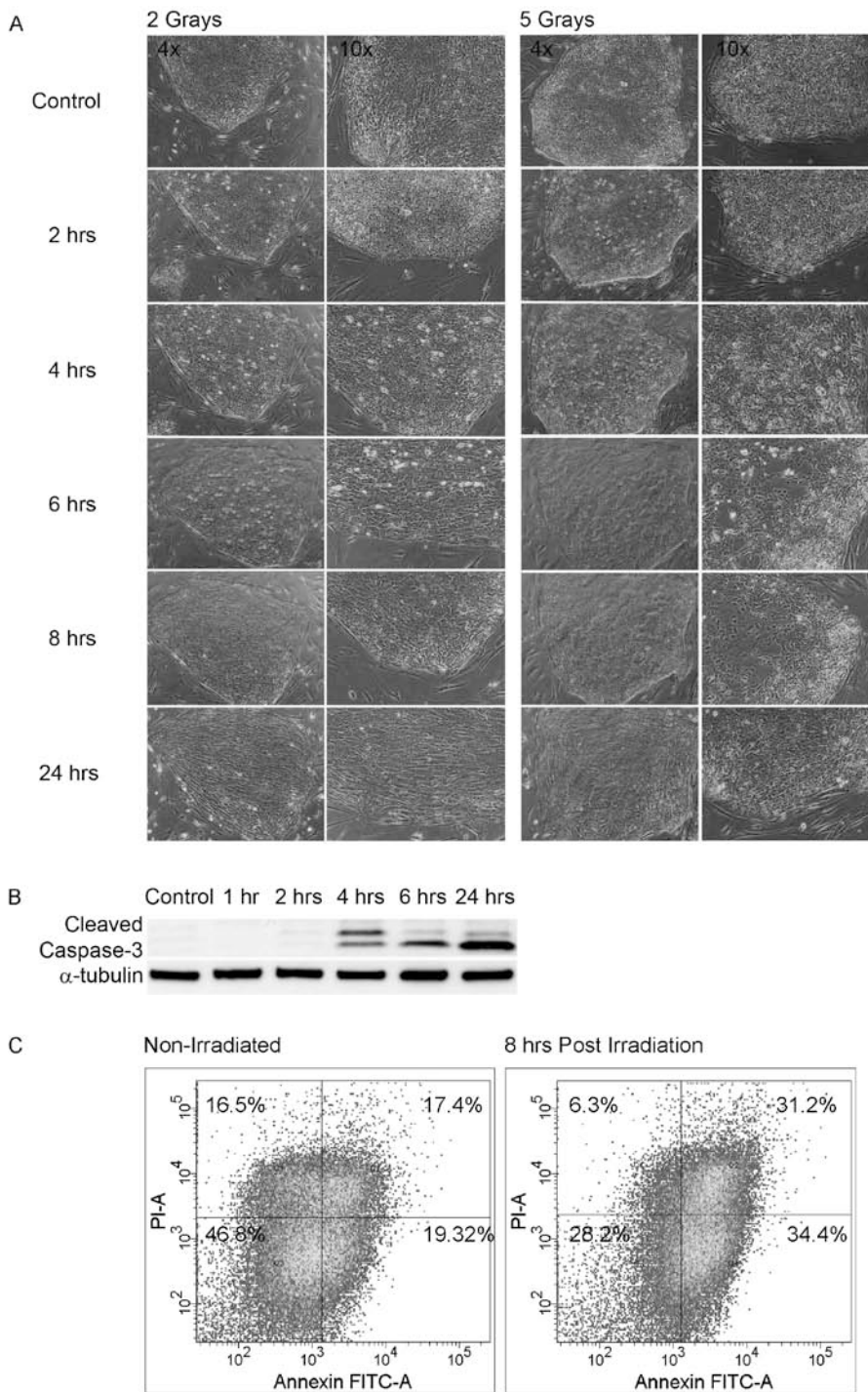
Figure 3: Radiosensitivity of human embryonic stem cells.
(A): Phase contrast imaging of irradiated and non-irradiated human ES cells at the indicated time points. (B): Western blot analysis for cleaved caspase-3 following irradiation. α-tubulin served as the loading control. (C): Flow cytometry for Annexin V-FITC and PI of non-irradiated cells and eight hours post irradiation of human ES cells.

3.3.2 ATM activation in human embryonic stem cells

ATM kinase activation is one of the earliest and most sensitive responses to DNA damage in irradiated cells (Abraham, 2001). Following γ-irradiation ATM is recruited to the sites of DSB, where it becomes activated through autophosphorylation at serine 1981 (Bakkenist and Kastan, 2003). We investigated ATM phosphorylation at this residue by Western blot (Figure 4A). Phosphorylation of ATM at serine 1981 was detected in human ES cells one hour following exposure to two grays of γ-radiation. High levels of this phosphorylation were maintained until four hours following irradiation, at which point the levels declined, but remained above steady state for at least 24 hours. During the same time frame, the level of total ATM protein did not change. Localization of ATM to the sites of DNA DSB was investigated by co-localization with the DNA DSB marker, γ-H2AX (Figure 4B).
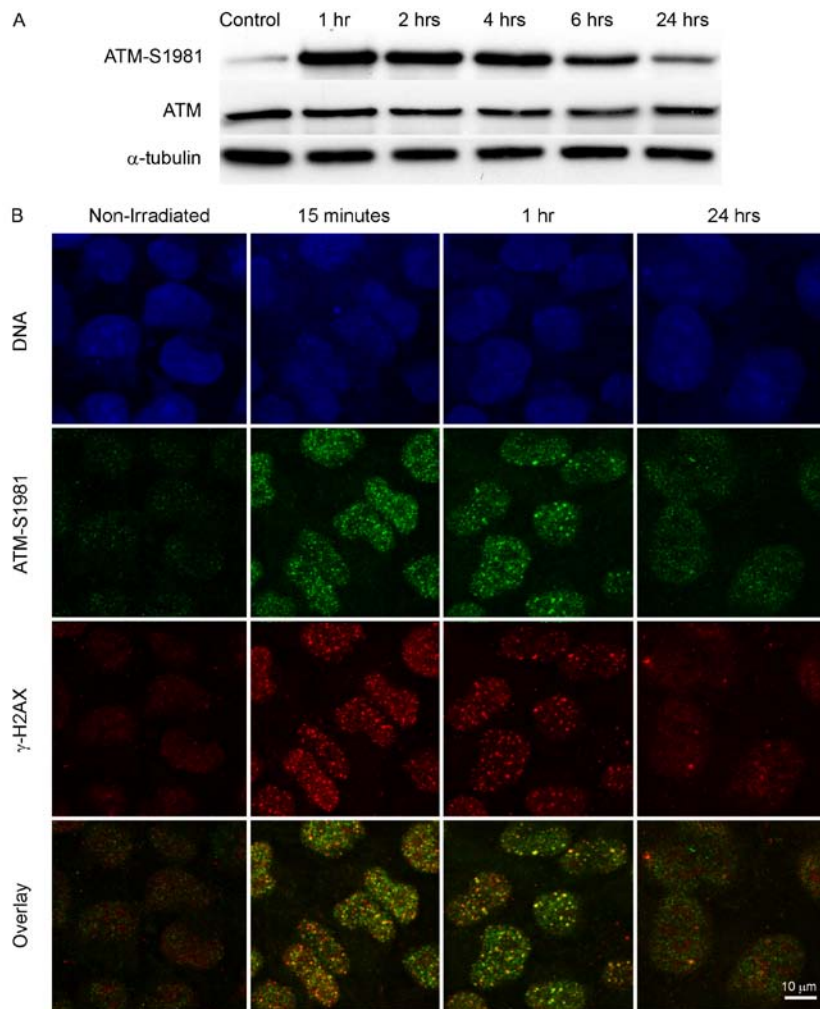
Figure 4: ATM autophosphorylation and localization in human embryonic stem cells.
(A): Western blot of ATM-serine 1981 and total ATM at the indicated time points following γ-irradiation. α-tubulin served as the loading control. (B): ATM-serine 1981 localizes to the sites of DNA DSB after irradiation, demonstrated by co-localization with a marker of DSB, γ-H2AX. Blue – DNA, Green – ATM-serine 1981, Red – γ-H2AX, Yellow – Co-localization. Bar = 10μm.

Phosphorylated ATM was detected only weakly in non-irradiated cells, but ATM-serine 1981 co-localized with γ-H2AX foci 15 minutes after irradiation. The number of γ-H2AX foci increased immediately following irradiation and returned close to basal levels within 24 hours. Furthermore, we double labeled cells for ATM-serine 1981 and NANOG and analyzed them by confocal microscopy (Figure 5), confirming that the ATM response occurs in pluripotent (NANOG-positive) human ES cells. Human ES cells are known to cycle rapidly through the growth phases following passaging and to decrease proliferation as they approach the next passage. We performed immunocytochemistry for ATM-Ser1981 and NANOG on day four and day seven following passaging to ensure that the kinetics of ATM signaling was not dependent on the cells' growth phase. The kinetics of ATM activation was identical in both cases, as is observed in Figure 5.
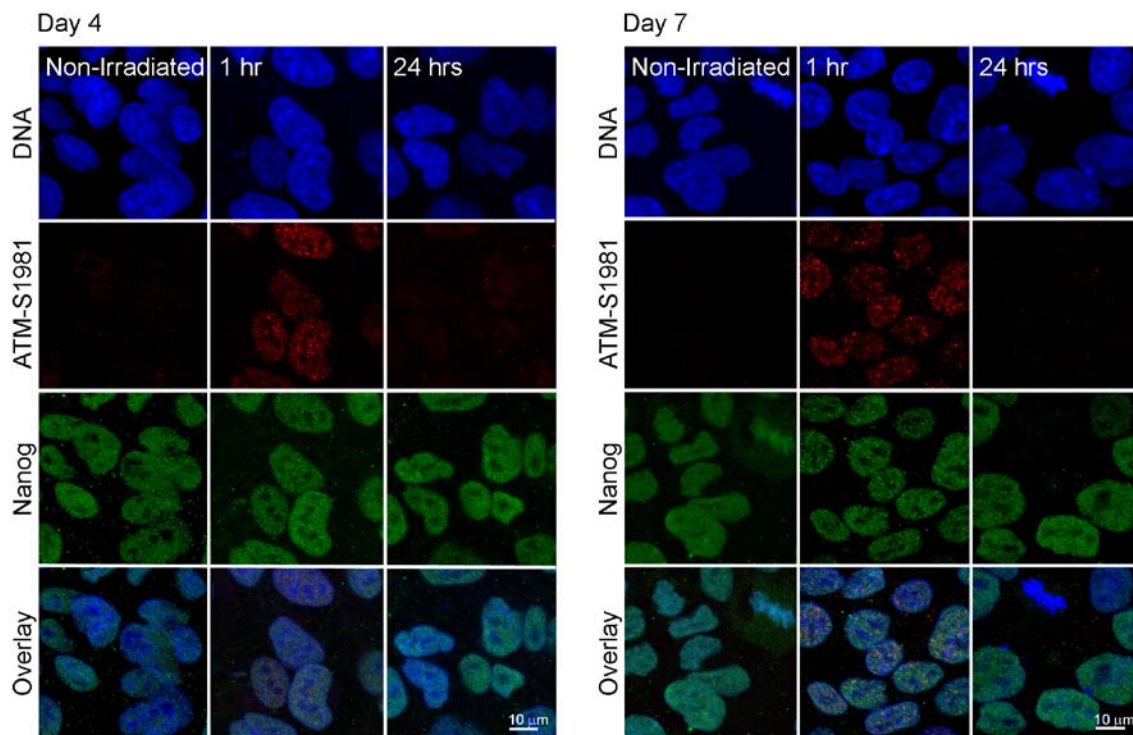
Figure 5: ATM activation in pluripotent human embryonic stem cells.
Double labeling of human ES cells with NANOG and ATM-serine 1981. Blue – DNA, Green – NANOG, Red – ATM-serine 1981. Bar = 10μm.

3.3.3 Activation of ATM downstream targets in human embryonic stem cells

Activated ATM phosphorylates numerous substrates at the sites of DSB, activating downstream signal transducers (Banin et al., 1998; Canman et al., 1998; Matsuoka et al., 2000; Melchionna et al., 2000). Phosphorylation of CHEK2 and TP53 is essential for induction of checkpoint arrest, whereas phosphorylation of NBS1 facilitates formation of MRE11/RAD50/NBS1 foci that are implicated in DNA repair (Carney et al. 1998). We monitored the phosphorylation of these ATM targets by Western blot analysis using phospho-specific antibodies (Figure 6). Phosphorylation of CHEK2 at threonine 68 (Figure 6A) was maximal one hour following irradiation and rapidly

declined thereafter, so that only a small fraction was still phosphorylated at six hours. The level of total CHEK2 did not change over the same time course. NBS1 phosphorylation at serine 343 (Figure 6A) followed a similar time course, peaking one hour after irradiation and returning to control levels by 24 hours. Again, there was no change in total protein level during this time frame.
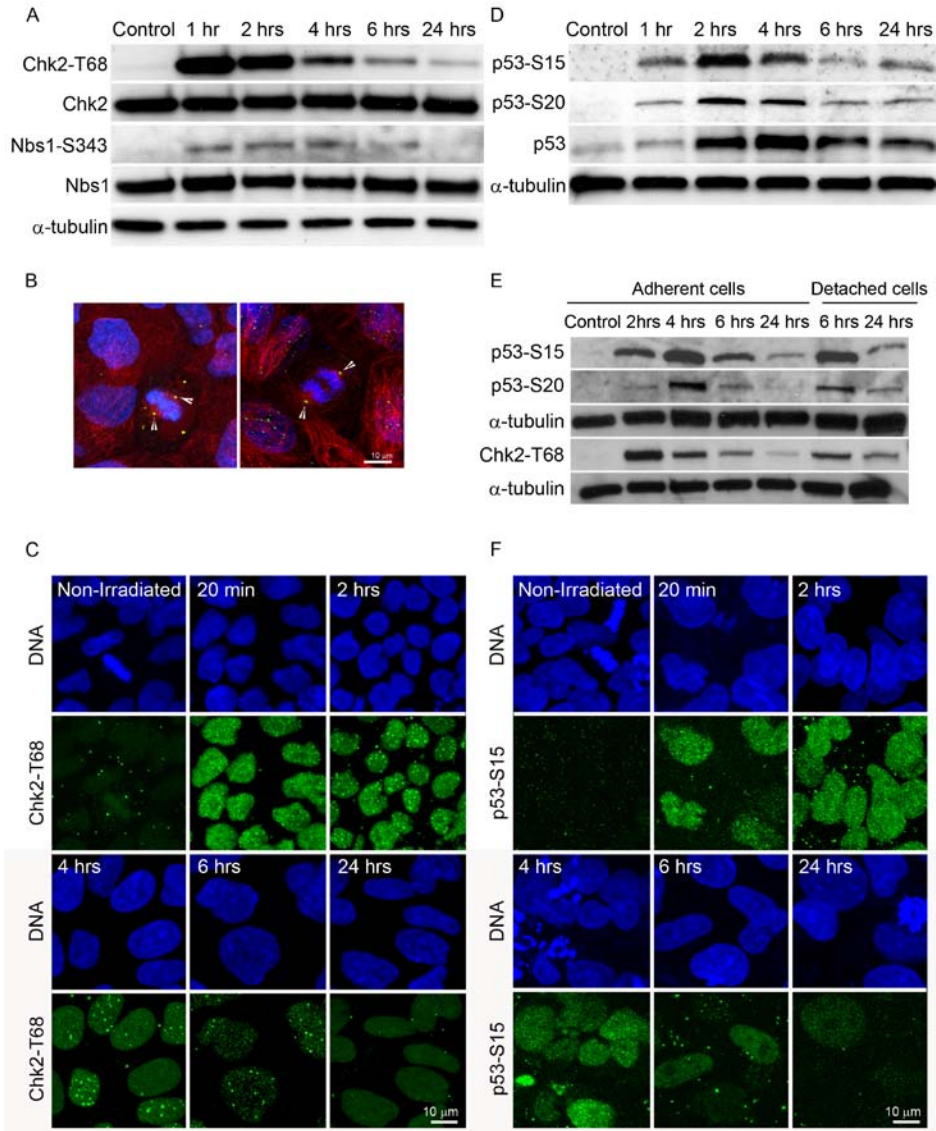
Figure 6: Phosphorylation and localization of CHEK2 and TP53 in human embryonic stem cells.
(A): Western blot of CHEK2-threonine 68, total CHEK2, NBS1-serine 343, and total NBS1. (B): Time-course immunocytochemistry of CHEK2-threonine 68 following irradiation of human ES cells. (C): Confocal microscopy of CHEK2-threonine 68 revealing its centrosomal location (arrowheads) in non-irradiated human ES cells. Blue – DNA, Green – CHEK2-threonine 68, Red – β-tubulin. Bar = 10μm. (C): Western blot of TP53-serine 15, TP53-serine 20, and total TP53. (D): Confocal microscopy of TP53-serine 15 following radiation treatment. α-tubulin served as the loading control for Western blots. Blue – DNA, Green – TP53-serine 15. Bar = 10μm.

Canonically, CHEK2 is activated at DNA DSB by a mechanism that requires ATM kinase dependent phosphorylation on threonine 68 (Matsuoka et al., 2000), and localizes diffusely throughout the nucleus of the irradiated somatic cells (Lukas et al., 2003). In contrast to observations in somatic cells, phosphorylated CHEK2 has been described to localize to the centrosomes of mouse ES cells (Hong and Stambrook, 2004). We have also observed localization of CHEK2-threonine 68 to the mitotic spindle poles in non-irradiated human ES cells (Figure 6B). However, phosphorylated CHEK2 was detected in the nucleus 20 minutes after irradiation of human ES cells (Figure 6C), unlike published reports in mouse ES cells (Hong and Stambrook, 2004). Levels detected by immunocytochemistry followed a similar time course to those observed by Western blot analysis, with nuclear levels decreasing rapidly after two hours.

Both ATM and CHEK2 kinases phosphorylate and thereby stabilize and activate TP53. ATM phosphorylates TP53 at serine 15 (Banin et al. 1998; Canman et al. 1998), whereas CHEK2 phosphorylates TP53 at serine 20 in response to activation by ATM (Hirao et al. 2000; Shieh et al. 2000). We examined phosphorylation of these serine residues following irradiation using Western blot analysis (Figure 6D). Non-irradiated human ES cells had no detectable TP53 phosphorylated at serine 15 or serine 20, but within one hour of irradiation, phosphorylation of serine 15 and serine 20 was detected, reached maximal levels by two hours, declined thereafter, remaining elevated above baseline for 24 hours. The level of total TP53 also increased after irradiation (Figure 6D) most likely due to TP53 stabilization following its phosphorylation (Chehab et al., 1999; Tibbetts et al., 1999). We also analyzed the phosphorylation of CHEK2 and TP53 in detached, presumably dying, human ES cells six and 24 hours after irradiation (Figure 6E). We observed the response in detached cells is in accordance with the response of adherent cells at these time points post irradiation.

Conflicting results regarding TP53 subcellular localization have been reported in mouse and human ES cells (Aladjem et al. 1998; Hong and Stambrook 2004; Lin et al. 2005; Qin et al. 2007; Chuykin et al. 2008). Our data show that TP53-serine 15, detected using two different TP53-serine 15 antibodies, is nuclear in two human ES cell lines (WA07, and WA09 not shown) following irradiation, by both immunocytochemistry (Figure 6F) and immunohistochemistry (Figure 7). Our results demonstrate that non-irradiated human ES cells have no detectable nuclear staining for phospho-TP53. Twenty minutes after irradiation, both the number of TP53-positive nuclei and the intensity of staining increased, peaked at two hours, and declined thereafter, similar to Western blot results (Figure 6D). Localization of TP53 to the nucleus followed a dose dependency, as higher levels of radiation induced a stronger response when examined at the same time point (three hours; Figure 8). Human ES cells were irradiated with 0, 2, 5, 7, 9, and 30 grays, and fixed three hours post irradiation. Immunohistochemistry demonstrates very faint nuclear staining for TP53-serine 15 in non-irradiated cells. Following increasing doses of irradiation the number of TP53-serine 15 positive nuclei and the intensity of staining increase at this time point. In addition, cell death becomes more prominent, and spaces between cells begin to appear at five grays, and holes in the colonies at seven grays.
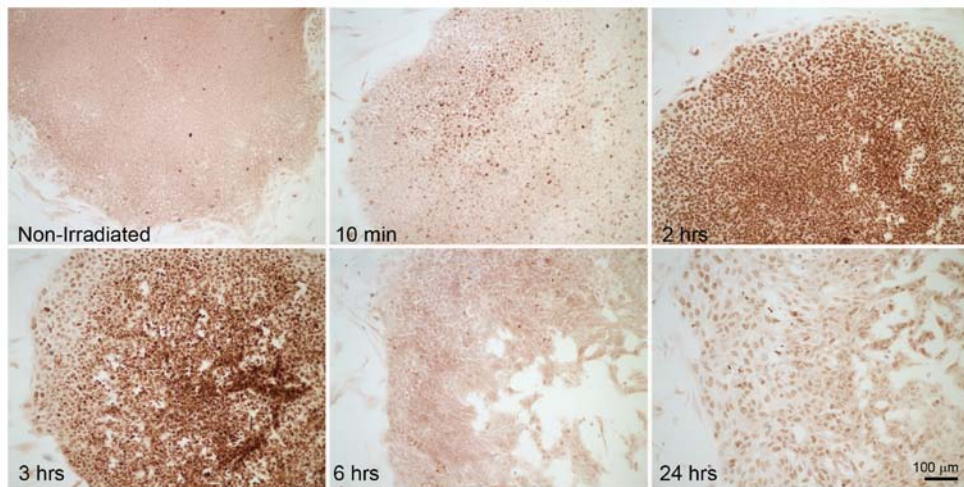
Figure 7: Localization of TP53-serine 15 to the nuclei of irradiated human embryonic stem (ES) cells.
Immunohistochemistry for TP53-serine 15. Note that six hours post irradiation holes in the colony appear, supporting the earlier observation of human ES cell sensitivity to irradiation. Bar = 100μm.
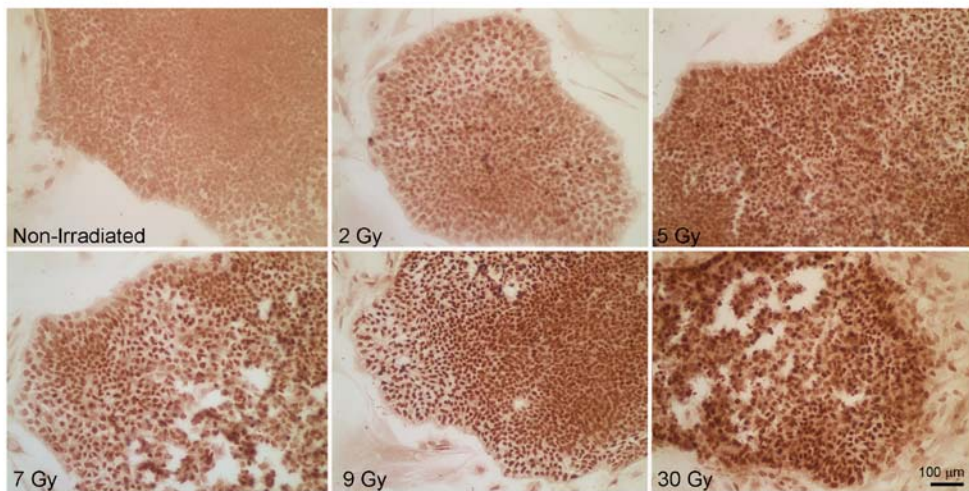
Figure 8: Dose-dependent TP53-serine 15 response in human ES cells.

3.3.4   Cell cycle arrest following irradiation in human embryonic stem cells

We next investigated whether human ES cells halt progression through the cell cycle in response to γ-irradiation. We compared the proliferation of the human ES cells on day five and day seven after passaging, and observed that the cells remain actively proliferating on the later day of the cell culture (Figure 9). Therefore, for the following studies we used cells on the later day of the cell culture.

	5 days	7 days
G_1/G_0	20.0%	25.8%
S	57.9%	53.9%
G_2/M	22.0%	20.1%
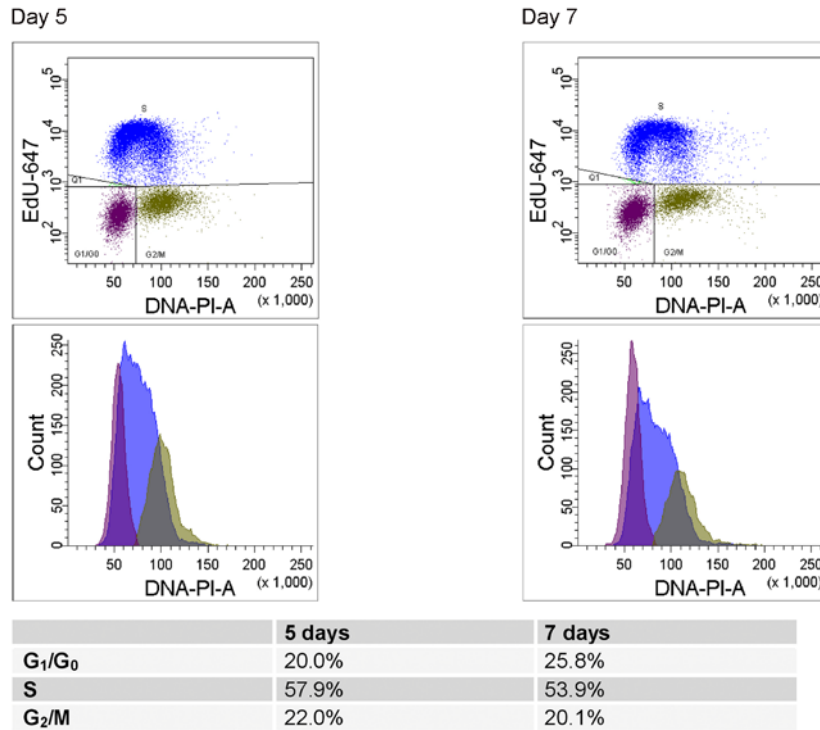
Figure 9: Human embryonic stem cell proliferation.
Human ES cells are actively proliferating on day five and day seven after passaging. Human ES cells were labeled with EdU 30 minutes prior to harvesting on day five (left) and day seven (right) after passaging. Cells were collected, stained for EdU and PI, and analyzed by flow cytometry. Dot plots (top) represent EdU fluorescence versus DNA content determined with PI. Following gating, the G_1, S, and G_2/M phase cells were depicted on the DNA histograms (bottom). The table represents the percentage of cells in each stage of the cell cycle on day five and day seven after passaging.

In order to assess the cell cycle profile of irradiated human ES cells, we performed flow cytometric analysis of DNA content using PI (Figure 10A). Similar to non-human primate (Fluckiger et al., 2006) and mouse (Hong and Stambrook, 2004) ES cells, irradiated human ES cells arrested in G_2/M phase of the cell cycle. The percentage of cells in G_1 was significantly reduced four hours following irradiation, and essentially no cells were detected in G_1 eight hours after irradiation. Human ES cells returned to the cell cycle 16 hours post irradiation indicated by a decrease in the percentage of cells in G_2/M between 16 and 20 hours (Figure 10A). By 48 hours the cell cycle distribution closely resembled non-irradiated cells.

In order to further understand the events that occurred following release from cell cycle arrest, we performed immunostaining with the mitosis-specific marker histone H3-serine 10 (Figure 10B).   Twenty minutes after irradiation, cells continued to divide and these mitotic figures were indistinguishable from controls (Figure 10B). Two hours following irradiation, no histone H3-serine 10 positive cells were detected, suggesting that cells were arrested in G_2 phase. Similarly, six hours following irradiation, no dividing cells were observed and there was a considerable amount of cell death. Mitotic figures began to be detected 20 hours after irradiation, indicating that cells returned to the cell cycle. We determined the mitotic indexes prior to, and 24 hours post irradiation (Figure 10C, right). There was no significant difference in quantified mitotic index between non-irradiated (3.91±0.50%)

and irradiated ($3.57 \pm 0.37\%$, $0.5 < p < 0.7$, n=3) cells, but a high percentage of cells entering mitosis 24 hours after irradiation displayed aberrant mitotic spindles (Figure 10D, Materials and Methods). The presence of aberrant mitotic figures, including anaphase bridges, multipolar spindles, lagging and misaligned chromosomes, was elevated to $414.51 \pm 45.98\%$, in comparison to non-irradiated cells ($100 \pm 38.86\%$, $p < 0.001$, n=3; Figure 10C, left).
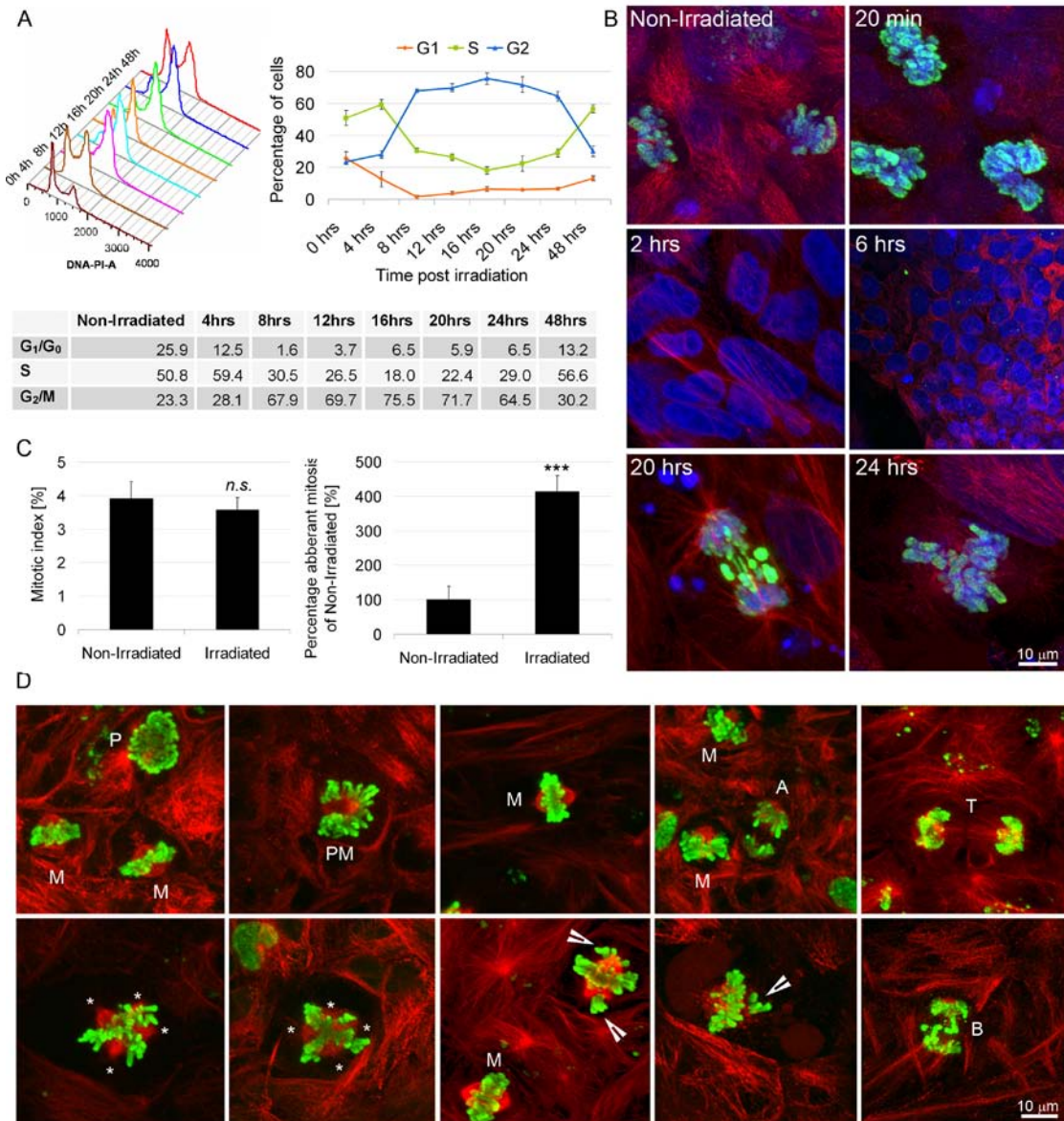
Figure 10: Cell cycle analysis of irradiated human embryonic stem cells.
(A): Analysis of DNA content of human ES cells after irradiation by flow cytometry using PI; left panel: cell cycle profiles, as measured 0-48 hours after irradiation of human ES cells; right panel: percentages of cells in G_1, S and G_2/M as a function of time following irradiation. Percentages were calculated using ModFit software (Verity Software house, Topsham, ME). Results were gated to exclude cellular debris, sub G_0 population, and doublets. Data presented are means ± SEM calculated from three independent experiments. The table represents the percentage of cells in each stage of the cell cycle after irradiation. (B): Histone H3-serine10 time course immunocytochemistry in irradiated human ES cells. (C): Left panel: Quantification of mitotic indexes in non-irradiated cells and 24 hours post irradiation. Human ES cells were irradiated, or left untreated and fixed 24 hours later. Coverslips were stained with histone H3-serine10 antibody and the percentage of histone H3-serine10 positive

(mitotic) cells was determined. The data represent mean ± SEM from three independent experiments. At least 1000 cells were analyzed per condition in each experiment. Statistical significance was determined by Chi-Square test. *n.s.* – not significant. Right panel: Quantification of percentage of aberrant mitotic figures in non-irradiated and irradiated human ES cells. Cells were treated as in left panel, and assayed for the presence of aberrant mitotic figures. Three independent experiments were performed, and at least 100 mitotic figures were analyzed per condition in each experiment. The result in non-irradiated cells was normalized to 100%, and the value in irradiated cells was calculated in respect to this. Statistical significance was determined by Chi-Square test. *** *p*<0.001. (D): Examples of normal (top row) and aberrant (bottom row) mitotic figures visualized by confocal microscopy. P – prophase, PM – prometaphase, M – metaphase, A – anaphase, T – telophase, B – anaphase bridge, asterisk – poles of mitotic spindle, arrowheads – misaligned chromosomes. Blue – DNA, green – histone H3-serine 10, red – β-tubulin. Bar = 10μm.

We assayed the expression of G_1/S cell cycle regulators – retinoblastoma (RB) tumor suppressor and CDKN1A (Figure 11). Retinoblastoma protein is a negative regulator of G_1 to S cell cycle transition, and has been reported to be in its inactive, hyperphosphorylated, form in the mouse ES cells (Savatier et al., 1994). CDKN1A is essential negative regulator of the cyclin dependent kinase 2 (CDK2) that is under TP53 transcriptional control, and whose expression is stimulated following DNA damage. Mouse ES cells have been shown to lack induction of Cdkn1A that explains the absence of the G_1/S cell cycle arrest in these cells (Hong and Stambrook, 2004). We determined the level of RB protein phosphorylated at several serine residues – serine 790, serine 795, and serine 807/811. We found that RB is phosphorylated at these residues at all investigated time points following irradiation, suggesting that it remains in its inactive and cell cycle permissive form (Figure 11). The induction of CDKN1A protein level was very weak, suggesting that it may be insufficient to maintain G_1/S arrest (Figure 11B).
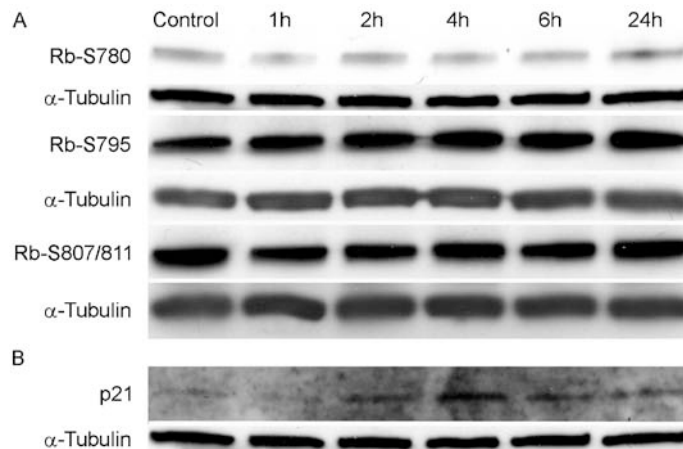
Figure 11: Protein level of G_1 cell cycle regulators in human embryonic stem cells.
(A): Western blot of RB-serine 790, RB-serine 795, and RB-serine 807/811. (B): Western blot of CDKN1A. α-tubulin served as the loading control for Western blots.

The appearance of mitotic cells 16-20 hours after irradiation can be explained 1) by arrested cells reentering the cell cycle, or 2) by cells that were in the very early stages of G_1 reaching mitosis 16-20 hours after irradiation and never arresting. We performed a pulse chase experiment in which we labeled human ES cells with a thymidine analogue, 5-ethynyl-2'-deoxyuridine (EdU) for 30 minutes just prior to irradiation in order to distinguish between these two possibilities. EdU was washed out following the 30 minute pulse, cells were collected at 4, 8, 16 and 24 hours post irradiation, and analyzed by flow cytometry (Figure 12). The pulse only labeled the human ES

cells in S phase at the time of irradiation. Eight hours after irradiation, these cells have clearly moved into the G_2/M phase of the cell cycle. At 16 hours, the first G_1 cells which stain for EdU are observed, indicating that arrested cells have undergone mitosis. Additionally, in the dot plot it is observed that the G_1 population has a lower EdU signal, as would be expected after mitosis.
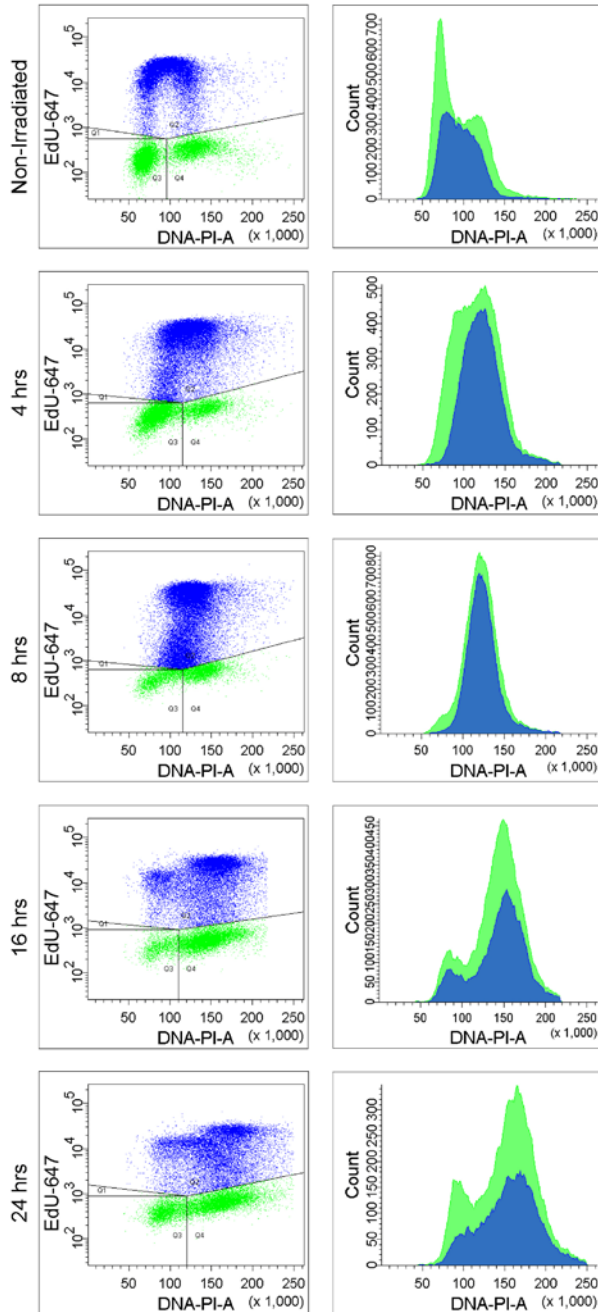
Figure 12: Human embryonic stem cells resume the cell cycle following irradiation induced G_2/M arrest.
Human ES cells were pulse labeled with EdU prior to irradiation, exposed to two grays of γ-radiation, and left to recover for 4, 8, 16, and 24 hours, without addition of EdU. At indicated time points following irradiation, human ES cells were collected, stained for EdU and propidium iodide, and analyzed by flow cytometry. Dot plots (left) represent EdU fluorescence versus DNA content determined with PI. Following gating, the EdU-positive cells (blue) were plotted together with the single cells (green) on DNA histograms (on the right). Note that EdU-positive

cells are cells that were in the S phase at the time of irradiation, and do not necessarily represent S-phase cells at any of the time points following irradiation.

3.3.5 ATM is required for the G$_2$/M arrest in human embryonic stem cells

In order to test if ATM signaling is necessary for G$_2$/M arrest, we inhibited ATM kinase using the ATM-specific inhibitor KU55933 (Hickson et al. 2004). To the best of our knowledge, KU55933 inhibits ATM kinase activity in all somatic cells examined to date, when added to the cell culture medium at a concentration of 10 μM (Hickson et al., 2004; White et al., 2008). However, our titration experiments revealed that this dose is only partially effective in human ES cells, and that 100 μM is needed to inhibit ATM signaling (Figure 13A). ATM phosphorylation and activity are maximal one hour after irradiation, thus, we titrated the concentration of KU55933 needed to inhibit the ATM function in human ES cells at this time point. We treated cells starting one hour prior to irradiation (minus one hour) until one hour post irradiation (plus one hour) with vehicle (DMSO), 10 μM, 50 μM and 100 μM KU55933. A dose-dependent decrease in the level of ATM-serine 1981, CHEK2-threonine 68, TP53-serine 15, and NBS1-serine 343 following the addition of increasing concentration of KU55933 confirmed inhibition of ATM signaling in irradiated human ES cells. Under the same treatment, the level of total ATM, CHEK2 and NBS1 did not change. Similarly, treatment with KU55933 dramatically reduced TP53 stabilization after irradiation.

In order to determine if ATM activation is necessary for G$_2$/M arrest, we performed histone H3-serine 10 immunocytochemistry and determined mitotic index two hours after irradiation in cells in which ATM kinase was inhibited. Human ES cells were treated starting one hour prior to irradiation (minus one hour) until two hours post irradiation (plus two hours) with vehicle (DMSO) or 100 μM KU55933, fixed and stained with histone H3-serine 10 antibody (Figure 13B). No significant difference in mitotic index was observed between non-irradiated cells treated with DMSO (2.85±0.53%) and KU55933 (2.60±0.21%, 0.3<p<0.5, n=3; Figure 13C). However, two hours after irradiation, KU55933 treated cells had higher mitotic index (1.35±0.34%) than DMSO treated cells (0.16±0.02%, p<0.001; Figure 13C), suggesting that ATM function is required for functional G$_2$/M arrest in human ES cells. However, even this high dose (100 μM) of ATM inhibitor did not completely restore the mitotic index in irradiated cells (1.35±0.34%) to the one detected in non-irradiated cells (2.60±0.21%).

Finally, we characterized mitotic cells that were observed following irradiation of KU55933 treated cells. The percentage of aberrant mitotic figures following irradiation of KU55933 treated cells was elevated (229.01±36.15%, p<0.001, n=3; Figure 13D) compared to KU55933 treated non-irradiated cells (100±4.56%). The most prevalent type of mitotic error was anaphase bridges. We did not observe a statistically significant difference in the frequency of aberrant mitotic figures between vehicle (78.03±22.44%) and KU55933 (100±4.56%, p>0.1, n=3) treated non-irradiated cells.
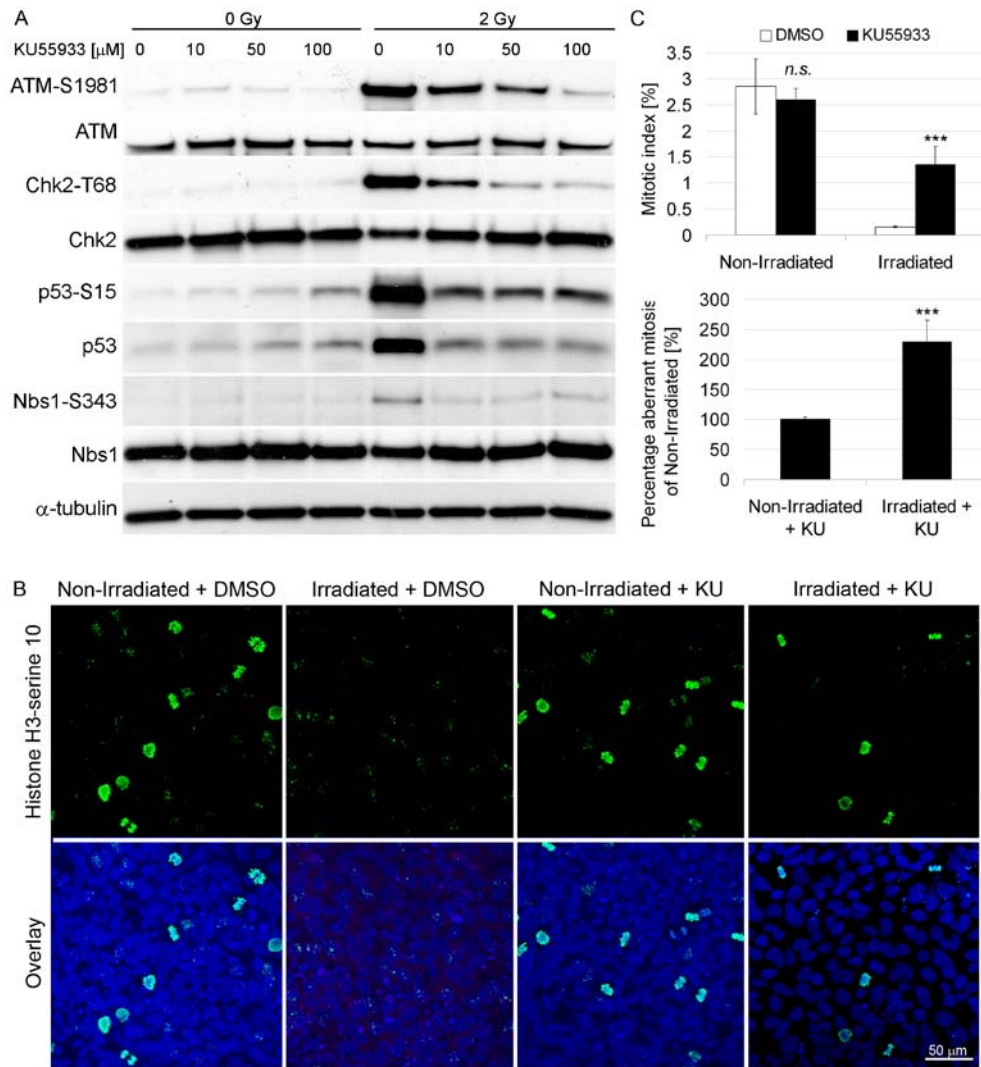
Figure 13: Inhibition of ATM signaling with KU55933 in human embryonic stem cells.
(A): Western blot for ATM-serine 1981, ATM, CHEK2-threonine 68, CHEK2, TP53-serine 15, TP53, NBS1-serine 343, and NBS1 in human ES cells. Human ES cells were pretreated with vehicle (DMSO) or 10 μM, 50 μM, and 100 μM KU55933 for one hour (minus one hour), irradiated, or left untreated, and harvested one hour later (plus one hour). α-tubulin served as the loading control. (B): Human ES cells were treated with vehicle (DMSO) or 100 μM KU55933 starting one hour before irradiation (minus one hour), irradiated, or left untreated, and fixed two hours later (plus two hours), stained for histone H3-serine10 and analyzed by confocal microscopy. (C): Quantification of mitotic indexes of KU55933 or vehicle treated non-irradiated and irradiated cells. Human ES cells were treated as in (B), and the percentage of mitotic cells was quantified two hours post irradiation. Three independent experiments were performed, and at least 1500 cells were analyzed per condition in each experiment. The data represents means ± SEM. Statistical significance was determined by Chi-Square test. *n.s.* – not significant; *** $p<0.001$. (D): Quantification of percentage of aberrant mitotic figures in KU55933 treated cells. Human ES cells were treated as in (A), and assayed for the presence of aberrant mitotic figures. The percentage of aberrant mitotic figures in non-irradiated KU55933 treated cells was normalized to 100%, and the value in irradiated KU55933 treated cells was calculated in respect to this. Three independent experiments were performed, and at least 100 mitotic figures were analyzed per condition in each experiment. Statistical significance was determined by Chi-Square test. *** $p<0.001$. Blue – DNA, green – histone H3-serine10. Bar = 50μm.

3.4   DISCUSSION

Several phenotypes associated with response of embryonic stem cells to DNA damage are: 1) they reduce expression of pluripotency factors (Lin et al., 2005; Qin et al., 2007), 2) they lack a G_1/S checkpoint (Fluckiger et al., 2006; Hong and Stambrook, 2004), and 3) they are extremely sensitive to DNA damaging agents resulting in cell death within several hours of exposure to DNA damaging agents (Aladjem et al., 1998; Hong and Stambrook, 2004; Qin et al., 2007). Additionally, a number of cell cycle regulatory proteins have been demonstrated to have aberrant functions in ES cells with sometimes conflicting results reported between laboratories. In this study, we sought to investigate the functioning of the ATM signaling cascade in human ES cells, including analysis of the cell cycle distribution after ionizing radiation. We found that ATM signaling is intact and that human ES cells activate and properly localize the checkpoint signaling proteins ATM, CHEK2 and TP53, resulting in a temporary G_2/M arrest before the cells resume mitosis. Furthermore, our results describe an essential role of ATM in induction of G_2/M arrest, as an ATM specific inhibitor, KU55933, inhibits this G_2/M arrest.

Firstly, we investigated the expression of pluripotency markers NANOG, OCT4, CD9, and SSEA4 after irradiation. Surprisingly, we found that the protein levels do not change over the 24 hour period following irradiation, suggesting that human ES cells remained pluripotent. This observation is in contradiction with reports of DNA damage induced differentiation of mouse (Lin et al., 2005) and human (Qin et al., 2007) ES cells. However, in these studies authors investigated the mRNA levels within six hours of irradiation. When we examined mRNA levels, we also observed a drop at six hours following irradiation. However, at 24 hours the levels returned to near that of controls.

Embryonic stem cells of different species show tremendous sensitivity to DNA damage and undergo extensive cell death within hours of DNA damage. In this paper, we demonstrated cell death within hours following exposure of human ES cells to two grays of γ-irradiation. Cleavage of caspase-3 was detected four hours after irradiation, and cell loss was visualized six hours post irradiation. Interestingly, human embryonal carcinoma (EC) cells display a higher survival rate following ionizing radiation, when compared to their differentiated counterparts (Wang et al., 2009). After confirming the radiosensitivity of human ES cells, we investigated checkpoint signaling and function in irradiated human ES cells.

ATM is rapidly activated in cells exposed to agents that induce DNA double strand breaks (Abraham, 2001). Cells deficient in ATM exhibit hypersensitivity to radiation and radiomimetic drugs, defective cell cycle arrest, increased chromosome breakage, and reduced TP53 response following irradiation (Rudolph and Latt, 1989; Taylor et al., 1979; Xu and Baltimore, 1996; Young and Painter, 1989). Cell cycle checkpoint defects include a diminished arrest in G_1, radioresistant DNA synthesis, and reduced arrest in G_2 (Rudolph and Latt, 1989; Xu and Baltimore, 1996; Young and Painter, 1989). In this study, we monitored the kinetics of ATM phosphorylation and localization to the sites of DNA DSB. Confocal microscopy revealed that ATM was phosphorylated and recruited to the DNA DSB in human ES cells within 15 minutes of irradiation. Phosphorylation of ATM and its target proteins CHEK2, TP53, and NBS1 reached maximum within the first hour of irradiation, suggesting activation of checkpoint signaling in human ES cells.

Hong and Stambrook (Hong and Stambrook, 2004) reported that CHEK2 is hyperphosphorylated and localized to the centrosomes in mouse ES cells rather than diffusely distributed in the nucleus, making it unavailable to act as a motile signal transducer. We also observed phosphorylated CHEK2 at the poles of mitotic spindle in non-irradiated human ES cells (Figure 6). However, in contrast to mouse ES cells, phospho-CHEK2 was mobilized to the nucleus of human ES cells within 20 minutes of irradiation. Centrosomal CHEK2 was detected in non-irradiated somatic cells as well, and mobilized to the nucleus in response to DNA damage (Zhang et al., 2007), in agreement with its canonical role as a mobile signal transducer. In addition, several proteins involved in DNA damage response, such as ATM (Oricchio et al., 2006; Zhang et al., 2007), ATR (Zhang et al., 2007), ATRIP (Zhang et al., 2007), CHEK1 (Kramer et al., 2004), TP53 (Ciciarello et al., 2001), and BRCA1 (Hsu and White, 1998) have been detected to associate with centrosomes during mitosis. Based on these emerging data, it has been suggested that centrosomes might have a functional role in DNA damage responses, serving either as "command centers" (Doxsey, 2001), where DNA damage response proteins come in close proximity and/or are sequestered from unfavorable interactions, or as a subject of DNA damage response (Loffler et al., 2006).

Conflicting results regarding TP53 localization have been reported in ES cells. Several groups have reported that TP53 is not translocated into the nucleus of mouse ES cells after DNA damage (Aladjem et al., 1998; Chuykin et al., 2008; Hong and Stambrook, 2004). In contrast, other data suggest that TP53 induces differentiation in mouse (Lin et al., 2005) and human (Qin et al., 2007) ES cells following DNA damage by binding to the *NANOG* promoter, and suppressing NANOG expression, implying that TP53 does translocate into the nucleus of ES cells following DNA damage. Our data demonstrate that TP53 is stabilized in irradiated human ES cells. The observation that both ATM kinase dependent TP53-serine 15, and ATM and CHEK2 dependent TP53-serine 20 phosphorylation are maximal two hours following irradiation, prior to maximal TP53 protein level four hours after irradiation, is consistent with a function of these two kinases in TP53 stabilization and activation. Furthermore, our results conclusively demonstrate that TP53 is nuclear in irradiated human ES cells.

Mouse (Hong and Stambrook, 2004) and non-human primate (Fluckiger et al., 2006) ES cells, as well as human EC cells (Wang et al., 2009), have been shown to lack DNA damage induced G_1 cell cycle arrest. Here we extend this finding to human ES cells. Flow cytometry revealed that irradiated human ES cells do not accumulate in G_1 but rather at the G_2/M stage of the cell cycle. However, this cell cycle arrest is temporary, and human ES cells re-enter the cell cycle approximately 16 hours after irradiation. Interestingly, in spite of the numerous similarities between ES and EC cells, human ES cells do not exhibit S phase delay as do human EC cells, and undergo G_2/M arrest much earlier in comparison to human EC cells.

Studies with histone H3-serine 10 immunocytochemistry demonstrated that human ES cells promptly cease mitosis, further indicating that cells are arresting in G_2. Twenty four hours following irradiation, a four fold higher proportion of mitotic figures appear aberrant in comparison to non-irradiated cells. It is unclear based on these results why aberrant mitoses are observed. It is possible that human ES cells resume cycling before all DNA damage is removed. However, this speculation is not supported by our γ-H2AX data, because the number of positive foci returns to near baseline levels by 24 hours. In addition, defective DNA DSB repair would increase DNA defects at mitosis such as chromosomal cross bridges. We do not observe this phenotype, and instead see

numerous types of defects including spindle pole abnormalities suggesting perhaps other cell cycle errors. Additional experiments will be required to discern the cause of these abnormal mitotic structures.

In order to determine if the observed accumulation of irradiated human ES cells in G_2 was ATM dependent, we employed a selective small molecule competitive ATM inhibitor, KU55933 (Hickson et al., 2004). KU55933 inhibits ATM kinase activity in all somatic cells examined to date when included into culture medium at a concentration of 10 μM (Hickson et al., 2004; White et al., 2008). Interestingly, we observed that a concentration of 100 μM KU55933 is necessary in human ES cells to inhibit ATM function, as determined by ATM-serine 1981, CHEK2-threonine 68, and NBS1-serine 343 phosphorylation, as well as TP53 stabilization. The partial inhibition of ATM kinase with 10 μM KU55933 is not due to insufficient time for inhibition, because White at al. (White et al., 2008) reported that ATM can be inhibited within five minutes of drug addition to the medium. It is of importance to note that even at 100 μM concentration KU55933 specifically targets ATM, and not other members of PI3K-related kinase family (Hickson et al., 2004). One possible explanation for this difference between human ES and somatic cells is high expression level of multi drug resistance proteins in ES cells, which could efficiently remove the drug from human ES cells. This is of particular importance for the potential use of KU55933 as a radiosensitizing drug in anti-cancer therapy, since an implication may be that cancer stem cells may not be radiosensitized with 10 μM KU55933.

We demonstrated an essential role of ATM in induction of G_2/M arrest in irradiated human ES cells. Following inhibition of ATM, we observed an escape of irradiated cells from G_2/M arrest. However, abrogation of the G_2/M checkpoint was not 100% effective, as the mitotic index two hours following irradiation of KU55933 treated human ES cells was not restored to the levels observed in non-irradiated KU55933 treated cells. Two explanations are possible for this observation: 1) ATM kinase activity and signaling are not completely inhibited with 100 μM KU55933, or 2) there are two independent checkpoint mechanisms in human ES cells. The observation that ATM kinase dependent phosphorylation of CHEK2, NBS1 and TP53 was entirely abrogated in 100 μM KU55933 treated irradiated human ES cells suggests that a second, ATM independent G_2/M checkpoint is operating in human ES cells. However, additional experiments will be required in order to identify this mechanism.

Finally, we characterized the cells that escape G_2/M arrest following KU55933 treatment, and enter mitosis two hours following irradiation. We detected two fold higher frequency of mitotic errors, in particular anaphase bridges, in comparison to KU55933 treated control cells. At this time point γ-H2AX foci are still numerous and DNA DSB are not completely removed; the presence of free chromosome ends provides conditions in which chromosome cross links and anaphase bridges can occur, explaining the high rate of mitotic errors in these conditions.

It is interesting that while ATM dependent signaling in human ES cells appears indistinguishable from that in human somatic cells, ATM dependent cell cycle arrest in G_1 phase does not occur in ES cells. Canonically, maintenance of G_1/S arrest is dependent upon up-regulation of CDKN1A by TP53. Mouse ES cells have been shown to lack this TP53-Cdkn1A axis (Hong and Stambrook, 2004), which explains the absence of G_1/S arrest in these cells. However, it is not clear whether human ES cells induce CDKN1A in response to DNA damage. Qin et al. reported the absence of *CDKN1A* gene up-regulation following UV irradiation, but noticed a two fold increase in

protein level (Qin et al., 2007). In contrast, Becker et al. demonstrated 250-300 fold induction of *CDKN1A* mRNA levels following irradiation with five grays of ionizing radiation (Becker et al. 2007). In our data, CDKN1A protein was undetectable in non-irradiated human ES cells, and we observed only weak induction of protein following two grays of γ-irradiation. Taken together, it is possible that human ES cells have extremely low basal levels of CDKN1A, and following DNA damage induce CDKN1A, but at levels that are insufficient to inhibit CDK2 activity in ES cells.

It has been suggested that the G_1 phase of the cell cycle is a time when ES cells are sensitive to differentiating cues from the environment, and that shortening of G_1 can protect ES cells from differentiation (Lukaszewicz et al., 2005; Mummery et al., 1987). Therefore, by escaping G_1/S arrest following DNA damage, ES cells might be reducing the risk of differentiation. Indeed, Maimets et al. recently demonstrated that activation of TP53 by nutlin induces rapid differentiation of human ES cells by promoting accumulation of cells in G_0/G_1 phase in CDKN1A dependent manner (Maimets et al., 2008). Another possibility is that ES cells prefer repairing DNA damage during G_2 when the sister chromatid is present allowing for error-free DNA repair by homologous recombination, rather than error prone non-homologous end joining. Under this hypothesis, cells that are in G_0/G_1 at the time when DNA damage is inflicted may undergo differentiation or apoptosis, and those cells that are in G_2 phase of the cell cycle would arrest and attempt repair of the damage. Further experiments need to be performed to test this hypothesis, as the kinetics and efficiency of DSB repair in human ES cells are unknown.

4.0   CHEKPOINT SIGNALING AND DNA DOUBLE STRAND REPAIR IN HUMAN PLURIPOTENT STEM CELLS

This chapter is submitted as a research article in PLoS ONE:

DNA DamageRresponses in Human Induced Pluripotent Stem Cells and Embryonic Stem Cells. Olga Momcilovic[1, 2], Leah Knobloch[3], Jamie Fornsaglio[3], Sandra Varum[2, 4], Charles Easley[2, 5], Gerald Schatten[2, 5].

[1]Department of Human Genetics, Graduate School of Public Health, University of Pittsburgh, Pittsburgh, PA, USA, [2]Pittsburgh Development Center, University of Pittsburgh, Pittsburgh, PA, USA, [3]Natural Health Sciences, Seton Hill University, Greensburg, PA, USA, [4]Centro de Neurociências e Biologia Celular, Departamento de Zoologia, Universidade de Coimbra, Portugal, [5]Obstetrics, Gynecology & Reproductive Sciences, University of Pittsburgh School of Medicine, Pittsburgh, PA, USA.

4.1   ABSTRACT

Induced pluripotent stem (iPS) cells have the capability to undergo self-renewal and differentiation into all somatic cell types. Since they can be produced through somatic cell reprogramming, which uses a defined set of transcription factors, iPS cells represent important sources of patient-specific cells for clinical applications. However, before these cells can be used in pharmaceutical or therapeutic designs, it is essential to understand their genetic stability, in particular because currently available iPS cells are produced using integrating viral vectors that carry risks of insertional mutagenesis. In this paper, we describe DNA damage responses in human iPS cells. We observe hypersensitivity to DNA damaging agents resulting in rapid induction of apoptosis following γ-irradiation. Following radiation exposure, iPS cells activate checkpoint signaling, as evidenced by phosphorylation of ATM, NBS1, CHEK2, and TP53, including localization of ATM to the double strand breaks (DSB) and TP53 to the nucleus of NANOG-positive cells. We demonstrate that iPS cells arrest cell cycle progression in the G_2 phase of the cell cycle, and display a similar lack of the G_1/S cell cycle arrest as human embryonic stem cells. The cell cycle arrest is temporary and by 24 hours post-irradiation cell cycle distribution is comparable to untreated cells. We further show that both cell types remove DSB within six hours of γ-irradiation and form RAD51 foci, a surrogate marker for homologous recombination repair (HRR). Repair of DSB by homologous recombination is also confirmed by sister chromatid exchanges after induction of DSB by 100 nM camptothecin. Finally, our results show

elevated expression of genes involved in DNA damage signaling, checkpoint function, and repair of various types of DNA lesion in ES and iPS cells relative to their differentiated counterparts. Together, our results reveal high degrees of similarity in DNA damage responses between these two types of pluripotent stem cells, and also suggest that reprogramming significantly alters the DNA damage response of iPS cells relative to their somatic parent line.

4.2   INTRODUCTION

Induced pluripotent stem (iPS) cells are produced by reprogramming somatic cells with a defined set of transcriptional factors. They share numerous characteristics with embryonic stem (ES) cells, such as the ability to undergo self-renewal and differentiation, as well as expression of the same pluripotency markers NANOG, OCT4, SOX2 and SSEA-4 (Takahashi and Yamanaka, 2006). Therefore, it is possible to envision numerous therapeutic applications for human iPS cells without the ethical challenges involved with human ES cells.

Studies in mouse and human somatic cell reprogramming utilized four transcription factors carried on integrating retroviral vectors. Two cocktails of transcription factors were successfully used: *OCT4, SOX2, KLF4* and *MYC* (Takahashi et al., 2007; Takahashi and Yamanaka, 2006), or *OCT4, NANOG, SOX2* and *LIN28* (Yu et al., 2007). OCT4, SOX2 and NANOG are master transcriptional regulators of the pluripotent state in embryonic stem (ES) cells (Chambers et al., 2003; Hart et al., 2004; Mitsui et al., 2003; Nichols et al., 1998). These three transcription factors bind to and activate expression of genes that are involved in maintaining pluripotency, while repressing genes involved in differentiation (Boyer et al., 2005). OCT4, SOX2, and NANOG also bind to and activate their own genes, creating a positive feedback loop that might "jumpstart" reprogramming (Hochedlinger and Plath, 2009). However, *MYC, LIN28* and *KLF4* have oncogenic properties and might activate tumor suppression response when expressed in somatic cells. These responses consist of cell cycle arrest, senescence and apoptosis, and may act as a roadblock to reprogramming. Indeed, reprogramming is a very inefficient process with 0.01 – 0.1% success rate (Okita et al., 2007; Takahashi et al., 2007; Takahashi and Yamanaka, 2006), suggesting that there are unknown limiting steps necessary for the generation of iPS cells. Low efficiency of somatic cell reprogramming can be partially explained by the activation of TP53 pathway and *INK4/ARF* locus by reprogramming factors. In fact, genetic impairment of *TP53* and *CDKN1A* (p21) levels, as well as *INK4/ARF* locus dramatically increase efficiency of generation of iPS clones, endowing almost every somatic cell with the potential to form an iPS clone (Hong et al., 2009; Kawamura et al., 2009; Li et al., 2009; Utikal et al., 2009).

Introduction of transcription factors also increases the γ-H2AX foci (Kawamura et al., 2009), which are markers of double strand breaks. Thus, it is possible that TP53 is activated following expression of reprogramming factors by DNA damage, and that oncogenes block reprogramming by activating DNA damage responses.

Since genetic manipulation of *TP53* or *INK4/ARF* locus significantly increases the efficiency of reprogramming, it has been suggested that reprogramming could potentially depend on rare spontaneous mutations or epigenetic silencing of *INK4/ARF* or *TP53*(Deng and Xu, 2009). Another potential explanation is that activation

of TP53 by damaged DNA prevents the generation of iPS cells with damaged DNA or DNA repair deficiencies (Deng and Xu, 2009). Taking into account the critical role of TP53 in mediating DNA damage response and tumor suppression, it is critical to investigate the function of TP53 and DNA damage response in iPS cells.

Embryonic stem cells are pluripotent cells that are isolated from the inner cell mass (ICM) of the blastocyst (Thomson et al., 1998). They represent the *in vitro* counterpart of cells that in developing embryo contribute to embryo proper and some extraembryonic tissues. Similar to cells of the early embryo, ES cells are rapidly dividing. The cell cycle in ES cells is shortened in comparison to somatic cells, mainly due to an abbreviated G_1 phase and facilitated G_1 to S transition (Becker et al., 2006). Rapid progression through successive rounds of DNA replication and mitotic division may expose ES cells to increased risk of replication errors, which are the most common source of double strand breaks (DSB) in proliferating cells. Double strand breaks can also be induced by various physical (ionizing radiation) and chemical (radiomimetic drugs) agents and represent the most difficult type of DNA damage to repair.

Following introduction of DNA damage, cells elicit a complex DNA damage response comprised of coordinated cell cycle arrest, DNA repair, and in some instances apoptosis. We have previously shown that human ES cells activate ataxia telangiectasia mutated (ATM)-dependent checkpoint signaling cascade, including phosphorylation and nuclear localization of TP53 and arrest in the G_2/M stage of the cell cycle following irradiation (Momcilovic et al., 2009). In this study we extend these findings to iPS cells and focus on understanding the DNA damage response of iPS cells. We investigated activation of checkpoint signaling and induction of cell cycle arrest following exposure of iPS cells to γ-radiation. We further examined double strand break (DSB) repair and contrast the response of iPS cells to ES cells. Finally, we compared the expression of DNA damage signaling and repair gene and protein levels between ES, iPS and differentiated cells. Our results show that reprogramming significantly alters the DNA damage response in iPS cells relative to their parent line, resulting in loss of the G_1/S checkpoint and a dramatic increase in radiosensitivity. Furthermore, iPS cells share numerous similarities in DNA damage response with ES cells, including G_2/M cell cycle arrest, efficient DSB repair, and high expression of DNA damage signaling and repair genes.

4.3   RESULTS

4.3.1   Pluripotency and radiosensitivity in human induced pluripotent stem cells

Induced pluripotent stem (iPS) cells share numerous similarities with embryonic stem (ES) cells, including self-renewal, differentiation into all three germ layers, and expression of markers found in ES cells, such as OCT4, NANOG, SOX2, SSEA-3 and SSEA4 (Takahashi et al., 2007). In order to confirm that we are investigating DNA damage response of pluripotent cells we examined expression of pluripotency markers NANOG, SSEA4 and OCT4 in both untreated cells and cells irradiated with one Gray (Gy) of γ-irradiation (Figure 14). We decided to use

NANOG and SSEA4 as markers of pluripotency because they were not used in the reprogramming cocktail to derive the AE iPS line. Furthermore, in the extremely remote case that irradiation reactivates the reprogramming factors, NANOG and SSEA4 would still reflect expression of endogenous genes. Both the untreated cell population and those exposed to radiation treatment show expression (Figure 14A) and nuclear localization of NANOG (Figure 14B), as well as cell surface expression of SSEA4 (Figure 14C), suggesting that, similar to human ES cells, iPS cells retain pluripotency markers after acute induction of DNA damage. We did not detect decreases in OCT4 protein levels by Western blot analysis (Figure 14A), confirming these results.
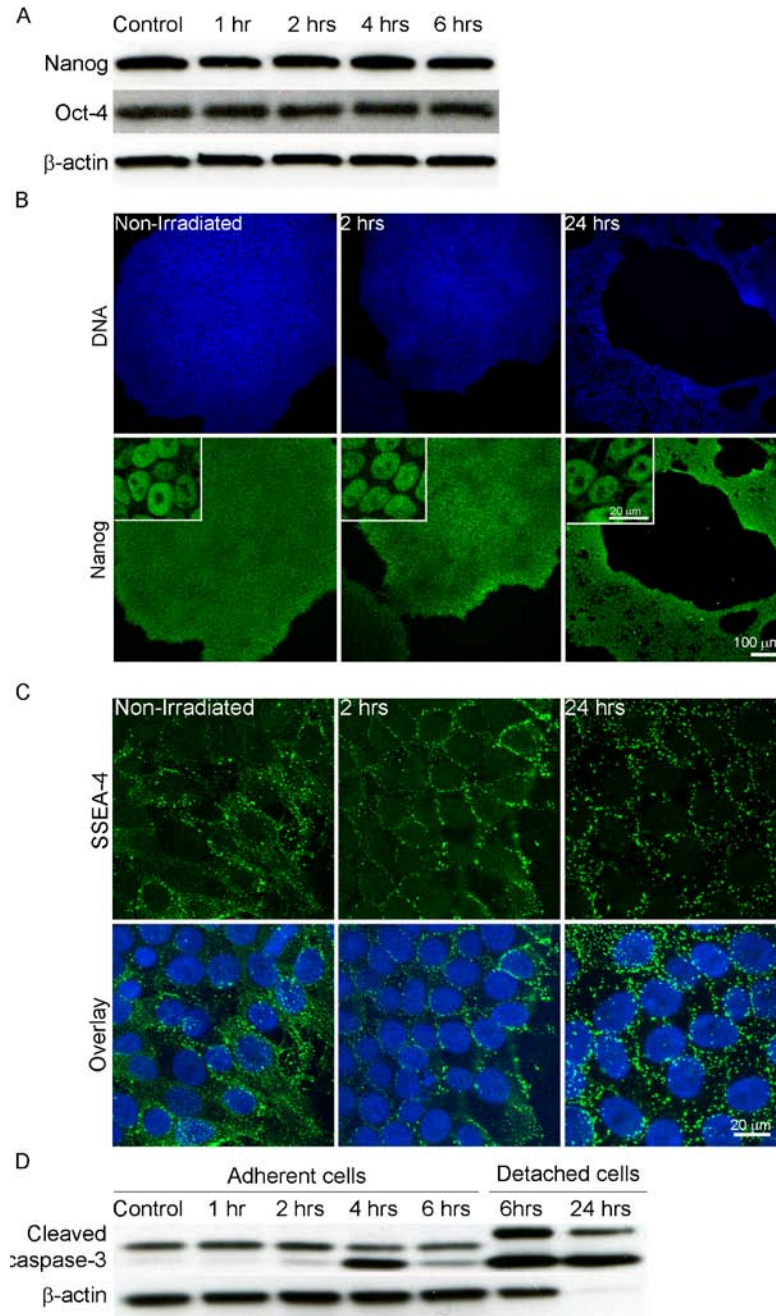
Figure 14: Pluripotency and radiosensitivity of human induced pluripotent stem (iPS) cells.

(A): Western blot analysis of NANOG and OCT4 after irradiation. β-actin served as the loading control. (B): Confocal microscopy for NANOG in iPS cells at indicated time periods after irradiation. Inset – zoomed region of a colony displaying nuclear localization of NANOG. Green – NANOG, Blue – DNA, scale bar = 100 µm (20 µm inset). (C): Confocal microscopy for SSEA4 in iPS cells at indicated time period after irradiation. Green – SSEA4, Blue – DNA, scale bar = 20 µm. (D): Western blot analysis for cleaved caspase-3 after irradiation. Human iPS cells were irradiated, or left untreated, returned to incubator and recovered for indicated periods of time. Adherent and detached cells were collected and analyzed separately. β-actin served as the loading control.

Human and mouse ES cells exhibit profound sensitivity to DNA damaging agents (Aladjem et al., 1998; Momcilovic et al., 2009). We also noted significant detachment of iPS cells from the surface of the cell culture dish by 24 hours following irradiation (Figure 14B), even when a radiation dose of one Gy was used. To confirm that cells were indeed undergoing cell death we performed Western blot analysis for cleaved caspase-3, including both adherent and detached (floating) cells (Figure 14D). Cleaved caspase-3 began to appear four hours after irradiation in adherent cells and continued to increase for 24 hours, particularly in the detached cells, suggesting that iPS cells undergo apoptosis.

4.3.2   Activation of checkpoint signaling in irradiated human induced pluripotent stem cells

Following introduction of double strand breaks (DSB) ATM undergoes auto-phosphorylation at serine 1981 and its kinase function is activated, leading to phosphorylation of numerous downstream targets (Abraham, 2001; Bakkenist and Kastan, 2003). We have previously demonstrated that ATM is phosphorylated at serine 1981 and localizes to DSB sites within 15 minutes of γ-irradiation in human ES cells (Momcilovic et al., 2009). We tested activation of ATM-dependent checkpoint signaling cascade in two iPS lines by Western blot (Figure 15A) and immunocytochemistry (Figure 15B, C) after one (Figure 15) and two Gy of γ-irradiation (Figure 16A). Both dosages induced strong checkpoint signaling response as evidenced by phosphorylation of ATM and its target proteins. Western blot analysis revealed ATM-serine 1981, CHEK2-threonine 68, NBS1-serine 343, and TP53-serine 15 phosphorylation within one hour of γ-irradiation. ATM-serine 1981 and CHEK2-threonine 68 phosphorylation was highest one hour after irradiation and declined subsequently, staying above steady-state level six hours later. NBS1-serine 343 phosphorylation peaked four hours after irradiation, returning to steady-state levels six hours following irradiation. ATM-dependent phosphorylation of TP53 at serine 15 was highest two hours after irradiation, and declined four hours post irradiation. During the same time period the level of total ATM, CHEK2 and NBS1 proteins did not change, whereas the level of total TP53 protein increased following TP53 phosphorylation, suggesting that TP53 is stabilized in response to radiation-induced DNA damage (Chehab et al., 1999; Tibbetts et al., 1999). We also investigated localization of ATM-serine 1981 and TP53-serine 15 in response to radiation exposure. Phosphorylated ATM was localized to sites of DNA damage as detected by co-localization with DSB marker γ-H2AX (Figure 15B). Furthermore, in order to confirm that we were observing the DNA damage response in pluripotent stem cells, we co-stained iPS cells with TP53-serine 15 and NANOG (Figure 15C), and detected nuclear localization of TP53-serine 15 in NANOG-positive cells after irradiation. Additionally, we compared expression of TP53 target genes between non-irradiated and irradiated iPS cells (Figure 15D). We

detected two-fold or greater upregulation of genes involved in cell cycle arrest: *p21 (CDKN1A), GADD45A, PPM1D, SESTRIN1 (SESN1), SESTRIN2 (SESN2),* and *MDM2*, suggesting that TP53 is transcriptionally activated after irradiation. Interestingly, we did not detect upregulation of TP53-dependent apoptosis genes *BAX* and *BCL2*. Collectively, these results are very similar to our previous observations in human ES cells and confirm activation of checkpoint signaling cascade in iPS cells following exposure to one and two Gy of γ-irradiation.
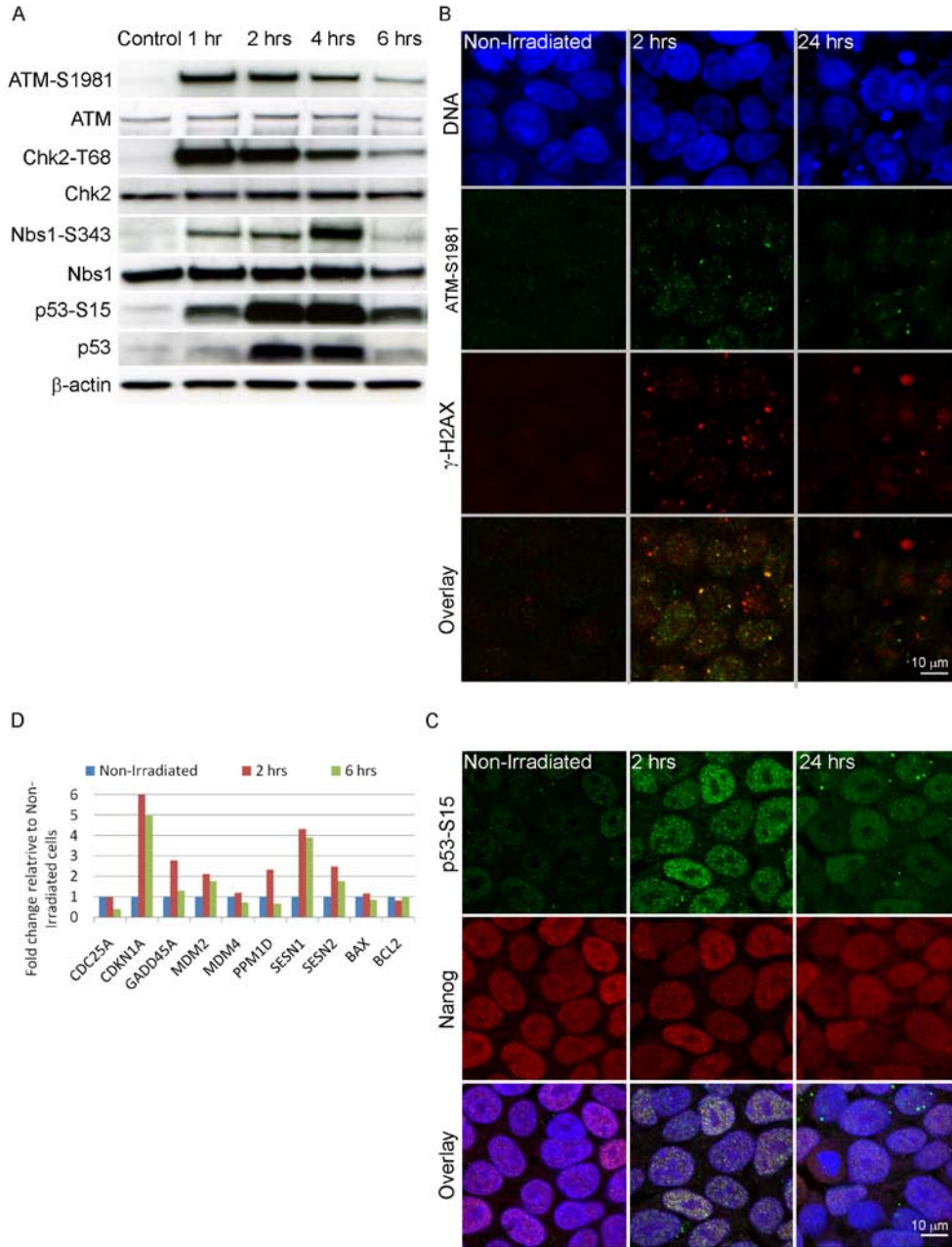
Figure 15: Activation of checkpoint signaling cascade in human induced pluripotent stem (iPS) cells.
(A): Western blot analysis of ATM-serine 1981, total ATM, CHEK2-threonine 68, total CHEK2, NBS1-serine 343, total NBS1, TP53-serine 15, and total TP53 at indicated time points after γ-irradiation of iPS cells. β-actin served as the loading control. (B): Confocal microscopy for ATM and γ-H2AX in iPS cells at indicated time points after

irradiation. Green – ATM-serine 1981, Red – γ-H2AX, Blue – DNA, Yellow – co-localization of ATM-serine 1981 and γ-H2AX. Scale bar = 10 µm. (C): Confocal microscopy for NANOG and TP53-serine 15 in irradiated iPS cells at indicated time points after irradiation. Green – NANOG, Red – TP53-serine 15, Blue – DNA. Scale bar = 10 µm. (D): Expression of TP53 target genes in irradiated human induced pluripotent stem (iPS) cells. Fold changes were calculated using the -ΔΔCt method relative to non-irradiated iPS cells and normalized using *ACTB* as endogenous control.
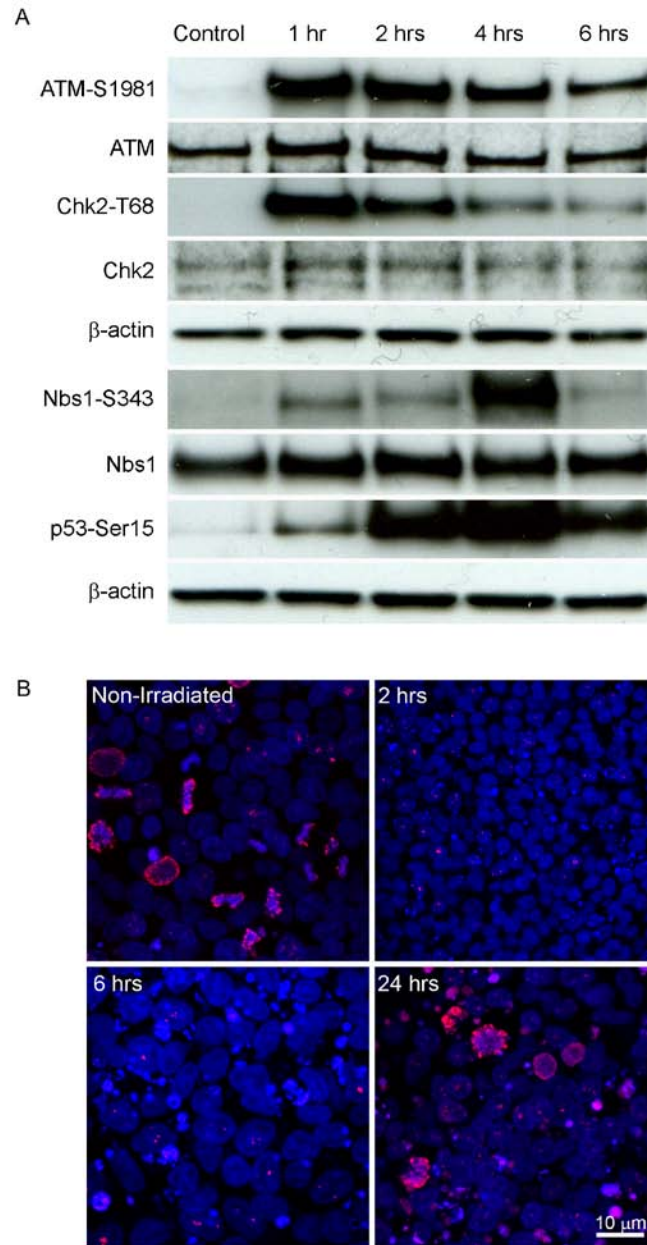
Figure 16: Activation of checkpoint signaling cascade and cell cycle arrest in human induced pluripotent stem (iPS) cells following 2 Grays of γ-irradiation.

(A): Western blot analysis of ATM-serine 1981, total ATM, CHEK2-threonine 68, total CHEK2, NBS1-serine 343, total NBS1 and TP53-serine 15 at indicated time points after γ-irradiation of iPS cells. β-actin served as the loading control. (B): Confocal microscopy for phospho-histone H3 after irradiation of human iPS cells. Red – phospho-histone H3, Blue – DNA. Scale bar = 10 µm.

4.3.3   Cell cycle arrest in irradiated human induced pluripotent stem cells

We next investigated whether iPS cells arrest in response to ionizing irradiation, and if so at which stage of the cell cycle. We employed flow cytometric analysis of DNA content using PI in order to monitor progression of irradiated iPS cells through the cell cycle (Figure 17A). As expected of self-renewing pluripotent cells, a high percentage of non-irradiated iPS cells were in S phase (Table 11). After exposure to one Gy of γ-irradiation, iPS cells arrested in
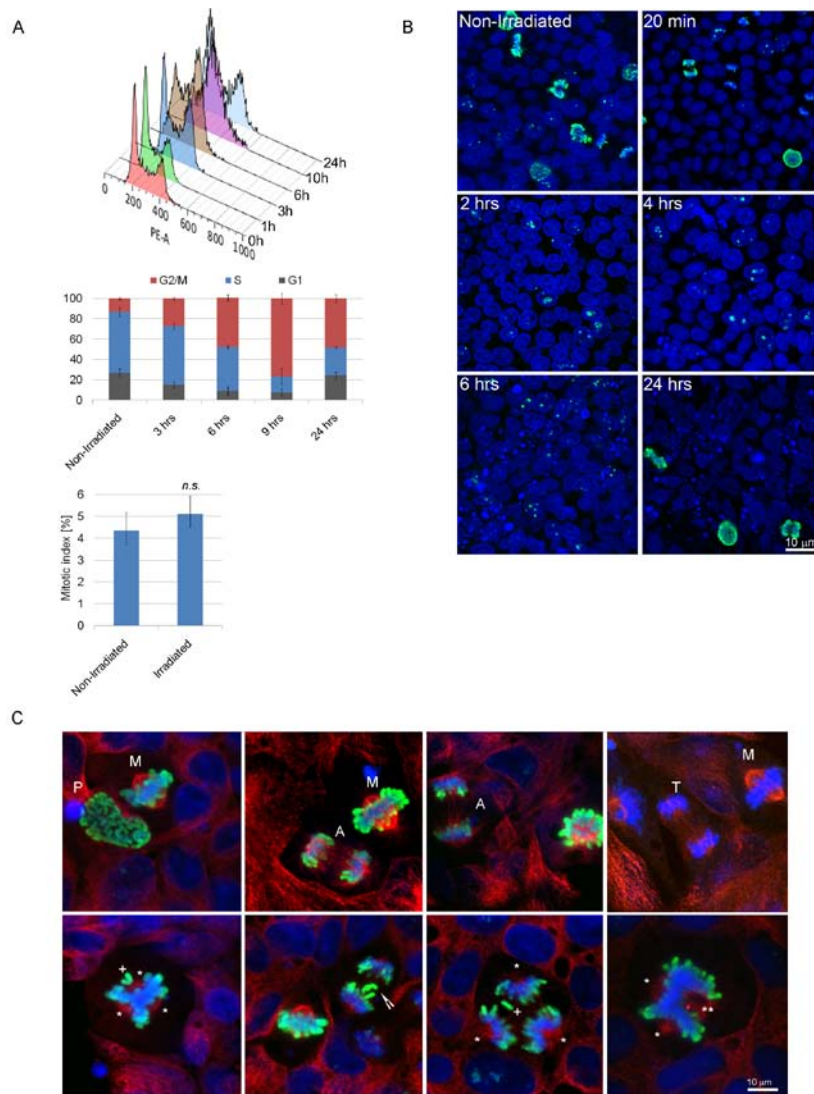
Figure 17: Induction of a temporary G_2/M cell cycle arrest in irradiated human induced pluripotent stem (iPS) cells.
(A): Analysis of DNA content of irradiated human iPS cells by flow cytometry using PI. Top panel: DNA histograms displaying cell cycle profiles measured 0 – 24 hours after irradiation. Bottom panel: percentages of cells in G_1, S, and G_2/M phase of the cell cycle at indicated time points after irradiation. Percentages were calculated using ModFit software (Verity Software House). Results were gated to exclude cellular debris, sub-G_0 population, and doublets. Data present mean ± SEM calculated from three independent experiments. (B): Confocal microscopy for phospho-histone H3 after irradiation of human iPS cells. Green – phospho-histone H3, Blue – DNA. Scale bar = 10 µm. (C): Quantification of mitotic indexes in non-irradiated cells and 24 hours after irradiation. At least 500 cells per condition were counted in three independent experiments, and statistical difference was determined with χ^2 test. The data represent mean ± SEM.   (D): Examples of normal (top row) and aberrant (bottom row) mitotic figures visualized by confocal microscopy after staining for mitotic marker phospho-histone H3. Abbreviations: A – anaphase, M – metaphase, P – prophase, T – telophase. Arrow – lagging chromosome, plus sign – misaligned chromosome, asterisks – pole of mitotic spindle. Green – phospho-histone H3, Red – β-tubulin, Blue – DNA. Scale bar = 10 µm.

the G_2/M stage of the cell cycle, displaying a similar absence of G_1/S cell cycle arrest as mouse, non-human primate and human ES cells (Fluckiger et al., 2006; Hong and Stambrook, 2004; Momcilovic et al., 2009). Three hours after irradiation a significant drop in the percentage of cells in G_1 phase was observed, whereas percentage of cells in G_2/M increased. This trend continued for six hours after irradiation, and by nine hours after irradiation the majority of cells (77%) were in G_2/M phase. By 24 hours post-irradiation, cell cycle distribution resembled non-irradiated cells (Table 11, Figure 17A).

Table 11: Percentage of cells at each stage of the cell cycle (mean ± SEM)

	Non-Irradiated	3 hrs	6 hrs	9 hrs	24 hrs
G_1	26.8±3.8	15.3±3	9.2±4.4	7.6±3.7	24.4±3.5
S	60±4.5	57.5±3.1	43.1±1.4	15.7±8.2	27.2±0.9
G_2/M	13.2±1.2	27.3±1.5	48.6±3.1	76.7±5	48.4±3.6

In order to better understand when cells arrest after irradiation (G_2 or M phase), as well as the events that occur following iPS cells' return to the cell cycle, we performed immunocytochemistry using mitosis-specific marker histone H3 phosphorylated at serine 10 (phospho-H3). In a population of non-irradiated cells we observed numerous phospho-H3-positive cells in various stages of mitosis (Figure 17B). Twenty minutes after exposure to one (Figure 17B) or two Gy (Figure 16B) of γ-radiation we still observed mitotic cells, presumably cells that were already undergoing mitosis at the time of irradiation. However, two, four, and six hours after irradiation, we could not detect any mitotic cells, suggesting that iPS cells arrest in the G_2 phase and do not enter mitosis following irradiation. Mitotic cells start reappearing 24 hours after irradiation (please see Figure 17D for examples), with no statistically significant difference in mitotic index (5.1 ± 0.34%; Figure 17C) compared to non-irradiated cells (4.3 ± 0.48%; n=3, 0.3>p>0.2). Note that a lot of cellular debris is present in cell colonies both at 6 and 24 hours after irradiation, in accordance with iPS cells' radiosensitivity. In aggregate, both flow cytometry and immunocytochemistry results reveal that iPS cells arrest in G_2 stage of the cell cycle and resume cell cycle progression by 24 hours following irradiation.

4.3.4 Double strand break repair in human embryonic stem and induced pluripotent stem cells

The fact that iPS cells resume the cell cycle within 24 hours of DNA damage suggests that DNA breaks are removed by that time and allowing recovery from the cell cycle arrest. We investigated DSB repair by monitoring formation and removal of γ-H2AX foci, which is frequently used as a DSB marker. Since open chromatin structure can lead to formation of microscopically visible foci in the absence of exogenous DNA damage (Banath et al., 2009) and since both human ES and iPS cells have open chromatin structure, we first tested the usefulness of γ-H2AX as a DSB marker in human ES cells by inducing localized damage. We employed a 405 nm laser to induce DNA damage in a specified nuclear region of several ES cells in the colony, as well as in several mouse embryonic fibroblasts (MEF) that were used to co-culture human ES cells (Figure 18). Thirty minutes after laser treatment, we detected γ-H2AX in MEF but only in affected cells and only in the nuclear region that was targeted, confirming our goal behind γ-

H2AX testing. In human ES cells we also detected DNA damage only in cells of colonies that were treated with the laser, and not in neighboring cells. However, unlike in MEF cells, γ-H2AX staining was not confined to the affected nuclear region; instead, staining was present in the whole nucleus (Figure 18), perhaps due to highly dynamic chromatin in pluripotent stem cells (Meshorer et al., 2006). Nevertheless, we confirmed that γ-H2AX staining is sensitive enough to detect DNA damage only in laser-treated human ES cells.
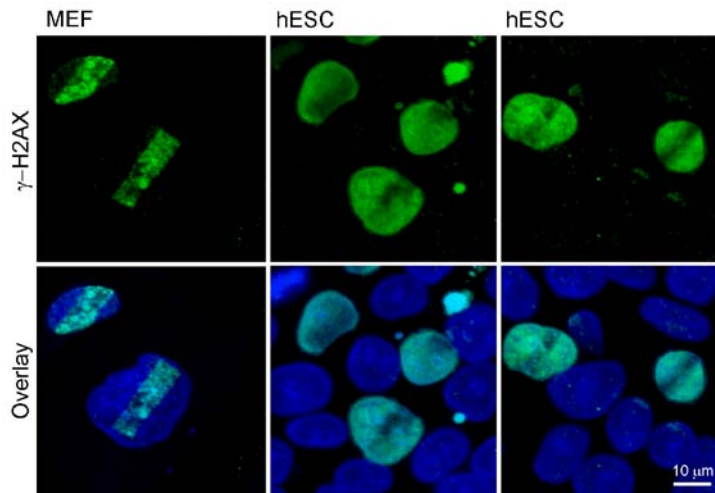
Figure 18: Induction of localized DNA damage in mouse embryonic fibroblasts (MEF) and human embryonic stem (ES) cells.
405 nm laser was used at 25% intensity to induce DNA damage in defined nuclear region of MEF and hESC. Thirty minutes following DNA damage, cells were fixed and stained for double strand break marker γ-H2AX. Green – γ-H2AX, Blue – DNA. Scale bar = 10 μm.

We irradiated human ES and iPS cells with one Gy of γ-irradiation and performed time-course immunocytochemistry for γ-H2AX (Figure 19). Non-irradiated human ES and iPS cells were not completely void of γ-H2AX foci, which may reflect endogenous DNA damage. However, within 20 minutes of γ-irradiation we detected strong induction of γ-H2AX foci in both cell types. Over the following four hours, both cell types lost many of these foci, so that by six hours post irradiation the number of γ-H2AX foci had returned to steady-state levels.

Two main pathways for DNA repair include error-prone non-homologous end joining (NHEJ) and error-free homologous recombination repair (HRR). Unlike NHEJ, HRR relies on the presence of the sister chromatid for use as a template for accurate DNA repair, and is hence limited to late S and G_2 phases of the cell cycle. We hypothesized that HRR plays a major role in DSB repair in ES cells due to their developmental role and the requirement that their genomic integrity be preserved, as well as the fact that, in any given moment, more than 70% of an ES cell population is in the S and G_2/M phases of the cell cycle (Momcilovic et al., 2009), when the sister chromatid is available. In order to test this, we irradiated ES and iPS cells with one Gy of γ-radiation and investigated the formation of RAD51 foci (Figure 20A). RAD51 is a recombinase that is essential for HRR and, following induction of DSB, localizes to the foci that are believed to represent sites where HRR takes place. Two hours following irradiation we detected formation of RAD51 foci in the majority of cells suggesting that both ES and iPS cells repair DSB by HRR. Even more direct evidence of HRR are the sister chromatid exchanges (SCE) that represent a subset of HRR events. We treated ES and iPS cells with 50 and 100 nM camptothecin for one hour

to induce breaks in S-phase cells (Figure 20B). Camptothecin is a topoisomerase I inhibitor that stabilizes the topoisomerase I – DNA complex. Topoisomerase I-introduced single strand nicks in DNA can be converted into DSB if the replication fork collides with stabilized topoisomerase I – DNA complex. Therefore, camptothecin specifically introduces DSB in replicating cells, eliciting HRR repair of DSB. We observed increase in the number of SCE following 50 nM and 100 nM treatments of ES and iPS cells. The increase was similar in both cell types, suggesting that iPS cells have similar HRR capacity as ES cells.
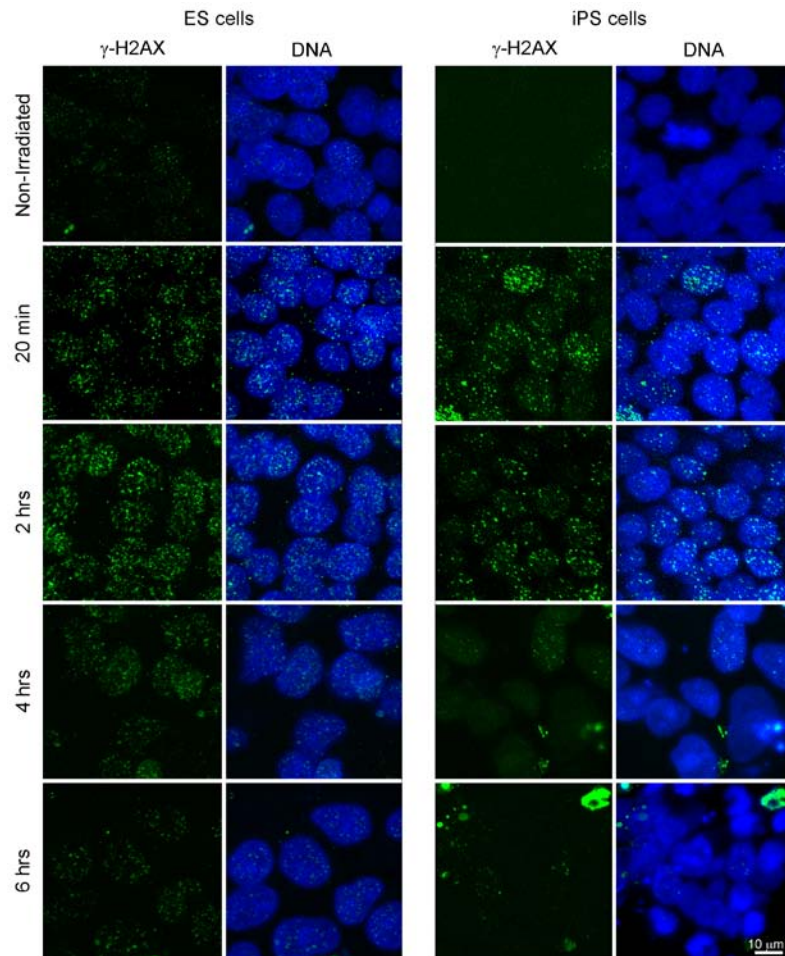
Figure 19:   Repair of double strand breaks (DSB) in human embryonic stem (ES) and induced pluripotent stem (iPS) cells.
Time course immunocytochemistry for marker of DSB γ-H2AX in ES cells (left panel) and iPS cells (right panel). Green – γ-H2AX, Blue – DNA. Scale bar = 10 μm.

69
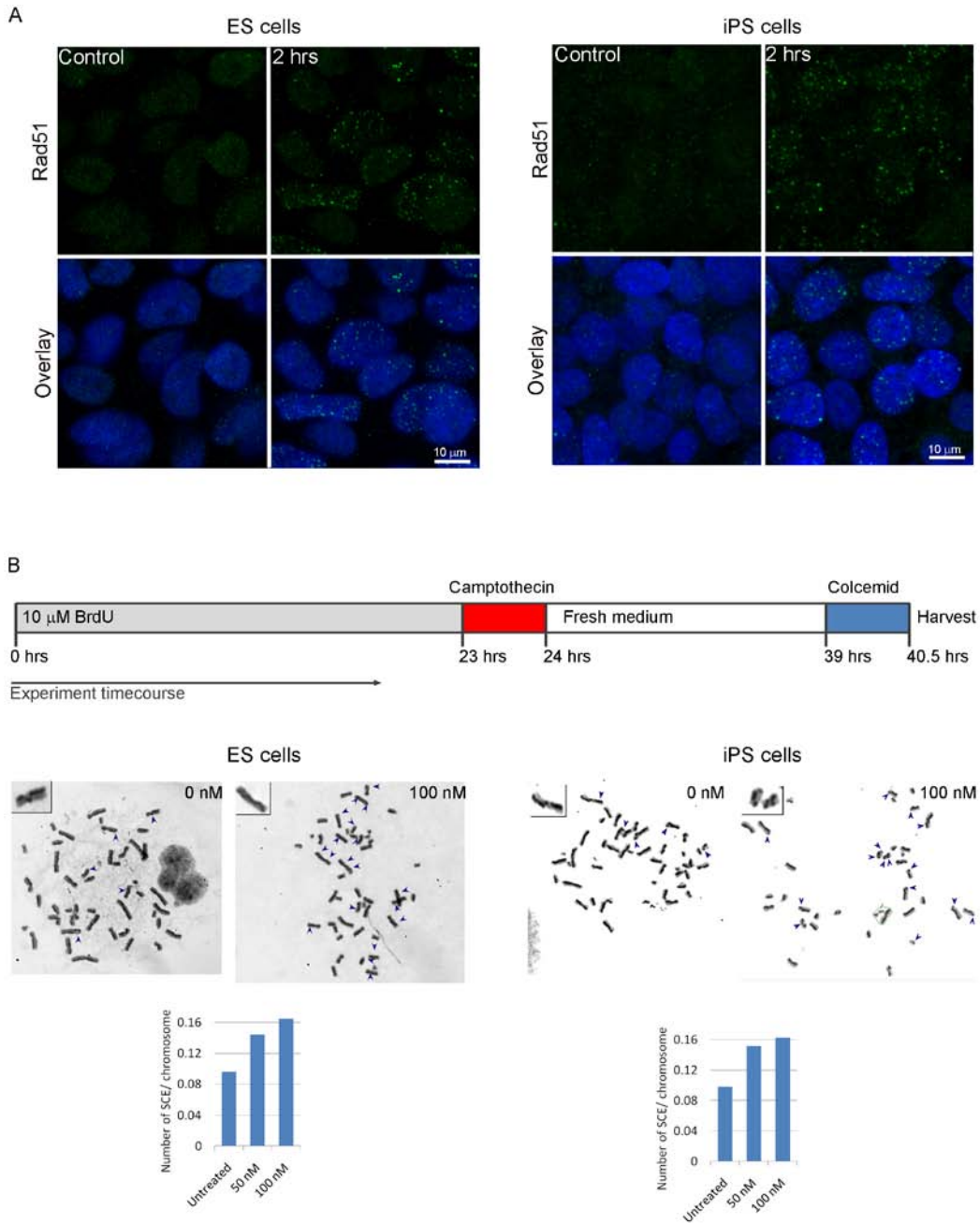
Figure 20: Homologous recombination repair in human stem (ES) and induced pluripotent stem (iPS) cells.
(A): Confocal microscopy for RAD51 in irradiated human ES cells (left panel) and iPS cells (right panel). Green – RAD51, Blue – DNA. Scale bar = 10 µm. (B): Sister chromatid exchanges (SCE) in untreated and 100 nM camptothecin treated human ES cells (left panel) and iPS cells (right panel). Cells were grown for one cell cycle in the presence of 10 µM BrdU, followed by one hour treatment with 100 nM camptothecin and 15 hours recovery in the fresh medium. Following 90 minute 120 ng/ml colcemid treatment cells were harvested for cytogenetic preparation and differential staining with Hoechst 33258 dye and Giemsa was performed. The number of reciprocal SCE was counted in 25 metaphase spreads.

4.3.5   Gene expression analysis in pluripotent and differentiated cells

ES cells have been reported to have greater capacities for DNA repair as compared with somatic cells, and have higher expression of some DNA repair genes (Maynard et al., 2008; Tichy et al.; Tichy and Stambrook, 2008). We explored this finding in human ES and iPS cells by comparing the expression level of genes participating in DNA damage signaling, cell cycle arrest, as well as DNA repair across three human ES cell lines (WA01, WA07, WA09), two iPS cell lines (IMR-90 iPS, AE iPS), and two differentiated cell lines (WA07 teratoma fibroblasts [TF] and IMR-90 fibroblasts), using quantitative PCR (qPCR) array (Figure 21). TF and IMR-90 served as differentiated counterparts for ES and iPS cell lines, respectively. We excluded from the data analysis ten genes with Ct values above 30 (*BTG2, CIDEA, DMC1, GADD45G, GML, IP6K3, PCBP4, RAD51, SEMA4A, TP73*). Since the ES cell lines did not show any significant difference in gene expression between each other ($p>0.05$, Figure 22), they were grouped together and used as a control for fold difference comparisons. Interestingly, we also could not detect significant difference in gene expression between ES and iPS lines, although AE iPS line did show increased (but not significant) gene expression relative to ES cells (less than two fold difference, $p>0.05$, Figure 22).   In fibroblasts, however, the general trend was reduced gene expression relative to ES and iPS cells (Figure 6A). Out of 57 analyzed genes, 38 (66.7%) showed two-fold or greater downregulation in IMR-90, whereas 31 genes (54.4%) displayed two-fold or greater downregulation in TF. In IMR-90, only two (3.5%) genes were two-fold or more upregulated (*MPG* and *TREX1*), while in TF three genes (5.3%) (*MPG, TREX1* and *GADD45A*) were upregulated. Based on the $p<0.05$ cut-off, 23 genes in IMR-90 displayed a statistically significant expression fold difference and nine in TF. These genes showed also at least two-fold difference in comparison to ES lines, so we considered their expression biologically altered.

We grouped genes according to their pathways and gene expression fold differences relative to ES cells: DNA damage signaling and cell cycle arrest (Figure 21B), DSB repair (Figure 21C), MMR (Figure 21D), BER (Figure 21E), and NER (Figure 21F). The corresponding p-values are shown in Tables 12 – 16. Out of 18 genes involved in cell cycle arrest and DNA damage signaling, seven showed statistically significant lower expression in IMR-90 cells (*ATR, BRCA1, CHEK1, PCNA, RAD9A, SMC1A, T*TP53), and one showed significant reduction in TF cells (*ATR*) while another showed increased expression (*GADD45A*) (Figure 21B; Table 12). In a group of 22 DSB repair genes, 13genes were expressed at significantly lower levels in IMR-90 (*ATR, BRCA1, FANCG, FEN1, XRCC6(Ku70), LIG1, MRE11A, PRKDC(PRKDC), RAD18, RAD9A, RPA1, XRCC2*), and five in TF (*ATR, FANCG, FEN1, MRE11A, PRKDC(PRKDC)*) (Figure 21C; Table 13). In the group of genes involved in MMR we detected five genes with lower expression in IMR-90 (*EXO1, MSH2, MSH3, MUTYH, N4BP2*) and two in TF (*MSH2, N4BP2*), whereas *TREX1* showed higher expression in TF when compared to ES cells (Figure 21D; Table 14). Among eight BER genes, three showed reduced expression in IMR-90 (*MUTYH, UNG, XRCC1*), whereas *MPG* showed increased expression in IMR-90 relative to ES cells (Figure 21 E; Table 15). Finally, TF did not show any significant difference in expression of genes involved in BER, nor NER (Figure 21E, F; Table 15, 16). But though there was no statistical significance in observed fold difference in gene expression, most of the analyzed genes showed lower expression in differentiated cells than in ES or iPS cells (Figure 21). Thus, ES and iPS cell lines

display a similar expression pattern for DNA damage signaling and repair genes, and exhibit generally elevated expression levels compared to their differentiated counterparts, TF and IMR-90, respectively (Figure 21A). These results suggest that differentiation and reprogramming significantly alter the expression pattern of DNA damage response genes.

Figure 21: **Analysis of D NA d amage s ignaling an d r epair g ene e xpression i n hum an pl uripotent stem c ells a nd differentiated cells.**

(A): Heat map of transcripts analyzed by PCR array. Expression values were normalized over the expression of β-actin and presented as $\log_{10}$ of relative changes compared to WA07. In comparison to WA07 genes with higher expression are depicted in red, genes with lower expression are depicted in green, and genes with no difference are depicted in black. Cell lines were clustered based on the overall similarity in gene expression. The genes were grouped according to the pathway they participate in: (B): DNA damage and cell cycle arrest signaling, (C): double strand break (DSB) repair, (D): mismatch repair (MMR), (E): base excision repair (BER), (F): nucleotide excision repair (NER). Expression fold differences were calculated using the -ΔΔCt method relative to averaged ES cell lines and normalized using *ACTB* as endogenous control. The data presented are from three independent experiments.

Figure 22: Gene expression comparison between pluripotent stem cell lines.
Volcano plots represent *p*-values (Y-axis) for observed difference in gene expression (X-axis). Blue horizontal line represents position of $-Log_{10}(0.05)$ for easier visualization of significant (p<0.05) difference. Horizontal lines represent two fold boundaries: on the left are shown genes with more than twofold downregulation (green), and on the right are genes with more than two fold upregulation (red) in comparison to control line. Genes in between vertical lines show less than two fold difference in gene expression and are depicted in black. Dots represent genes on the array.

Table 12: *p*-value comparing to ES cell expression: DNA damage signaling and cell cycle arrest genes.

Gene	IMR-90 iPS	AE iPS	IMR-90	TF
ATM	0.57631	0.506295	0.085474	0.298853
ATR	0.224651	0.136748	0.00012	0.007757
BRCA1	0.696705	0.80286	0.039688	0.173745
CCNH	0.94397	0.428333	0.224058	0.853943
CDK7	0.955632	0.259967	0.819881	0.682147
CHEK1	0.987316	0.118751	0.031091	0.103799
CHEK2	0.859196	0.844377	0.054215	0.106662
GADD45A	0.328035	0.92211	0.183808	0.045834
GTSE1	0.648524	0.406655	0.069732	0.255467
HUS1	0.960966	0.949327	0.059013	0.309369
MNAT1	0.955009	0.478443	0.255932	0.611328
PCNA	0.850991	0.233539	0.023314	0.121541
RAD1	0.771902	0.536311	0.291469	0.20101
RAD17	0.955772	0.473923	0.120408	0.406977
RAD9A	0.597626	0.537845	0.023091	0.122588
RBBP8	0.824502	0.345977	0.084385	0.28663
SMC1A	0.737524	0.272268	0.049401	0.094141
TTP53	0.773965	0.377934	0.023513	0.098894

Table 13: *p*-value comparing to ES cell expression: DSB repair genes.

Gene	IMR-90 iPS	AE iPS	IMR-90	TF
ABL1	0.949231	0.549173	0.504224	0.452685
ATM	0.57631	0.506295	0.085474	0.298853
ATR	0.224651	0.136748	0.00012	0.007757
BRCA1	0.696705	0.80286	0.039688	0.173745
FANCG	0.947707	0.562551	0.005944	0.042056
FEN1	0.398639	0.310912	0.000734	0.015698
XRCC6 (Ku70)	0.943276	0.654172	0.033858	0.123937
XRCC6BP1	0.754221	0.505813	0.069761	0.389662
LIG1	0.930717	0.546939	0.011995	0.067929
MRE11A	0.413568	0.515739	0.019145	0.046147
NBN (NBS1)	0.973539	0.711284	0.053436	0.543504
PRKDC (DNA-PKcs)	0.821906	0.694589	0.00513	0.029441
RAD1	0.771902	0.536311	0.291469	0.20101
RAD17	0.955772	0.473923	0.120408	0.406977
RAD18	0.995641	0.545698	0.04567	0.203224
RAD21	0.916088	0.790471	0.071021	0.223934
RAD50	0.824122	0.711063	0.185977	0.696658
RAD51L1	0.982636	0.809205	0.084185	0.331463
RAD9A	0.597626	0.537845	0.023091	0.122588

Table 13 continued.

RPA1	0.735362	0.536414	0.023445	0.072859
XRCC2	0.573091	0.769153	0.027158	0.066824
XRCC3	0.325782	0.994872	0.834946	0.68676

Table 14: *p*-**value comparing to ES cell expression: MMR genes.**

Gene	IMR-90 iPS	AE iPS	IMR-90	TF
ABL1	0.949231	0.549173	0.504224	0.452685
ANKRD17	0.934429	0.731614	0.09786	0.204471
EXO1	0.492576	0.522098	0.031245	0.095152
MLH1	0.416364	0.465582	0.081946	0.23796
MLH3	0.997759	0.965141	0.174521	0.328437
MSH2	0.857991	0.435612	0.023702	0.060512
MSH3	0.869539	0.269519	0.041186	0.430153
MUTYH	0.451588	0.259017	0.016515	0.056259
N4BP2	0.864914	0.672229	0.009036	0.031524
PMS1	0.937467	0.754491	0.081887	0.186824
PMS2	0.292682	0.415731	0.641265	0.838477
PMS2L3	0.725087	0.863888	0.818104	0.401013
TREX1	0.916034	0.528133	0.191454	0.035572

Table 15: *p*-**value comparing to ES cell expression: BER genes.**

Gene	IMR-90 iPS	AE iPS	IMR-90	TF
APEX1	0.881701	0.216286	0.085594	0.381403
MBD4	0.877766	0.361172	0.267382	0.230659
MPG	0.487583	0.456759	0.011145	0.068083
MUTYH	0.451588	0.259017	0.016515	0.056259
NTHL1	0.815198	0.135108	0.063159	0.177981
OGG1	0.816398	0.570708	0.116337	0.49135
UNG	0.540893	0.21115	0.033375	0.078898
XRCC1	0.811104	0.168127	0.029069	0.152095

Table 16: *p*-**value comparing to ES cell expression: NER genes.**

Gene	IMR-90 iPS	AE iPS	IMR-90	TF
ERCC1	0.467596	0.353567	0.240213	0.29478
ERCC2	0.3228	0.588618	0.124794	0.314321
RPA1	0.735362	0.536414	0.023445	0.072859
XPA	0.949872	0.933206	0.673024	0.879367
XPC	0.808056	0.690012	0.256061	0.601866
XRCC1	0.811104	0.168127	0.029069	0.152095

We also validated gene expression data by comparing DSB repair protein levels between human ES, iPS and differentiated cell lines (Figure 23). We detected a lower level of proteins involved in HRR (MRE11, NBS1 and RAD52) and NHEJ (XRCC4 and ligase IV) in TF and IMR-90 compared to ES and iPS cells, thereby confirming our gene expression results.
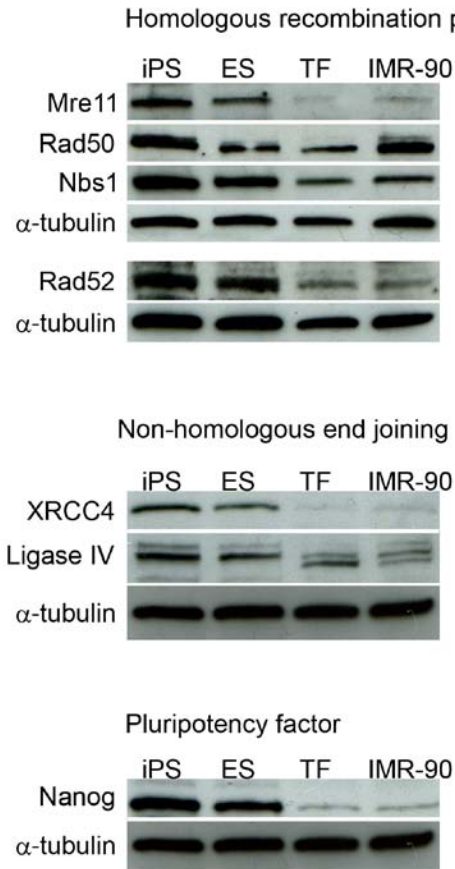
Figure 23: Comparison of DNA repair protein levels between pluripotent stem cells and differentiated cells.
Western blot analysis of basal level of proteins involved in homologous recombination, non-homologous end joining, and pluripotency maintenance. α-tubulin served as the loading control.

4.4   DISCUSSION

In this study we set forth to investigate DNA damage response, including checkpoint signaling, cell cycle arrest, apoptosis and DNA repair in iPS cells. We found that overall response of iPS cells to ionizing radiation is very similar to that in human ES cells. Following activation of the ATM-dependent checkpoint signaling cascade by

ionizing radiation, iPS cells arrest cell cycle progression in G_2 phase. Furthermore, keeping in mind that DSB repair efficiently removes DNA breaks, we present evidence for homologous recombination in human ES and iPS cells. More generally, human ES and iPS cells exhibit elevated expression of DNA repair genes, perhaps explaining the high capacity for DNA repair in human ES cells.

Irradiation of iPS cells induced strong apoptotic response, resulting in visual loss of iPS cells from the colony in the 24 hours after irradiation, and increased cleavage of caspase-3 four hours following radiation treatment (Figure 14B, D). We conducted initial experiments using the same two Gy dose of γ-radiation as we did for studies using human ES cells. The iPS cells responded with such a high level of cell death that almost all cells had died by 24 hours post-irradiation (data not shown). Therefore, we limited the dosage used in this study to one Gy, which elicited a DNA damage response while preserving enough cells to perform experiments. Thus, human iPS cells exhibit profound radiosensitivity, similar to observations in mouse, non-human primate and human ES cells (Aladjem et al., 1998; Fluckiger et al., 2006; Hong and Stambrook, 2004; Momcilovic et al., 2009). We did not detect such a level of cell death in IMR-90 fibroblasts, the parent line for IMR-90 iPS cells (data not shown), suggesting that radiosensitivity is specifically associated with pluripotent state.

We also investigated the expression of pluripotency markers NANOG, SSEA4 and OCT4 in untreated and irradiated iPS cells. As expected, iPS cells show robust expression of NANOG and OCT4 proteins, nuclear localization of NANOG, and cell surface expression of SSEA4 (Figure 14). Similar to previous findings in human ES cells, γ-irradiation does not lead to downregulation of OCT4 and NANOG protein levels during the six hours after irradiation, and confocal microscopy confirmed expression and appropriate localization of NANOG and SSEA4 up to 24 hours after DNA damage.

We next studied activation of ATM and its target proteins, CHEK2, NBS1 and TP53, using Western blot analysis and confocal microscopy (Figure 15). The kinetics of ATM, CHEK2, NBS1 and TP53 phosphorylation was remarkably similar to observations made in human ES cells. In addition, we verified canonical localization of ATM-serine 1981 to the sites of DSB by co-localization with γ-H2AX. In addition, double labeling of irradiated iPS cells with NANOG and TP53-serine 15 confirmed activation of checkpoint signaling in pluripotent cells. Finally, examination of expression of TP53 target genes revealed upregulation of *CDKN1A, GADD45A, SESN1, SESN2, MDM2* and *PPM1D*, indicating that TP53 is transcriptionally active. Studies that showed that TP53 knockout improves reprogramming efficiency, led some authors to question the status of TP53 in iPS cells (Deng and Xu, 2009). Our finding suggests that TP53 is active in iPS cells and that reprogramming does not affect TP53.

The analysis of iPS cell cycle distribution revealed a lack of G_1/S arrest in irradiated iPS cells (Figure 17). Instead, iPS cells arrest in the G_2 phase of the cell cycle, analogous to data in ES cells. Cell cycle analysis revealed that reprogramming induces changes in the cell cycle structure, resulting in highly proliferative cell populations with $60 \pm 4.5\%$ cells in the S phase, and $4.3 \pm 0.5\%$ in mitosis, mirroring findings in the human ES cells. Since it has been proposed that the G_1 phase of the cell cycle is a time when ES cells are sensitive to differentiating signals, it is not surprising that reprogramming also leads to loss of G_1/S cell cycle arrest in iPS cells, which may protect them from differentiation.

Cell cycle analysis, as well as staining for mitotic marker phospho-histone H3, showed that cell cycle arrest is temporary and that 24 hours after irradiation iPS cells restart cell cycle progression. This finding suggests that iPS cells repair damaged DNA during this time frame. We followed DSB repair by examining the kinetics of γ-H2AX foci formation and removal (Figure 19). H2AX is a histone variant that is phosphorylated at serine 139 (and referred to as γ-H2AX) by ATM, DNA-PK and ATR at DSB sites and covers mega base-long stretches of DNA surrounding the DSB (Rogakou et al., 1999; Rogakou et al., 1998). In mouse ES cells, γ-H2AX forms visible foci even in the absence of externally-induced DNA damage and, following irradiation, endogenous γ-H2AX foci cannot be clearly distinguished from irradiation-induced foci (Banath et al., 2009). This has been attributed to open chromatin structure and global chromatin decondensation that favors formation of visible γ-H2AX foci and limits the use of this marker in following DNA repair in mouse ES cells (Banath et al., 2009). Since both human ES and iPS cells also have open chromatin structure, we first validated γ-H2AX as a DSB marker in human ES cells by inducing localized damage with a 405 nm laser. We observed localized γ-H2AX staining in laser-irradiated MEF, but relatively spread out γ-H2AX staining in laser-treated ES cells (Figure 18). This can be explained because of highly dynamic chromatin in pluripotent stem cells (Meshorer et al., 2006), so that chromatin movement distributes damaged DNA from a localized region throughout the nucleus; γ-H2AX staining was not observed in untreated MEF and ES cells, justifying the use of γ-H2AX as a DSB marker. When we irradiated ES and iPS cells with γ-irradiation, we observed γ-H2AX foci forming within 20 minutes of irradiation. The foci were gone within six hours of irradiation, indicating that DNA repair took place within that time frame, consistent with earlier observations of efficient DNA repair in human ES cells (Maynard et al., 2008).

The two main pathways for repairing DSB are homologous recombination repair (HRR) and non-homologous end joining (NHEJ). Homologous recombination is critically dependent on the presence of the homologous sequence on the sister chromatids, so it typically occurs in the late S and G_2 phases of the cell cycle. The use of the homologous chromosome during G_1 phase could lead to loss of heterozygosity and be potentially harmful. The advantage of HRR is that the original DNA sequence is restored without any loss of information because it uses the sister chromatid as a template, making it an error-free method of repair. In contrast, NHEJ does not require regions of homology and can operate in any stage of the cell cycle. However, due to the complex nature of DSB (non-ligatable groups, 3' or 5' overhangs), processing DSB without a template can likely lead to the loss of some genetic information. The advantage of NHEJ is that it is fast and independent of whatever cell cycle stage the cell is at. Focusing on ES cells, it has long been speculated that HRR is the predominant form of DSB repair in this developmentally critical cell type, and this was recently confirmed in mouse ES cells (Banuelos et al., 2008; Serrano et al.; Tichy et al.). Mouse ES cells also demonstrate lower expression of key NHEJ repair factors, such as Ligase IV and PRKDC (Banuelos et al., 2008; Tichy et al.), and show elevated expression or HRR factors (RAD51, RAD54 and RAD52) (Tichy et al.) compared to MEF. Here we show evidence that human ES and iPS cells repair DSB through HRR, which uses RAD51 as a surrogate marker for HRR and visualization of SCE (Figure 20). Gene and protein expression analysis revealed that both human ES and iPS cells have higher expression levels of factors involved in DNA damage signaling and DNA repair than their differentiated counterparts (Figure 21, Figure 23). Maynard and colleagues (Maynard et al., 2008) reported similar data in human ES cells and showed that human ES

cells exhibit a higher capacity for repairing multiple forms of DNA lesions. Interestingly, human ES and iPS cells display elevated expression of genes involved in HRR (RAD52, MRE11, NBS1) and, unlike in mouse ES cells (Tichy et al.), NHEJ (PRKDC, XRCC6, Ligase IV, XRCC4) relative to differentiated cells (Figure 21). Other researchers also described differences in expression levels of NHEJ factors in human ES cells relative to mouse ES cells: human ES cells expressed higher levels of PRKDC and XRCC6 than mouse ES cells, and showed proficiency in end-joining, which mouse ES cells lack (Banuelos et al., 2008). Therefore, it appears that there are species-specific differences between mouse and human ES cells regarding the roles of HRR and NHEJ. Additionally, it seems there is a general difference between mouse and human somatic cells in their dependence on NHEJ. For example, DNA-PK activity (Finnie et al., 1995) and XRCC6 expression (Anderson and Lees-Miller, 1992) are higher in human somatic cells relative to mouse cells, and XRCC5 is an essential protein in human but not mouse cells (Li et al., 2002). Nevertheless, the relative contributions and importance of HRR and NHEJ in human ES and iPS cells still need to be clarified.

5.0   CONCLUSIONS AND FUTURE DIRECTIONS

Embryonic stem (ES) cells are pluripotent cells that are isolated from the inner cell mass (ICM) of the blastocyst (Thomson et al., 1998). They represent in vitro counterpart of cells that in developing embryo contribute to embryo proper and some extraembryonic tissues. Since ES cells inherited behavior of the ICM cells, they can be used to study various aspects of early development. The two most important characteristics of ES cells are 1) capability to undergo self-renewal and 2) ability to differentiate into all cell types of an organism. Self-renewal depends on the ability of cells to divide and replenish stem cell pool, whereas pluripotency depends on plasticity of cells and ability to respond to differentiation signals. Similar to cells of the early embryo, ES cells divide rapidly. The cell cycle in ES cells is shortened in comparison to somatic cells, mainly due to abbreviated G_1 phase and facilitated G_1 to S transition (Becker et al., 2006). Rapid progression through successive rounds of DNA replication and mitotic division may expose ES cells to increased risk of replication errors that may induce double strand breaks (DSB). The fact that ES cells can differentiate into numerous cell types emphasizes the importance of the safe-keeping of genomic integrity.

In this study we investigated DNA damage responses in two types of pluripotent stem (PS) cells, namely embryonic stem (ES) cells, and induced pluripotent stem (iPS) cells. DNA damage response has been studied in great detail in somatic cells, and is comprised of coordinated cell cycle arrest, DNA repair, and apoptosis. However, little is known about the events occurring following introduction of DNA damage into ES cells, and iPS cells are even less explored.

Human ES and iPS cells are extremely sensitive to DNA damage and undergo cells death within hours of introduction of DNA lesions. The hypersensitivity to DNA damaging agents has been reported in mouse and non-human primate ES cells as well (Aladjem et al., 1998; Fluckiger et al., 2006; Hong and Stambrook, 2004), and appears to be a common characteristic of pluripotent stem cells representing one line of defense against genomic instability. Both human ES and iPS cells activate checkpoint signaling cascade following γ-irradiation, leading to G_2/M, but not G_1/S arrest, similar to observations in mouse ES cells (Hong and Stambrook, 2004). However, despite sharing similarities with mouse ES cells, human ES cell also show differences in DNA damage response, including robust phosphorylation and nuclear localization of CHEK2 and TP53 after irradiation. It is interesting that even though checkpoint signaling is fully activated, ES cells do not arrest in G_1/S phase. G_1 phase of the cell cycle has been argued to be a phase when ES cells are particularly sensitive to differentiation signals, which might explain the absence of G_1/S arrest. Indeed, direct reprogramming of somatic cells by transcription factors appears to eliminate G_1/S arrest of the starting somatic cell population (iPS cells also show absence of G_1/S arrest, and stop

their cycle in G_2/M), suggesting it is a part of PS cell phenotype. The fate of cells that are in G_1 and early S phase at the time of irradiation is unknown, and would be interesting to investigate. One speculation is that these cells would die before reaching G_2 phase. Taking into account the extent of cell death after irradiation this explanation is possible. However, even the cell death of the entire G_1 population after irradiation does not explain the observed level of apoptosis. This further suggests that the cell cycle phase at the time of irradiation is not the only determinant affecting the life and death decision in PS cells. Our results also demonstrate that cells that were in S phase of the cell cycle at the time of irradiation arrest at G_2/M and continue cycling approximately 16 hours after irradiation. We do not know, however, which percentage of initial population of cells in S phase survives and enters G_1 phase after checkpoint recovery.

Another curious observation is that within hours of UV irradiation or exposure to radiomimetic drugs, mouse ES cells decrease expression of pluripotency marker NANOG due to TP53-dependent repression (Lin et al., 2005). However, in this study we show that γ-irradiation results in a temporary reduction in *NANOG* gene expression, and that NANOG mRNA level returns to pre-irradiation level 24 hours later. This suggests that perhaps in human ES cells *NANOG* down-regulation occurs concurrent with TP53 activation (six hours after irradiation), but when TP53 response fades, *NANOG* expression returns to steady state level. It is possible that continuous exposure of ES cells to DNA damaging agents results in long-term TP53 activation and *NANOG* downregulation, which would lead to ES cell differentiation in the presence of persistent DNA damage. However, acute DNA damage that leads to temporary activation of checkpoint signaling and cell cycle arrest may not necessarily induce differentiation of ES cells. In agreement with this hypothesis, ES cells recover one week after irradiation and are able to produce teratomas in immunocompromised mice. Even though iPS cells retain expression of pluripotency markers after irradiation, we have not tested their ability to form teratomas; it would be interesting to determine iPS cells' differentiation potential after DNA damage and contrast it to findings in ES cells. Together, these results suggest that at least some pluripotent stem cells survive irradiation, and raise interesting question of identity of cells that survive and those that undergo apoptosis.

Following checkpoint recovery we observed higher incidence of aberrant mitotic figures, but the origin of these abnormal mitotic spindles in human ES cells remains unknown. The observed defects in mitotic figures are classified to the following categories: misaligned chromosomes, multipolar spindles, lagging chromosomes, and anaphase bridges. Each of these defects may have distinct causes, and need to be further studied. For example, it has been demonstrated that irradiation induces supernumerary mitotic poles due to centrosomes amplification. Indeed, centrosome amplification occurs in numerous tumors and is a potential source of chromosome instability, chromosomal aberrations and aneuploidy. It would be instrumental, then, to investigate the centrosomes cycle following irradiation and establish whether centrosomes undergo duplication in the absence of cellular division and when DNA cycle has been arrested. In general, the issue of mitotic regulation is largely unexplored in ES cells. Mitotic spindles need to be formed in limited space due to tight packing of the cells in the colony, while still allowing accurate segregation of chromosomes between daughter cells. Therefore, future studies need to address mitotic spindle formation and checkpoint function in ES cells.

While ATM function is clearly important for induction of G_2/M cell cycle arrest, our results suggest there is an ATM independent pathway operating in irradiated human ES cells. Following the inhibition of ATM with KU55933, a partial escape from cell cycle arrest can be observed two hours following irradiation of human ES cells, illustrating the role of ATM in cell cycle arrest. However, the escape from G_2/M is not complete, suggesting the existence of an additional cell cycle arrest mechanism. A potential checkpoint target could be Polo-like kinase 1 (PLK1). This kinase is not only an important regulator of mitotic entry, but also necessary for the checkpoint recovery and entry of cells back into the cell cycle after the checkpoint response is completed (Macurek et al., 2008). Importantly, PLK1 was shown to play role in ATM-independent cell cycle arrest in somatic cells (Bassermann et al., 2008). Its expression, localization, and function are unknown in human ES cells, and provide another interesting research topic.

The fact that ES and iPS cells restart the cell cycle by 24 hours post-irradiation implies that DNA damage has been repaired within this time period. The timecourse immunocytochemistry of γ-H2AX demonstrated removal of most of the γ-H2AX foci by six hours after irradiation, which is in agreement with observed high capacity of human ES cells to repair multiple forms of DNA damage. We hypothesized that in the population of self-renewing pluripotent stem cells error-free homologous recombination repair (HRR) would be the primary pathway for repair of double strand breaks (DSB). Both ES and iPS cells form RAD51 foci after irradiation suggesting HRR is taking place. The gene and protein expression analysis revealed higher level of DNA repair transcripts and protein in ES and iPS cells relative to their undifferentiated counterparts. Again, it appears that high capacity of DNA repair is a feature of pluripotent stem cells and participates in maintenance of genomic integrity in this cell type. Interestingly, unlike in mouse ES cells (Banuelos et al., 2008; Tichy et al.), we observe high expression of genes and proteins involved in both HRR and error prone non-homologous end joining (NHEJ). The role of NHEJ in human PS cells remains unknown and it would be beneficial to test the activity of this pathway in human ES cells by inhibiting or down-regulating key players in NHEJ in PS and determining its role in survival of ES cells after irradiation, as well as their ability to differentiate.

Taken together, we demonstrate several approaches to the maintenance of genomic stability in ES cells, including susceptibility to apoptosis in the presence of DNA damage, G_2/M arrest that may favor error free homologous recombination repair of double strand breaks, and high level of expression of proteins involved in repair of multiple forms of DNA damage. Finally, we report that reprogramming of somatic cells significantly alters DNA damage response, which becomes greatly similar to ES cells' behavior after DNA damage, and represents characteristic of pluripotent state.

BIBLIOGRAPHY

Aasen, T., A. Raya, M.J. Barrero, E. Garreta, A. Consiglio, F. Gonzalez, R. Vassena, J. Bilic, V. Pekarik, G. Tiscornia, M. Edel, S. Boue, and J.C. Belmonte. 2008. Efficient and rapid generation of induced pluripotent stem cells from human keratinocytes. *Nat Biotechnol*. 26:1276-1284.

Abraham, R.T. 2001. Cell cycle checkpoint signaling through the ATM and ATR kinases. *Genes Dev*. 15:2177-2196.

Acquaviva, C., and J. Pines. 2006. The anaphase-promoting complex/cyclosome: APC/C. *J Cell Sci*. 119:2401-2404.

Aladjem, M.I., B.T. Spike, L.W. Rodewald, T.J. Hope, M. Klemm, R. Jaenisch, and G.M. Wahl. 1998. ES cells do not activate p53-dependent stress responses and undergo p53-independent apoptosis in response to DNA damage. *Curr Biol*. 8:145-155.

Alexandru, G., F. Uhlmann, K. Mechtler, M.A. Poupart, and K. Nasmyth. 2001. Phosphorylation of the cohesin subunit Scc1 by Polo/Cdc5 kinase regulates sister chromatid separation in yeast. *Cell*. 105:459-472.

Amit, M., M.K. Carpenter, M.S. Inokuma, C.P. Chiu, C.P. Harris, M.A. Waknitz, J. Itskovitz-Eldor, and J.A. Thomson. 2000. Clonally derived human embryonic stem cell lines maintain pluripotency and proliferative potential for prolonged periods of culture. *Dev Biol*. 227:271-278.

Anderson, C.W., and S.P. Lees-Miller. 1992. The nuclear serine/threonine protein kinase DNA-PK. *Crit Rev Eukaryot Gene Expr*. 2:283-314.

Andrews, P.W., P.N. Goodfellow, L.H. Shevinsky, D.L. Bronson, and B.B. Knowles. 1982. Cell-surface antigens of a clonal human embryonal carcinoma cell line: morphological and antigenic differentiation in culture. *Int J Cancer*. 29:523-531.

Aoi, T., K. Yae, M. Nakagawa, T. Ichisaka, K. Okita, K. Takahashi, T. Chiba, and S. Yamanaka. 2008. Generation of pluripotent stem cells from adult mouse liver and stomach cells. *Science*. 321:699-702.

Arata, Y., M. Fujita, K. Ohtani, S. Kijima, and J.Y. Kato. 2000. Cdk2-dependent and -independent pathways in E2F-mediated S phase induction. *J Biol Chem*. 275:6337-6345.

Atherton-Fessler, S., L.L. Parker, R.L. Geahlen, and H. Piwnica-Worms. 1993. Mechanisms of p34cdc2 regulation. *Mol Cell Biol*. 13:1675-1685.

Atkin, N.B., M.C. Baker, R. Robinson, and S.E. Gaze. 1974. Chromosome studies on 14 near-diploid carcinomas of the ovary. *Eur J Cancer*. 10:144-146.

Babaie, Y., R. Herwig, B. Greber, T.C. Brink, W. Wruck, D. Groth, H. Lehrach, T. Burdon, and J. Adjaye. 2007. Analysis of Oct4-dependent transcriptional networks regulating self-renewal and pluripotency in human embryonic stem cells. *Stem Cells*. 25:500-510.

Bakkenist, C.J., and M.B. Kastan. 2003. DNA damage activates ATM through intermolecular autophosphorylation and dimer dissociation. *Nature*. 421:499-506.

Banath, J.P., C.A. Banuelos, D. Klokov, S.M. MacPhail, P.M. Lansdorp, and P.L. Olive. 2009. Explanation for excessive DNA single-strand breaks and endogenous repair foci in pluripotent mouse embryonic stem cells. *Exp Cell Res*. 315:1505-1520.

Banin, S., L. Moyal, S. Shieh, Y. Taya, C.W. Anderson, L. Chessa, N.I. Smorodinsky, C. Prives, Y. Reiss, Y. Shiloh, and Y. Ziv. 1998. Enhanced phosphorylation of p53 by ATM in response to DNA damage. *Science*. 281:1674-1677.

Banuelos, C.A., J.P. Banath, S.H. Macphail, J. Zhao, C.A. Eaves, M.D. O'Connor, P.M. Lansdorp, and P.L. Olive. 2008. Mouse but not human embryonic stem cells are deficient in rejoining of ionizing radiation-induced DNA double-strand breaks. *DNA Repair (Amst)*. 7:1471-1483.

Barnes, D.E., G. Stamp, I. Rosewell, A. Denzel, and T. Lindahl. 1998. Targeted disruption of the gene encoding DNA ligase IV leads to lethality in embryonic mice. *Curr Biol*. 8:1395-1398.

Bassermann, F., D. Frescas, D. Guardavaccaro, L. Busino, A. Peschiaroli, and M. Pagano. 2008. The Cdc14B-Cdh1-Plk1 axis controls the G2 DNA-damage-response checkpoint. *Cell*. 134:256-267.

Bassing, C.H., K.F. Chua, J. Sekiguchi, H. Suh, S.R. Whitlow, J.C. Fleming, B.C. Monroe, D.N. Ciccone, C. Yan, K. Vlasakova, D.M. Livingston, D.O. Ferguson, R. Scully, and F.W. Alt. 2002. Increased ionizing radiation sensitivity and genomic instability in the absence of histone H2AX. *Proc Natl Acad Sci U S A*. 99:8173-8178.

Baumann, P., F.E. Benson, and S.C. West. 1996. Human Rad51 protein promotes ATP-dependent homologous pairing and strand transfer reactions in vitro. *Cell*. 87:757-766.

Baumann, P., and S.C. West. 1999. Heteroduplex formation by human Rad51 protein: effects of DNA end-structure, hRP-A and hRad52. *J Mol Biol*. 291:363-374.

Beattie, G.M., A.D. Lopez, N. Bucay, A. Hinton, M.T. Firpo, C.C. King, and A. Hayek. 2005. Activin A maintains pluripotency of human embryonic stem cells in the absence of feeder layers. *Stem Cells*. 23:489-495.

Becker, K.A., P.N. Ghule, J.A. Therrien, J.B. Lian, J.L. Stein, A.J. van Wijnen, and G.S. Stein. 2006. Self-renewal of human embryonic stem cells is supported by a shortened G1 cell cycle phase. *J Cell Physiol*. 209:883-893.

Becker, K.A., J.L. Stein, J.B. Lian, A.J. van Wijnen, and G.S. Stein. 2007. Establishment of histone gene regulation and cell cycle checkpoint control in human embryonic stem cells. *J Cell Physiol*. 210:517-526.

Benson, F.E., P. Baumann, and S.C. West. 1998. Synergistic actions of Rad51 and Rad52 in recombination and DNA repair. *Nature*. 391:401-404.

Bertocci, B., A. De Smet, J.C. Weill, and C.A. Reynaud. 2006. Nonoverlapping functions of DNA polymerases mu, lambda, and terminal deoxynucleotidyltransferase during immunoglobulin V(D)J recombination in vivo. *Immunity*. 25:31-41.

Blangy, A., H.A. Lane, P. d'Herin, M. Harper, M. Kress, and E.A. Nigg. 1995. Phosphorylation by p34cdc2 regulates spindle association of human Eg5, a kinesin-related motor essential for bipolar spindle formation in vivo. *Cell*. 83:1159-1169.

Bongso, A., C.Y. Fong, S.C. Ng, and S. Ratnam. 1994. Isolation and culture of inner cell mass cells from human blastocysts. *Hum Reprod*. 9:2110-2117.

Booher, R.N., P.S. Holman, and A. Fattaey. 1997. Human Myt1 is a cell cycle-regulated kinase that inhibits Cdc2 but not Cdk2 activity. *J Biol Chem*. 272:22300-22306.

Boulton, S.J., and S.P. Jackson. 1998. Components of the Ku-dependent non-homologous end-joining pathway are involved in telomeric length maintenance and telomeric silencing. *Embo J*. 17:1819-1828.

Boyer, L.A., T.I. Lee, M.F. Cole, S.E. Johnstone, S.S. Levine, J.P. Zucker, M.G. Guenther, R.M. Kumar, H.L. Murray, R.G. Jenner, D.K. Gifford, D.A. Melton, R. Jaenisch, and R.A. Young. 2005. Core transcriptional regulatory circuitry in human embryonic stem cells. *Cell*. 122:947-956.

Bradley, A., M. Evans, M.H. Kaufman, and E. Robertson. 1984. Formation of germ-line chimaeras from embryo-derived teratocarcinoma cell lines. *Nature*. 309:255-256.

Branzei, D., and M. Foiani. 2008. Regulation of DNA repair throughout the cell cycle. *Nat Rev Mol Cell Biol*. 9:297-308.

Bressan, D.A., B.K. Baxter, and J.H. Petrini. 1999. The Mre11-Rad50-Xrs2 protein complex facilitates homologous recombination-based double-strand break repair in Saccharomyces cerevisiae. *Mol Cell Biol*. 19:7681-7687.

Brons, I.G., L.E. Smithers, M.W. Trotter, P. Rugg-Gunn, B. Sun, S.M. Chuva de Sousa Lopes, S.K. Howlett, A. Clarkson, L. Ahrlund-Richter, R.A. Pedersen, and L. Vallier. 2007. Derivation of pluripotent epiblast stem cells from mammalian embryos. *Nature*. 448:191-195.

Budman, J., and G. Chu. 2005. Processing of DNA for nonhomologous end-joining by cell-free extract. *Embo J*. 24:849-860.

Bunz, F., A. Dutriaux, C. Lengauer, T. Waldman, S. Zhou, J.P. Brown, J.M. Sedivy, K.W. Kinzler, and B. Vogelstein. 1998. Requirement for p53 and p21 to sustain G2 arrest after DNA damage. *Science*. 282:1497-1501.

Burdon, T., C. Stracey, I. Chambers, J. Nichols, and A. Smith. 1999. Suppression of SHP-2 and ERK signalling promotes self-renewal of mouse embryonic stem cells. *Dev Biol*. 210:30-43.

Byrne, J.A., D.A. Pedersen, L.L. Clepper, M. Nelson, W.G. Sanger, S. Gokhale, D.P. Wolf, and S.M. Mitalipov. 2007. Producing primate embryonic stem cells by somatic cell nuclear transfer. *Nature*. 450:497-502.

Campbell, K.H., J. McWhir, W.A. Ritchie, and I. Wilmut. 1996. Sheep cloned by nuclear transfer from a cultured cell line. *Nature*. 380:64-66.

Canman, C.E., D.S. Lim, K.A. Cimprich, Y. Taya, K. Tamai, K. Sakaguchi, E. Appella, M.B. Kastan, and J.D. Siliciano. 1998. Activation of the ATM kinase by ionizing radiation and phosphorylation of p53. *Science*. 281:1677-1679.

Carney, J.P., R.S. Maser, H. Olivares, E.M. Davis, M. Le Beau, J.R. Yates, 3rd, L. Hays, W.F. Morgan, and J.H. Petrini. 1998. The hMre11/hRad50 protein complex and Nijmegen breakage syndrome: linkage of double-strand break repair to the cellular DNA damage response. *Cell*. 93:477-486.

Cartwright, P., C. McLean, A. Sheppard, D. Rivett, K. Jones, and S. Dalton. 2005. LIF/STAT3 controls ES cell self-renewal and pluripotency by a Myc-dependent mechanism. *Development*. 132:885-896.

Celeste, A., S. Petersen, P.J. Romanienko, O. Fernandez-Capetillo, H.T. Chen, O.A. Sedelnikova, B. Reina-San-Martin, V. Coppola, E. Meffre, M.J. Difilippantonio, C. Redon, D.R. Pilch, A. Olaru, M. Eckhaus, R.D. Camerini-Otero, L. Tessarollo, F. Livak, K. Manova, W.M. Bonner, M.C. Nussenzweig, and A. Nussenzweig. 2002. Genomic instability in mice lacking histone H2AX. *Science*. 296:922-927.

Chae, H.D., J. Yun, Y.J. Bang, and D.Y. Shin. 2004. Cdk2-dependent phosphorylation of the NF-Y transcription factor is essential for the expression of the cell cycle-regulatory genes and cell cycle G1/S and G2/M transitions. *Oncogene*. 23:4084-4088.

Chambers, I., D. Colby, M. Robertson, J. Nichols, S. Lee, S. Tweedie, and A. Smith. 2003. Functional expression cloning of Nanog, a pluripotency sustaining factor in embryonic stem cells. *Cell*. 113:643-655.

Chan, D.W., and S.P. Lees-Miller. 1996. The DNA-dependent protein kinase is inactivated by autophosphorylation of the catalytic subunit. *J Biol Chem*. 271:8936-8941.

Chan, E.H., A. Santamaria, H.H. Sillje, and E.A. Nigg. 2008. Plk1 regulates mitotic Aurora A function through betaTrCP-dependent degradation of hBora. *Chromosoma*. 117:457-469.

Chappell, C., L.A. Hanakahi, F. Karimi-Busheri, M. Weinfeld, and S.C. West. 2002. Involvement of human polynucleotide kinase in double-strand break repair by non-homologous end joining. *Embo J*. 21:2827-2832.

Chehab, N.H., A. Malikzay, E.S. Stavridi, and T.D. Halazonetis. 1999. Phosphorylation of Ser-20 mediates stabilization of human p53 in response to DNA damage. *Proc Natl Acad Sci U S A*. 96:13777-13782.

Chuykin, I.A., M.S. Lianguzova, T.V. Pospelova, and V.A. Pospelov. 2008. Activation of DNA damage response signaling in mouse embryonic stem cells. *Cell Cycle*. 7:2922-2928.

Ciciarello, M., R. Mangiacasale, M. Casenghi, M. Zaira Limongi, M. D'Angelo, S. Soddu, P. Lavia, and E. Cundari. 2001. p53 displacement from centrosomes and p53-mediated G1 arrest following transient inhibition of the mitotic spindle. *J Biol Chem*. 276:19205-19213.

Cortez, D., Y. Wang, J. Qin, and S.J. Elledge. 1999. Requirement of ATM-dependent phosphorylation of brca1 in the DNA damage response to double-strand breaks. *Science*. 286:1162-1166.

Davis, B.J., J.M. Havener, and D.A. Ramsden. 2008. End-bridging is required for pol mu to efficiently promote repair of noncomplementary ends by nonhomologous end joining. *Nucleic Acids Res*. 36:3085-3094.

Davis, R.L., H. Weintraub, and A.B. Lassar. 1987. Expression of a single transfected cDNA converts fibroblasts to myoblasts. *Cell*. 51:987-1000.

Delacote, F., M. Han, T.D. Stamato, M. Jasin, and B.S. Lopez. 2002. An xrcc4 defect or Wortmannin stimulates homologous recombination specifically induced by double-strand breaks in mammalian cells. *Nucleic Acids Res*. 30:3454-3463.

Deng, W., and Y. Xu. 2009. Genome integrity: linking pluripotency and tumorgenicity. *Trends Genet*. 25:425-427.

Dimos, J.T., K.T. Rodolfa, K.K. Niakan, L.M. Weisenthal, H. Mitsumoto, W. Chung, G.F. Croft, G. Saphier, R. Leibel, R. Goland, H. Wichterle, C.E. Henderson, and K. Eggan. 2008. Induced pluripotent stem cells generated from patients with ALS can be differentiated into motor neurons. *Science*. 321:1218-1221.

Ding, Q., Y.V. Reddy, W. Wang, T. Woods, P. Douglas, D.A. Ramsden, S.P. Lees-Miller, and K. Meek. 2003. Autophosphorylation of the catalytic subunit of the DNA-dependent protein kinase is required for efficient end processing during DNA double-strand break repair. *Mol Cell Biol*. 23:5836-5848.

Douglas, P., S. Gupta, N. Morrice, K. Meek, and S.P. Lees-Miller. 2005. DNA-PK-dependent phosphorylation of Ku70/80 is not required for non-homologous end joining. *DNA Repair (Amst)*. 4:1006-1018.

Doxsey, S.J. 2001. Centrosomes as command centres for cellular control. *Nat Cell Biol*. 3:E105-108.

Dynlacht, B.D., O. Flores, J.A. Lees, and E. Harlow. 1994. Differential regulation of E2F transactivation by cyclin/cdk2 complexes. *Genes Dev*. 8:1772-1786.

Ebert, A.D., J. Yu, F.F. Rose, Jr., V.B. Mattis, C.L. Lorson, J.A. Thomson, and C.N. Svendsen. 2009. Induced pluripotent stem cells from a spinal muscular atrophy patient. *Nature*. 457:277-280.

el-Deiry, W.S., T. Tokino, V.E. Velculescu, D.B. Levy, R. Parsons, J.M. Trent, D. Lin, W.E. Mercer, K.W. Kinzler, and B. Vogelstein. 1993. WAF1, a potential mediator of p53 tumor suppression. *Cell*. 75:817-825.

Essers, J., R.W. Hendriks, S.M. Swagemakers, C. Troelstra, J. de Wit, D. Bootsma, J.H. Hoeijmakers, and R. Kanaar. 1997. Disruption of mouse RAD54 reduces ionizing radiation resistance and homologous recombination. *Cell*. 89:195-204.

Evans, M.J., and M.H. Kaufman. 1981. Establishment in culture of pluripotential cells from mouse embryos. *Nature*. 292:154-156.

Falck, J., N. Mailand, R.G. Syljuasen, J. Bartek, and J. Lukas. 2001. The ATM-Chk2-Cdc25A checkpoint pathway guards against radioresistant DNA synthesis. *Nature*. 410:842-847.

Ferguson, D.O., and W.K. Holloman. 1996. Recombinational repair of gaps in DNA is asymmetric in Ustilago maydis and can be explained by a migrating D-loop model. *Proc Natl Acad Sci U S A*. 93:5419-5424.

Finnie, N.J., T.M. Gottlieb, T. Blunt, P.A. Jeggo, and S.P. Jackson. 1995. DNA-dependent protein kinase activity is absent in xrs-6 cells: implications for site-specific recombination and DNA double-strand break repair. *Proc Natl Acad Sci U S A*. 92:320-324.

Fluckiger, A.C., G. Marcy, M. Marchand, D. Negre, F.L. Cosset, S. Mitalipov, D. Wolf, P. Savatier, and C. Dehay. 2006. Cell cycle features of primate embryonic stem cells. *Stem Cells*. 24:547-556.

Fong, H., K.A. Hohenstein, and P.J. Donovan. 2008. Regulation of self-renewal and pluripotency by Sox2 in human embryonic stem cells. *Stem Cells*. 26:1931-1938.

Forsburg, S.L. 2000. Cell Cycle Lecture Notes. Vol. 2010.

Fouse, S.D., Y. Shen, M. Pellegrini, S. Cole, A. Meissner, L. Van Neste, R. Jaenisch, and G. Fan. 2008. Promoter CpG methylation contributes to ES cell gene regulation in parallel with Oct4/Nanog, PcG complex, and histone H3 K4/K27 trimethylation. *Cell Stem Cell*. 2:160-169.

Frank-Vaillant, M., and S. Marcand. 2002. Transient stability of DNA ends allows nonhomologous end joining to precede homologous recombination. *Mol Cell*. 10:1189-1199.

Frank, K.M., N.E. Sharpless, Y. Gao, J.M. Sekiguchi, D.O. Ferguson, C. Zhu, J.P. Manis, J. Horner, R.A. DePinho, and F.W. Alt. 2000. DNA ligase IV deficiency in mice leads to defective neurogenesis and embryonic lethality via the p53 pathway. *Mol Cell*. 5:993-1002.

Friedberg Errol C, W.G.C., Siede Wolfram, Wood Richard D, Schultz Roger A, Ellenberger Tom. 2006. DNA Repair and Mutagenesis. ASM Press. 1118 pp.

Fujikura, J., E. Yamato, S. Yonemura, K. Hosoda, S. Masui, K. Nakao, J. Miyazaki Ji, and H. Niwa. 2002. Differentiation of embryonic stem cells is induced by GATA factors. *Genes Dev*. 16:784-789.

Fukushima, T., M. Takata, C. Morrison, R. Araki, A. Fujimori, M. Abe, K. Tatsumi, M. Jasin, P.K. Dhar, E. Sonoda, T. Chiba, and S. Takeda. 2001. Genetic analysis of the DNA-dependent protein kinase reveals an inhibitory role of Ku in late S-G2 phase DNA double-strand break repair. *J Biol Chem*. 276:44413-44418.

Furnari, B., A. Blasina, M.N. Boddy, C.H. McGowan, and P. Russell. 1999. Cdc25 inhibited in vivo and in vitro by checkpoint kinases Cds1 and Chk1. *Mol Biol Cell*. 10:833-845.

Gachelin, G., R. Kemler, F. Kelly, and F. Jacob. 1977. PCC4, a new cell surface antigen common to multipotential embryonal carcinoma cells, spermatozoa, and mouse early embryos. *Dev Biol*. 57:199-209.

Gao, Y., J. Chaudhuri, C. Zhu, L. Davidson, D.T. Weaver, and F.W. Alt. 1998. A targeted DNA-PKcs-null mutation reveals DNA-PK-independent functions for KU in V(D)J recombination. *Immunity*. 9:367-376.

Gatei, M., D. Young, K.M. Cerosaletti, A. Desai-Mehta, K. Spring, S. Kozlov, M.F. Lavin, R.A. Gatti, P. Concannon, and K. Khanna. 2000. ATM-dependent phosphorylation of nibrin in response to radiation exposure. *Nat Genet*. 25:115-119.

Giono, L.E., and J.J. Manfredi. 2006. The p53 tumor suppressor participates in multiple cell cycle checkpoints. *J Cell Physiol*. 209:13-20.

Goodhead, D.T. 1989. The initial physical damage produced by ionizing radiations. *Int J Radiat Biol*. 56:623-634.

Gottlieb, T.M., and S.P. Jackson. 1993. The DNA-dependent protein kinase: requirement for DNA ends and association with Ku antigen. *Cell*. 72:131-142.

Gould, K.L., and P. Nurse. 1989. Tyrosine phosphorylation of the fission yeast cdc2+ protein kinase regulates entry into mitosis. *Nature*. 342:39-45.

Grawunder, U., M. Wilm, X. Wu, P. Kulesza, T.E. Wilson, M. Mann, and M.R. Lieber. 1997. Activity of DNA ligase IV stimulated by complex formation with XRCC4 protein in mammalian cells. *Nature*. 388:492-495.

Grawunder, U., D. Zimmer, and M.R. Leiber. 1998. DNA ligase IV binds to XRCC4 via a motif located between rather than within its BRCT domains. *Curr Biol*. 8:873-876.

Greber, B., H. Lehrach, and J. Adjaye. 2007. Fibroblast growth factor 2 modulates transforming growth factor beta signaling in mouse embryonic fibroblasts and human ESCs (hESCs) to support hESC self-renewal. *Stem Cells*. 25:455-464.

Gu, Y., S. Jin, Y. Gao, D.T. Weaver, and F.W. Alt. 1997. Ku70-deficient embryonic stem cells have increased ionizing radiosensitivity, defective DNA end-binding activity, and inability to support V(D)J recombination. *Proc Natl Acad Sci U S A*. 94:8076-8081.

Guo, Z., A. Kumagai, S.X. Wang, and W.G. Dunphy. 2000. Requirement for Atr in phosphorylation of Chk1 and cell cycle regulation in response to DNA replication blocks and UV-damaged DNA in Xenopus egg extracts. *Genes Dev*. 14:2745-2756.

Gupta, R.C., L.R. Bazemore, E.I. Golub, and C.M. Radding. 1997. Activities of human recombination protein Rad51. *Proc Natl Acad Sci U S A*. 94:463-468.

Gurdon, J.B., and V. Uehlinger. 1966. "Fertile" intestine nuclei. *Nature*. 210:1240-1241.

Haber, J.E. 2000. Partners and pathwaysrepairing a double-strand break. *Trends Genet*. 16:259-264.

Hanna, J., S. Markoulaki, P. Schorderet, B.W. Carey, C. Beard, M. Wernig, M.P. Creyghton, E.J. Steine, J.P. Cassady, R. Foreman, C.J. Lengner, J.A. Dausman, and R. Jaenisch. 2008. Direct reprogramming of terminally differentiated mature B lymphocytes to pluripotency. *Cell*. 133:250-264.

Hanna, J., M. Wernig, S. Markoulaki, C.W. Sun, A. Meissner, J.P. Cassady, C. Beard, T. Brambrink, L.C. Wu, T.M. Townes, and R. Jaenisch. 2007. Treatment of sickle cell anemia mouse model with iPS cells generated from autologous skin. *Science*. 318:1920-1923.

Hansis, C., J.A. Grifo, and L.C. Krey. 2000. Oct-4 expression in inner cell mass and trophectoderm of human blastocysts. *Mol Hum Reprod*. 6:999-1004.

Harper, J.W., G.R. Adami, N. Wei, K. Keyomarsi, and S.J. Elledge. 1993. The p21 Cdk-interacting protein Cip1 is a potent inhibitor of G1 cyclin-dependent kinases. *Cell*. 75:805-816.

Hart, A.H., L. Hartley, M. Ibrahim, and L. Robb. 2004. Identification, cloning and expression analysis of the pluripotency promoting Nanog genes in mouse and human. *Dev Dyn*. 230:187-198.

Hermeking, H., C. Lengauer, K. Polyak, T.C. He, L. Zhang, S. Thiagalingam, K.W. Kinzler, and B. Vogelstein. 1997. 14-3-3 sigma is a p53-regulated inhibitor of G2/M progression. *Mol Cell*. 1:3-11.

Hickson, I., Y. Zhao, C.J. Richardson, S.J. Green, N.M. Martin, A.I. Orr, P.M. Reaper, S.P. Jackson, N.J. Curtin, and G.C. Smith. 2004. Identification and characterization of a novel and specific inhibitor of the ataxia-telangiectasia mutated kinase ATM. *Cancer Res*. 64:9152-9159.

Hirao, A., Y.Y. Kong, S. Matsuoka, A. Wakeham, J. Ruland, H. Yoshida, D. Liu, S.J. Elledge, and T.W. Mak. 2000. DNA damage-induced activation of p53 by the checkpoint kinase Chk2. *Science*. 287:1824-1827.

Hochedlinger, K., and K. Plath. 2009. Epigenetic reprogramming and induced pluripotency. *Development*. 136:509-523.

Hoffmann, I., P.R. Clarke, M.J. Marcote, E. Karsenti, and G. Draetta. 1993. Phosphorylation and activation of human cdc25-C by cdc2--cyclin B and its involvement in the self-amplification of MPF at mitosis. *Embo J*. 12:53-63.

Hogan, B., M. Fellous, P. Avner, and F. Jacob. 1977. Isolation of a human teratoma cell line which expresses F9 antigen. *Nature*. 270:515-518.

Hong, H., K. Takahashi, T. Ichisaka, T. Aoi, O. Kanagawa, M. Nakagawa, K. Okita, and S. Yamanaka. 2009. Suppression of induced pluripotent stem cell generation by the p53-p21 pathway. *Nature*. 460:1132-1135.

Hong, Y., R.B. Cervantes, E. Tichy, J.A. Tischfield, and P.J. Stambrook. 2006. Protecting genomic integrity in somatic cells and embryonic stem cells. *Mutat Res*.

Hong, Y., and P.J. Stambrook. 2004. Restoration of an absent G1 arrest and protection from apoptosis in embryonic stem cells after ionizing radiation. *Proc Natl Acad Sci U S A*. 101:14443-14448.

Hooker, C.W., and P.J. Hurlin. 2006. Of Myc and Mnt. *J Cell Sci*. 119:208-216.

Hsu, L.C., and R.L. White. 1998. BRCA1 is associated with the centrosome during mitosis. *Proc Natl Acad Sci U S A*. 95:12983-12988.

Hutchinson, F. 1985. Chemical changes induced in DNA by ionizing radiation. *Prog Nucleic Acid Res Mol Biol*. 32:115-154.

Hutterer, A., D. Berdnik, F. Wirtz-Peitz, M. Zigman, A. Schleiffer, and J.A. Knoblich. 2006. Mitotic activation of the kinase Aurora-A requires its binding partner Bora. *Dev Cell*. 11:147-157.

Hyslop, L., M. Stojkovic, L. Armstrong, T. Walter, P. Stojkovic, S. Przyborski, M. Herbert, A. Murdoch, T. Strachan, and M. Lako. 2005. Downregulation of NANOG induces differentiation of human embryonic stem cells to extraembryonic lineages. *Stem Cells*. 23:1035-1043.

Inoue, D., and N. Sagata. 2005. The Polo-like kinase Plx1 interacts with and inhibits Myt1 after fertilization of Xenopus eggs. *Embo J*. 24:1057-1067.

Ivanova, N., R. Dobrin, R. Lu, I. Kotenko, J. Levorse, C. DeCoste, X. Schafer, Y. Lun, and I.R. Lemischka. 2006. Dissecting self-renewal in stem cells with RNA interference. *Nature*. 442:533-538.

Jackson, S.P. 2001. Detecting, signalling and repairing DNA double-strand breaks. *Biochem Soc Trans*. 29:655-661.

Jackson, S.P. 2002. Sensing and repairing DNA double-strand breaks. *Carcinogenesis*. 23:687-696.

James, D., A.J. Levine, D. Besser, and A. Hemmati-Brivanlou. 2005. TGFbeta/activin/nodal signaling is necessary for the maintenance of pluripotency in human embryonic stem cells. *Development*. 132:1273-1282.

Jin, S., S. Inoue, and D.T. Weaver. 1998. Differential etoposide sensitivity of cells deficient in the Ku and DNA-PKcs components of the DNA-dependent protein kinase. *Carcinogenesis*. 19:965-971.

Kahan, B.W., and B. Ephrussi. 1970. Developmental potentialities of clonal in vitro cultures of mouse testicular teratoma. *J Natl Cancer Inst*. 44:1015-1036.

Kannagi, R., N.A. Cochran, F. Ishigami, S. Hakomori, P.W. Andrews, B.B. Knowles, and D. Solter. 1983. Stage-specific embryonic antigens (SSEA-3 and -4) are epitopes of a unique globo-series ganglioside isolated from human teratocarcinoma cells. *Embo J*. 2:2355-2361.

Karagiannis, T.C., and A. El-Osta. 2004. Double-strand breaks: signaling pathways and repair mechanisms. *Cell Mol Life Sci*. 61:2137-2147.

Karimi-Busheri, F., A. Rasouli-Nia, J. Allalunis-Turner, and M. Weinfeld. 2007. Human polynucleotide kinase participates in repair of DNA double-strand breaks by nonhomologous end joining but not homologous recombination. *Cancer Res*. 67:6619-6625.

Kawamura, T., J. Suzuki, Y.V. Wang, S. Menendez, L.B. Morera, A. Raya, G.M. Wahl, and J.C. Belmonte. 2009. Linking the p53 tumour suppressor pathway to somatic cell reprogramming. *Nature*. 460:1140-1144.

Keenen, B., and I.L. de la Serna. 2009. Chromatin remodeling in embryonic stem cells: regulating the balance between pluripotency and differentiation. *J Cell Physiol*. 219:1-7.

Keirstead, H.S., G. Nistor, G. Bernal, M. Totoiu, F. Cloutier, K. Sharp, and O. Steward. 2005. Human embryonic stem cell-derived oligodendrocyte progenitor cell transplants remyelinate and restore locomotion after spinal cord injury. *J Neurosci*. 25:4694-4705.

Khanna, K.K., and S.P. Jackson. 2001. DNA double-strand breaks: signaling, repair and the cancer connection. *Nat Genet*. 27:247-254.

Kim, J.B., H. Zaehres, G. Wu, L. Gentile, K. Ko, V. Sebastiano, M.J. Arauzo-Bravo, D. Ruau, D.W. Han, M. Zenke, and H.R. Scholer. 2008. Pluripotent stem cells induced from adult neural stem cells by reprogramming with two factors. *Nature*. 454:646-650.

Kimura, K., M. Hirano, R. Kobayashi, and T. Hirano. 1998. Phosphorylation and activation of 13S condensin by Cdc2 in vitro. *Science*. 282:487-490.

Kironmai, K.M., and K. Muniyappa. 1997. Alteration of telomeric sequences and senescence caused by mutations in RAD50 of Saccharomyces cerevisiae. *Genes Cells*. 2:443-455.

Kleinsmith, L.J., and G.B. Pierce, Jr. 1964. Multipotentiality Of Single Embryonal Carcinoma Cells. *Cancer Res*. 24:1544-1551.

Knowles, B.B., D.P. Aden, and D. Solter. 1978. Monoclonal antibody detecting a stage-specific embryonic antigen (SSEA-1) on preimplantation mouse embryos and teratocarcinoma cells. *Curr Top Microbiol Immunol*. 81:51-53.

Kramer, A., N. Mailand, C. Lukas, R.G. Syljuasen, C.J. Wilkinson, E.A. Nigg, J. Bartek, and J. Lukas. 2004. Centrosome-associated Chk1 prevents premature activation of cyclin-B-Cdk1 kinase. *Nat Cell Biol*. 6:884-891.

Labosky, P.A., D.P. Barlow, and B.L. Hogan. 1994. Mouse embryonic germ (EG) cell lines: transmission through the germline and differences in the methylation imprint of insulin-like growth factor 2

receptor (Igf2r) gene compared with embryonic stem (ES) cell lines. *Development*. 120:3197-3204.

Lamba, D.A., J. Gust, and T.A. Reh. 2009. Transplantation of human embryonic stem cell-derived photoreceptors restores some visual function in Crx-deficient mice. *Cell Stem Cell*. 4:73-79.

Larsen, W. 2001. Human Embryology. CHURCHILL LIVINGSTONE. 548 pp.

Lavin, M.F., G. Birrell, P. Chen, S. Kozlov, S. Scott, and N. Gueven. 2005. ATM signaling and genomic stability in response to DNA damage. *Mutat Res*. 569:123-132.

Lee, S.E., R.A. Mitchell, A. Cheng, and E.A. Hendrickson. 1997. Evidence for DNA-PK-dependent and -independent DNA double-strand break repair pathways in mammalian cells as a function of the cell cycle. *Mol Cell Biol*. 17:1425-1433.

Lees-Miller, S.P., and K. Meek. 2003. Repair of DNA double strand breaks by non-homologous end joining. *Biochimie*. 85:1161-1173.

Lewis, L.K., F. Storici, S. Van Komen, S. Calero, P. Sung, and M.A. Resnick. 2004. Role of the nuclease activity of Saccharomyces cerevisiae Mre11 in repair of DNA double-strand breaks in mitotic cells. *Genetics*. 166:1701-1713.

Li, G., C. Nelsen, and E.A. Hendrickson. 2002. Ku86 is essential in human somatic cells. *Proc Natl Acad Sci U S A*. 99:832-837.

Li, H., M. Collado, A. Villasante, K. Strati, S. Ortega, M. Canamero, M.A. Blasco, and M. Serrano. 2009. The Ink4/Arf locus is a barrier for iPS cell reprogramming. *Nature*. 460:1136-1139.

Li, S., N.S. Ting, L. Zheng, P.L. Chen, Y. Ziv, Y. Shiloh, E.Y. Lee, and W.H. Lee. 2000. Functional link of BRCA1 and ataxia telangiectasia gene product in DNA damage response. *Nature*. 406:210-215.

Li, Z., T. Otevrel, Y. Gao, H.L. Cheng, B. Seed, T.D. Stamato, G.E. Taccioli, and F.W. Alt. 1995. The XRCC4 gene encodes a novel protein involved in DNA double-strand break repair and V(D)J recombination. *Cell*. 83:1079-1089.

Lieber, M.R., Y. Ma, U. Pannicke, and K. Schwarz. 2003. Mechanism and regulation of human non-homologous DNA end-joining. *Nat Rev Mol Cell Biol*. 4:712-720.

Lim, D.S., and P. Hasty. 1996. A mutation in mouse rad51 results in an early embryonic lethal that is suppressed by a mutation in p53. *Mol Cell Biol*. 16:7133-7143.

Lim, D.S., S.T. Kim, B. Xu, R.S. Maser, J. Lin, J.H. Petrini, and M.B. Kastan. 2000. ATM phosphorylates p95/nbs1 in an S-phase checkpoint pathway. *Nature*. 404:613-617.

Lin, T., C. Chao, S. Saito, S.J. Mazur, M.E. Murphy, E. Appella, and Y. Xu. 2005. p53 induces differentiation of mouse embryonic stem cells by suppressing Nanog expression. *Nat Cell Biol*. 7:165-171.

Liu, F., J.J. Stanton, Z. Wu, and H. Piwnica-Worms. 1997. The human Myt1 kinase preferentially phosphorylates Cdc2 on threonine 14 and localizes to the endoplasmic reticulum and Golgi complex. *Mol Cell Biol*. 17:571-583.

Loffler, H., J. Lukas, J. Bartek, and A. Kramer. 2006. Structure meets function--centrosomes, genome maintenance and the DNA damage response. *Experimental Cell Research*. 312:2633-2640.

Loh, Y.H., S. Agarwal, I.H. Park, A. Urbach, H. Huo, G.C. Heffner, K. Kim, J.D. Miller, K. Ng, and G.Q. Daley. 2009. Generation of induced pluripotent stem cells from human blood. *Blood*. 113:5476-5479.

Ludwig, T.E., M.E. Levenstein, J.M. Jones, W.T. Berggren, E.R. Mitchen, J.L. Frane, L.J. Crandall, C.A. Daigh, K.R. Conard, M.S. Piekarczyk, R.A. Llanas, and J.A. Thomson. 2006. Derivation of human embryonic stem cells in defined conditions. *Nat Biotechnol*. 24:185-187.

Lukas, C., J. Falck, J. Bartkova, J. Bartek, and J. Lukas. 2003. Distinct spatiotemporal dynamics of mammalian checkpoint regulators induced by DNA damage. *Nat Cell Biol*. 5:255-260.

Lukas, C., F. Melander, M. Stucki, J. Falck, S. Bekker-Jensen, M. Goldberg, Y. Lerenthal, S.P. Jackson, J. Bartek, and J. Lukas. 2004. Mdc1 couples DNA double-strand break recognition by Nbs1 with its H2AX-dependent chromatin retention. *Embo J*. 23:2674-2683.

Lukaszewicz, A., P. Savatier, V. Cortay, P. Giroud, C. Huissoud, M. Berland, H. Kennedy, and C. Dehay. 2005. G1 phase regulation, area-specific cell cycle control, and cytoarchitectonics in the primate cortex. *Neuron*. 47:353-364.

Luo, G., M.S. Yao, C.F. Bender, M. Mills, A.R. Bladl, A. Bradley, and J.H. Petrini. 1999. Disruption of mRad50 causes embryonic stem cell lethality, abnormal embryonic development, and sensitivity to ionizing radiation. *Proc Natl Acad Sci U S A*. 96:7376-7381.

Ma, Y., U. Pannicke, H. Lu, D. Niewolik, K. Schwarz, and M.R. Lieber. 2005a. The DNA-dependent protein kinase catalytic subunit phosphorylation sites in human Artemis. *J Biol Chem*. 280:33839-33846.

Ma, Y., U. Pannicke, K. Schwarz, and M.R. Lieber. 2002. Hairpin opening and overhang processing by an Artemis/DNA-dependent protein kinase complex in nonhomologous end joining and V(D)J recombination. *Cell*. 108:781-794.

Ma, Y., K. Schwarz, and M.R. Lieber. 2005b. The Artemis:DNA-PKcs endonuclease cleaves DNA loops, flaps, and gaps. *DNA Repair (Amst)*. 4:845-851.

Macurek, L., A. Lindqvist, D. Lim, M.A. Lampson, R. Klompmaker, R. Freire, C. Clouin, S.S. Taylor, M.B. Yaffe, and R.H. Medema. 2008. Polo-like kinase-1 is activated by aurora A to promote checkpoint recovery. *Nature*. 455:119-123.

Mahajan, K.N., S.A. Nick McElhinny, B.S. Mitchell, and D.A. Ramsden. 2002. Association of DNA polymerase mu (pol mu) with Ku and ligase IV: role for pol mu in end-joining double-strand break repair. *Mol Cell Biol*. 22:5194-5202.

Mahaney, B.L., K. Meek, and S.P. Lees-Miller. 2009. Repair of ionizing radiation-induced DNA double-strand breaks by non-homologous end-joining. *Biochem J*. 417:639-650.

Mailand, N., J. Falck, C. Lukas, R.G. Syljuasen, M. Welcker, J. Bartek, and J. Lukas. 2000. Rapid destruction of human Cdc25A in response to DNA damage. *Science*. 288:1425-1429.

Maimets, T., I. Neganova, L. Armstrong, and M. Lako. 2008. Activation of p53 by nutlin leads to rapid differentiation of human embryonic stem cells. *Oncogene*.

Mari, P.O., B.I. Florea, S.P. Persengiev, N.S. Verkaik, H.T. Bruggenwirth, M. Modesti, G. Giglia-Mari, K. Bezstarosti, J.A. Demmers, T.M. Luider, A.B. Houtsmuller, and D.C. van Gent. 2006. Dynamic assembly of end-joining complexes requires interaction between Ku70/80 and XRCC4. *Proc Natl Acad Sci U S A*. 103:18597-18602.

Martin, G.R. 1980. Teratocarcinomas and mammalian embryogenesis. *Science*. 209:768-776.

Martin, G.R. 1981. Isolation of a pluripotent cell line from early mouse embryos cultured in medium conditioned by teratocarcinoma stem cells. *Proc Natl Acad Sci U S A*. 78:7634-7638.

Matsuda, T., T. Nakamura, K. Nakao, T. Arai, M. Katsuki, T. Heike, and T. Yokota. 1999. STAT3 activation is sufficient to maintain an undifferentiated state of mouse embryonic stem cells. *Embo J*. 18:4261-4269.

Matsui, Y., K. Zsebo, and B.L. Hogan. 1992. Derivation of pluripotential embryonic stem cells from murine primordial germ cells in culture. *Cell*. 70:841-847.

Matsuoka, S., G. Rotman, A. Ogawa, Y. Shiloh, K. Tamai, and S.J. Elledge. 2000. Ataxia telangiectasia-mutated phosphorylates Chk2 in vivo and in vitro. *Proc Natl Acad Sci U S A*. 97:10389-10394.

Maynard, S., A.M. Swistikowa, J.W. Lee, Y. Liu, S.T. Liu, D.A.C. A, M. Rao, N. de Souza-Pinto, X. Zeng, and V.A. Bohr. 2008. Human Embryonic Stem Cells have Enhanced Repair of Multiple Forms of DNA Damage. *Stem Cells*.

Melchionna, R., X.B. Chen, A. Blasina, and C.H. McGowan. 2000. Threonine 68 is required for radiation-induced phosphorylation and activation of Cds1. *Nat Cell Biol*. 2:762-765.

Merkle, D., P. Douglas, G.B. Moorhead, Z. Leonenko, Y. Yu, D. Cramb, D.P. Bazett-Jones, and S.P. Lees-Miller. 2002. The DNA-dependent protein kinase interacts with DNA to form a protein-DNA complex that is disrupted by phosphorylation. *Biochemistry*. 41:12706-12714.

Meshorer, E., D. Yellajoshula, E. George, P.J. Scambler, D.T. Brown, and T. Misteli. 2006. Hyperdynamic plasticity of chromatin proteins in pluripotent embryonic stem cells. *Dev Cell*. 10:105-116.

Mikkelsen, T.S., J. Hanna, X. Zhang, M. Ku, M. Wernig, P. Schorderet, B.E. Bernstein, R. Jaenisch, E.S. Lander, and A. Meissner. 2008. Dissecting direct reprogramming through integrative genomic analysis. *Nature*. 454:49-55.

Mirzoeva, O.K., and J.H. Petrini. 2001. DNA damage-dependent nuclear dynamics of the Mre11 complex. *Mol Cell Biol*. 21:281-288.

Mitalipov, S., and D. Wolf. 2009. Totipotency, Pluripotency and Nuclear Reprogramming. *Adv Biochem Eng Biotechnol*.

Mitsui, K., Y. Tokuzawa, H. Itoh, K. Segawa, M. Murakami, K. Takahashi, M. Maruyama, M. Maeda, and S. Yamanaka. 2003. The homeoprotein Nanog is required for maintenance of pluripotency in mouse epiblast and ES cells. *Cell*. 113:631-642.

Momcilovic, O., S. Choi, S. Varum, C. Bakkenist, G. Schatten, and C. Navara. 2009. Ionizing radiation induces ataxia telangiectasia mutated-dependent checkpoint signaling and G(2) but not G(1) cell cycle arrest in pluripotent human embryonic stem cells. *Stem Cells*. 27:1822-1835.

Mummery, C.L., C.E. van den Brink, and S.W. de Laat. 1987. Commitment to differentiation induced by retinoic acid in P19 embryonal carcinoma cells is cell cycle dependent. *Dev Biol*. 121:10-19.

Nakagawa, M., M. Koyanagi, K. Tanabe, K. Takahashi, T. Ichisaka, T. Aoi, K. Okita, Y. Mochiduki, N. Takizawa, and S. Yamanaka. 2008. Generation of induced pluripotent stem cells without Myc from mouse and human fibroblasts. *Nat Biotechnol*. 26:101-106.

Nakajima, H., F. Toyoshima-Morimoto, E. Taniguchi, and E. Nishida. 2003. Identification of a consensus motif for Plk (Polo-like kinase) phosphorylation reveals Myt1 as a Plk1 substrate. *J Biol Chem*. 278:25277-25280.

Nassif, N., J. Penney, S. Pal, W.R. Engels, and G.B. Gloor. 1994. Efficient copying of nonhomologous sequences from ectopic sites via P-element-induced gap repair. *Mol Cell Biol*. 14:1613-1625.

Navara, C.S., C. Redinger, J. Mich-Basso, S. Oliver, A. Ben-Yehudah, C. Castro, and C. Simerly. 2007. Derivation and characterization of nonhuman primate embryonic stem cells. *Curr Protoc Stem Cell Biol*. Chapter 1:Unit 1A 1.

Neganova, I., X. Zhang, S. Atkinson, and M. Lako. 2009. Expression and functional analysis of G1 to S regulatory components reveals an important role for CDK2 in cell cycle regulation in human embryonic stem cells. *Oncogene*. 28:20-30.

Nichols, J., B. Zevnik, K. Anastassiadis, H. Niwa, D. Klewe-Nebenius, I. Chambers, H. Scholer, and A. Smith. 1998. Formation of pluripotent stem cells in the mammalian embryo depends on the POU transcription factor Oct4. *Cell*. 95:379-391.

Niida, H., and M. Nakanishi. 2006. DNA damage checkpoints in mammals. *Mutagenesis*. 21:3-9.

Niwa, H., J. Miyazaki, and A.G. Smith. 2000. Quantitative expression of Oct-3/4 defines differentiation, dedifferentiation or self-renewal of ES cells. *Nat Genet*. 24:372-376.

Niwa, H., Y. Toyooka, D. Shimosato, D. Strumpf, K. Takahashi, R. Yagi, and J. Rossant. 2005. Interaction between Oct3/4 and Cdx2 determines trophectoderm differentiation. *Cell*. 123:917-929.

Norbury, C.J., and I.D. Hickson. 2001. Cellular responses to DNA damage. *Annu Rev Pharmacol Toxicol*. 41:367-401.

Nussenzweig, A., K. Sokol, P. Burgman, L. Li, and G.C. Li. 1997. Hypersensitivity of Ku80-deficient cell lines and mice to DNA damage: the effects of ionizing radiation on growth, survival, and development. *Proc Natl Acad Sci U S A*. 94:13588-13593.

Nyberg, K.A., R.J. Michelson, C.W. Putnam, and T.A. Weinert. 2002. Toward maintaining the genome: DNA damage and replication checkpoints. *Annu Rev Genet*. 36:617-656.

Okamoto, K., H. Okazawa, A. Okuda, M. Sakai, M. Muramatsu, and H. Hamada. 1990. A novel octamer binding transcription factor is differentially expressed in mouse embryonic cells. *Cell*. 60:461-472.

Okita, K., T. Ichisaka, and S. Yamanaka. 2007. Generation of germline-competent induced pluripotent stem cells. *Nature*. 448:313-317.

Oricchio, E., C. Saladino, S. Iacovelli, S. Soddu, and E. Cundari. 2006. ATM is activated by default in mitosis, localizes at centrosomes and monitors mitotic spindle integrity. *Cell Cycle*. 5:88-92.

Palmieri, S.L., W. Peter, H. Hess, and H.R. Scholer. 1994. Oct-4 transcription factor is differentially expressed in the mouse embryo during establishment of the first two extraembryonic cell lineages involved in implantation. *Dev Biol*. 166:259-267.

Park, I.H., N. Arora, H. Huo, N. Maherali, T. Ahfeldt, A. Shimamura, M.W. Lensch, C. Cowan, K. Hochedlinger, and G.Q. Daley. 2008. Disease-specific induced pluripotent stem cells. *Cell*. 134:877-886.

Paull, T.T. 2005. Saving the ends for last: the role of pol mu in DNA end joining. *Mol Cell*. 19:294-296.

Paull, T.T., and M. Gellert. 1998. The 3' to 5' exonuclease activity of Mre 11 facilitates repair of DNA double-strand breaks. *Mol Cell*. 1:969-979.

Paull, T.T., and M. Gellert. 1999. Nbs1 potentiates ATP-driven DNA unwinding and endonuclease cleavage by the Mre11/Rad50 complex. *Genes Dev*. 13:1276-1288.

Peng, C.Y., P.R. Graves, R.S. Thoma, Z. Wu, A.S. Shaw, and H. Piwnica-Worms. 1997. Mitotic and G2 checkpoint control: regulation of 14-3-3 protein binding by phosphorylation of Cdc25C on serine-216. *Science*. 277:1501-1505.

Peter, M., E. Heitlinger, M. Haner, U. Aebi, and E.A. Nigg. 1991. Disassembly of in vitro formed lamin head-to-tail polymers by CDC2 kinase. *Embo J*. 10:1535-1544.

Pierce, A.J., P. Hu, M. Han, N. Ellis, and M. Jasin. 2001. Ku DNA end-binding protein modulates homologous repair of double-strand breaks in mammalian cells. *Genes Dev*. 15:3237-3242.

Qi, X., T.G. Li, J. Hao, J. Hu, J. Wang, H. Simmons, S. Miura, Y. Mishina, and G.Q. Zhao. 2004. BMP4 supports self-renewal of embryonic stem cells by inhibiting mitogen-activated protein kinase pathways. *Proc Natl Acad Sci U S A*. 101:6027-6032.

Qin, H., T. Yu, T. Qing, Y. Liu, Y. Zhao, J. Cai, J. Li, Z. Song, X. Qu, P. Zhou, J. Wu, M. Ding, and H. Deng. 2007. Regulation of apoptosis and differentiation by p53 in human embryonic stem cells. *J Biol Chem*. 282:5842-5852.

Rasband, W.S. 1997-2008. ImageJ

U. S. National Institutes of Health, Bethesda, Maryland, USA.

Resnick, J.L., L.S. Bixler, L. Cheng, and P.J. Donovan. 1992. Long-term proliferation of mouse primordial germ cells in culture. *Nature*. 359:550-551.

Rich, T., R.L. Allen, and A.H. Wyllie. 2000. Defying death after DNA damage. *Nature*. 407:777-783.

Rijkers, T., J. Van Den Ouweland, B. Morolli, A.G. Rolink, W.M. Baarends, P.P. Van Sloun, P.H. Lohman, and A. Pastink. 1998. Targeted inactivation of mouse RAD52 reduces homologous recombination but not resistance to ionizing radiation. *Mol Cell Biol*. 18:6423-6429.

Rodriguez, R.T., J.M. Velkey, C. Lutzko, R. Seerke, D.B. Kohn, K.S. O'Shea, and M.T. Firpo. 2007. Manipulation of OCT4 levels in human embryonic stem cells results in induction of differential cell types. *Exp Biol Med (Maywood)*. 232:1368-1380.

Rogakou, E.P., C. Boon, C. Redon, and W.M. Bonner. 1999. Megabase chromatin domains involved in DNA double-strand breaks in vivo. *J Cell Biol*. 146:905-916.

Rogakou, E.P., D.R. Pilch, A.H. Orr, V.S. Ivanova, and W.M. Bonner. 1998. DNA double-stranded breaks induce histone H2AX phosphorylation on serine 139. *J Biol Chem*. 273:5858-5868.

Roshak, A.K., E.A. Capper, C. Imburgia, J. Fornwald, G. Scott, and L.A. Marshall. 2000. The human polo-like kinase, PLK, regulates cdc2/cyclin B through phosphorylation and activation of the cdc25C phosphatase. *Cell Signal*. 12:405-411.

Rothkamm, K., I. Kruger, L.H. Thompson, and M. Lobrich. 2003. Pathways of DNA double-strand break repair during the mammalian cell cycle. *Mol Cell Biol*. 23:5706-5715.

Rudolph, N.S., and S.A. Latt. 1989. Flow cytometric analysis of X-ray sensitivity in ataxia telangiectasia. *Mutat Res*. 211:31-41.

San Filippo, J., P. Sung, and H. Klein. 2008. Mechanism of eukaryotic homologous recombination. *Annu Rev Biochem*. 77:229-257.

Saretzki, G., L. Armstrong, A. Leake, M. Lako, and T. von Zglinicki. 2004. Stress defense in murine embryonic stem cells is superior to that of various differentiated murine cells. *Stem Cells*. 22:962-971.

Saretzki, G., T. Walter, S. Atkinson, J.F. Passos, B. Bareth, W.N. Keith, R. Stewart, S. Hoare, M. Stojkovic, L. Armstrong, T. von Zglinicki, and M. Lako. 2008. Downregulation of multiple stress defense mechanisms during differentiation of human embryonic stem cells. *Stem Cells*. 26:455-464.

Sato, N., L. Meijer, L. Skaltsounis, P. Greengard, and A.H. Brivanlou. 2004. Maintenance of pluripotency in human and mouse embryonic stem cells through activation of Wnt signaling by a pharmacological GSK-3-specific inhibitor. *Nat Med*. 10:55-63.

Savatier, P., S. Huang, L. Szekely, K.G. Wiman, and J. Samarut. 1994. Contrasting patterns of retinoblastoma protein expression in mouse embryonic stem cells and embryonic fibroblasts. *Oncogene*. 9:809-818.

Savatier, P., H. Lapillonne, L.A. van Grunsven, B.B. Rudkin, and J. Samarut. 1996. Withdrawal of differentiation inhibitory activity/leukemia inhibitory factor up-regulates D-type cyclins and cyclin-dependent kinase inhibitors in mouse embryonic stem cells. *Oncogene*. 12:309-322.

Seki, A., J.A. Coppinger, C.Y. Jang, J.R. Yates, and G. Fang. 2008. Bora and the kinase Aurora a cooperatively activate the kinase Plk1 and control mitotic entry. *Science*. 320:1655-1658.

Serrano, L., L. Liang, Y. Chang, L. Deng, C. Maulion, S.C. Nguyen, and J.A. Tischfield. Homologous Recombination conserves DNA sequence integrity throughout the cell cycle in embryonic stem cells. *Stem Cells Dev*.

Sherr, C.J. 1994. G1 phase progression: cycling on cue. *Cell*. 79:551-555.

Shieh, S.Y., J. Ahn, K. Tamai, Y. Taya, and C. Prives. 2000. The human homologs of checkpoint kinases Chk1 and Cds1 (Chk2) phosphorylate p53 at multiple DNA damage-inducible sites. *Genes Dev*. 14:289-300.

Shiloh, Y. 2001. ATM and ATR: networking cellular responses to DNA damage. *Curr Opin Genet Dev*. 11:71-77.

Smith, A.G., J.K. Heath, D.D. Donaldson, G.G. Wong, J. Moreau, M. Stahl, and D. Rogers. 1988. Inhibition of pluripotential embryonic stem cell differentiation by purified polypeptides. *Nature*. 336:688-690.

Soldner, F., D. Hockemeyer, C. Beard, Q. Gao, G.W. Bell, E.G. Cook, G. Hargus, A. Blak, O. Cooper, M. Mitalipova, O. Isacson, and R. Jaenisch. 2009. Parkinson's disease patient-derived induced pluripotent stem cells free of viral reprogramming factors. *Cell*. 136:964-977.

Solter, D., N. Skreb, and I. Damjanov. 1970. Extrauterine growth of mouse egg-cylinders results in malignant teratoma. *Nature*. 227:503-504.

Stead, E., J. White, R. Faast, S. Conn, S. Goldstone, J. Rathjen, U. Dhingra, P. Rathjen, D. Walker, and S. Dalton. 2002. Pluripotent cell division cycles are driven by ectopic Cdk2, cyclin A/E and E2F activities. *Oncogene*. 21:8320-8333.

Stevens, L.C. 1970. The development of transplantable teratocarcinomas from intratesticular grafts of pre- and postimplantation mouse embryos. *Dev Biol*. 21:364-382.

Stewart, C.L., I. Gadi, and H. Bhatt. 1994. Stem cells from primordial germ cells can reenter the germ line. *Dev Biol*. 161:626-628.

Strathern, J.N., A.J. Klar, J.B. Hicks, J.A. Abraham, J.M. Ivy, K.A. Nasmyth, and C. McGill. 1982. Homothallic switching of yeast mating type cassettes is initiated by a double-stranded cut in the MAT locus. *Cell*. 31:183-192.

Sugawara, N., X. Wang, and J.E. Haber. 2003. In vivo roles of Rad52, Rad54, and Rad55 proteins in Rad51-mediated recombination. *Mol Cell*. 12:209-219.

Sumi, T., N. Tsuneyoshi, N. Nakatsuji, and H. Suemori. 2007. Apoptosis and differentiation of human embryonic stem cells induced by sustained activation of c-Myc. *Oncogene*. 26:5564-5576.

Sung, P. 1997. Function of yeast Rad52 protein as a mediator between replication protein A and the Rad51 recombinase. *J Biol Chem*. 272:28194-28197.

Sung, P., and D.L. Robberson. 1995. DNA strand exchange mediated by a RAD51-ssDNA nucleoprotein filament with polarity opposite to that of RecA. *Cell*. 82:453-461.

Suwa, A., M. Hirakata, Y. Takeda, S.A. Jesch, T. Mimori, and J.A. Hardin. 1994. DNA-dependent protein kinase (Ku protein-p350 complex) assembles on double-stranded DNA. *Proc Natl Acad Sci U S A*. 91:6904-6908.

Szostak, J.W., T.L. Orr-Weaver, R.J. Rothstein, and F.W. Stahl. 1983. The double-strand-break repair model for recombination. *Cell*. 33:25-35.

Tada, M., T. Tada, L. Lefebvre, S.C. Barton, and M.A. Surani. 1997. Embryonic germ cells induce epigenetic reprogramming of somatic nucleus in hybrid cells. *Embo J*. 16:6510-6520.

Takahashi-Tezuka, M., Y. Yoshida, T. Fukada, T. Ohtani, Y. Yamanaka, K. Nishida, K. Nakajima, M. Hibi, and T. Hirano. 1998. Gab1 acts as an adapter molecule linking the cytokine receptor gp130 to ERK mitogen-activated protein kinase. *Mol Cell Biol*. 18:4109-4117.

Takahashi, K., K. Tanabe, M. Ohnuki, M. Narita, T. Ichisaka, K. Tomoda, and S. Yamanaka. 2007. Induction of pluripotent stem cells from adult human fibroblasts by defined factors. *Cell*. 131:861-872.

Takahashi, K., and S. Yamanaka. 2006. Induction of pluripotent stem cells from mouse embryonic and adult fibroblast cultures by defined factors. *Cell*. 126:663-676.

Takata, M., M.S. Sasaki, E. Sonoda, C. Morrison, M. Hashimoto, H. Utsumi, Y. Yamaguchi-Iwai, A. Shinohara, and S. Takeda. 1998. Homologous recombination and non-homologous end-joining pathways of DNA double-strand break repair have overlapping roles in the maintenance of chromosomal integrity in vertebrate cells. *Embo J*. 17:5497-5508.

Tassan, J.P., S.J. Schultz, J. Bartek, and E.A. Nigg. 1994. Cell cycle analysis of the activity, subcellular localization, and subunit composition of human CAK (CDK-activating kinase). *J Cell Biol*. 127:467-478.

Taylor, A.M., C.M. Rosney, and J.B. Campbell. 1979. Unusual sensitivity of ataxia telangiectasia cells to bleomycin. *Cancer Res*. 39:1046-1050.

Tesar, P.J., J.G. Chenoweth, F.A. Brook, T.J. Davies, E.P. Evans, D.L. Mack, R.L. Gardner, and R.D. McKay. 2007. New cell lines from mouse epiblast share defining features with human embryonic stem cells. *Nature*. 448:196-199.

Thomson, J.A., J. Itskovitz-Eldor, S.S. Shapiro, M.A. Waknitz, J.J. Swiergiel, V.S. Marshall, and J.M. Jones. 1998. Embryonic stem cell lines derived from human blastocysts. *Science*. 282:1145-1147.

Thomson, J.A., J. Kalishman, T.G. Golos, M. Durning, C.P. Harris, R.A. Becker, and J.P. Hearn. 1995. Isolation of a primate embryonic stem cell line. *Proc Natl Acad Sci U S A*. 92:7844-7848.

Thomson, J.A., J. Kalishman, T.G. Golos, M. Durning, C.P. Harris, and J.P. Hearn. 1996. Pluripotent cell lines derived from common marmoset (Callithrix jacchus) blastocysts. *Biol Reprod*. 55:254-259.

Tibbetts, R.S., K.M. Brumbaugh, J.M. Williams, J.N. Sarkaria, W.A. Cliby, S.Y. Shieh, Y. Taya, C. Prives, and R.T. Abraham. 1999. A role for ATR in the DNA damage-induced phosphorylation of p53. *Genes Dev*. 13:152-157.

Tichy, E.D., R. Pillai, L. Deng, L. Liang, J.A. Tischfield, S. Schwemberger, G.F. Babcock, and P.J. Stambrook. Mouse embryonic stem cells but not somatic cells predominantly use homologous recombination to repair double strand DNA breaks. *Stem Cells Dev*.

Tichy, E.D., and P.J. Stambrook. 2008. DNA repair in murine embryonic stem cells and differentiated cells. *Exp Cell Res*. 314:1929-1936.

Toyoshima-Morimoto, F., E. Taniguchi, and E. Nishida. 2002. Plk1 promotes nuclear translocation of human Cdc25C during prophase. *EMBO Rep*. 3:341-348.

Toyoshima-Morimoto, F., E. Taniguchi, N. Shinya, A. Iwamatsu, and E. Nishida. 2001. Polo-like kinase 1 phosphorylates cyclin B1 and targets it to the nucleus during prophase. *Nature*. 410:215-220.

Tsuzuki, T., Y. Fujii, K. Sakumi, Y. Tominaga, K. Nakao, M. Sekiguchi, A. Matsushiro, Y. Yoshimura, and MoritaT. 1996. Targeted disruption of the Rad51 gene leads to lethality in embryonic mice. *Proc Natl Acad Sci U S A*. 93:6236-6240.

Uematsu, N., E. Weterings, K. Yano, K. Morotomi-Yano, B. Jakob, G. Taucher-Scholz, P.O. Mari, D.C. van Gent, B.P. Chen, and D.J. Chen. 2007. Autophosphorylation of DNA-PKCS regulates its dynamics at DNA double-strand breaks. *J Cell Biol*. 177:219-229.

Utikal, J., J.M. Polo, M. Stadtfeld, N. Maherali, W. Kulalert, R.M. Walsh, A. Khalil, J.G. Rheinwald, and K. Hochedlinger. 2009. Immortalization eliminates a roadblock during cellular reprogramming into iPS cells. *Nature*. 460:1145-1148.

Vallier, L., M. Alexander, and R.A. Pedersen. 2005. Activin/Nodal and FGF pathways cooperate to maintain pluripotency of human embryonic stem cells. *J Cell Sci*. 118:4495-4509.

Van Dyck, E., N.M. Hajibagheri, A. Stasiak, and S.C. West. 1998. Visualisation of human rad52 protein and its complexes with hRad51 and DNA. *J Mol Biol*. 284:1027-1038.

Viswanathan, S.R., G.Q. Daley, and R.I. Gregory. 2008. Selective blockade of microRNA processing by Lin28. *Science*. 320:97-100.

Wang, G., H. Zhang, Y. Zhao, J. Li, J. Cai, P. Wang, S. Meng, J. Feng, C. Miao, M. Ding, D. Li, and H. Deng. 2005. Noggin and bFGF cooperate to maintain the pluripotency of human embryonic stem cells in the absence of feeder layers. *Biochem Biophys Res Commun*. 330:934-942.

Wang, X., V.C. Lui, R.T. Poon, P. Lu, and R.Y. Poon. 2009. DNA Damage Mediated S and G(2) Checkpoints in Human Embryonal Carcinoma Cells. *Stem Cells*. 27:568-576.

Wang, Y.G., C. Nnakwe, W.S. Lane, M. Modesti, and K.M. Frank. 2004. Phosphorylation and regulation of DNA ligase IV stability by DNA-dependent protein kinase. *J Biol Chem*. 279:37282-37290.

Ward, J.F. 1988. DNA damage produced by ionizing radiation in mammalian cells: identities, mechanisms of formation, and reparability. *Prog Nucleic Acid Res Mol Biol*. 35:95-125.

Watanabe, N., H. Arai, J. Iwasaki, M. Shiina, K. Ogata, T. Hunter, and H. Osada. 2005. Cyclin-dependent kinase (CDK) phosphorylation destabilizes somatic Wee1 via multiple pathways. *Proc Natl Acad Sci U S A*. 102:11663-11668.

Watanabe, N., H. Arai, Y. Nishihara, M. Taniguchi, N. Watanabe, T. Hunter, and H. Osada. 2004. M-phase kinases induce phospho-dependent ubiquitination of somatic Wee1 by SCFbeta-TrCP. *Proc Natl Acad Sci U S A*. 101:4419-4424.

Watanabe, S., H. Umehara, K. Murayama, M. Okabe, T. Kimura, and T. Nakano. 2006. Activation of Akt signaling is sufficient to maintain pluripotency in mouse and primate embryonic stem cells. *Oncogene*. 25:2697-2707.

Welham, M.J., M.P. Storm, E. Kingham, and H.K. Bone. 2007. Phosphoinositide 3-kinases and regulation of embryonic stem cell fate. *Biochem Soc Trans*. 35:225-228.

Wernig, M., A. Meissner, J.P. Cassady, and R. Jaenisch. 2008. c-Myc is dispensable for direct reprogramming of mouse fibroblasts. *Cell Stem Cell*. 2:10-12.

White, J., E. Stead, R. Faast, S. Conn, P. Cartwright, and S. Dalton. 2005. Developmental activation of the Rb-E2F pathway and establishment of cell cycle-regulated cyclin-dependent kinase activity during embryonic stem cell differentiation. *Mol Biol Cell*. 16:2018-2027.

White, J.S., S. Choi, and C.J. Bakkenist. 2008. Irreversible chromosome damage accumulates rapidly in the absence of ATM kinase activity. *Cell Cycle*. 7:1277-1284.

Williams, R.L., D.J. Hilton, S. Pease, T.A. Willson, C.L. Stewart, D.P. Gearing, E.F. Wagner, D. Metcalf, N.A. Nicola, and N.M. Gough. 1988. Myeloid leukaemia inhibitory factor maintains the developmental potential of embryonic stem cells. *Nature*. 336:684-687.

Wolner, B., S. van Komen, P. Sung, and C.L. Peterson. 2003. Recruitment of the recombinational repair machinery to a DNA double-strand break in yeast. *Mol Cell*. 12:221-232.

Wu, X., V. Ranganathan, D.S. Weisman, W.F. Heine, D.N. Ciccone, T.B. O'Neill, K.E. Crick, K.A. Pierce, W.S. Lane, G. Rathbun, D.M. Livingston, and D.T. Weaver. 2000. ATM phosphorylation of Nijmegen breakage syndrome protein is required in a DNA damage response. *Nature*. 405:477-482.

Xiao, L., X. Yuan, and S.J. Sharkis. 2006. Activin A maintains self-renewal and regulates fibroblast growth factor, Wnt, and bone morphogenic protein pathways in human embryonic stem cells. *Stem Cells*. 24:1476-1486.

Xiao, Y., and D.T. Weaver. 1997. Conditional gene targeted deletion by Cre recombinase demonstrates the requirement for the double-strand break repair Mre11 protein in murine embryonic stem cells. *Nucleic Acids Res*. 25:2985-2991.

Xie, H., M. Ye, R. Feng, and T. Graf. 2004. Stepwise reprogramming of B cells into macrophages. *Cell*. 117:663-676.

Xu, C., M.S. Inokuma, J. Denham, K. Golds, P. Kundu, J.D. Gold, and M.K. Carpenter. 2001. Feeder-free growth of undifferentiated human embryonic stem cells. *Nat Biotechnol*. 19:971-974.

Xu, C., E. Rosler, J. Jiang, J.S. Lebkowski, J.D. Gold, C. O'Sullivan, K. Delavan-Boorsma, M. Mok, A. Bronstein, and M.K. Carpenter. 2005a. Basic fibroblast growth factor supports undifferentiated human embryonic stem cell growth without conditioned medium. *Stem Cells*. 23:315-323.

Xu, R.H., X. Chen, D.S. Li, R. Li, G.C. Addicks, C. Glennon, T.P. Zwaka, and J.A. Thomson. 2002. BMP4 initiates human embryonic stem cell differentiation to trophoblast. *Nat Biotechnol*. 20:1261-1264.

Xu, R.H., R.M. Peck, D.S. Li, X. Feng, T. Ludwig, and J.A. Thomson. 2005b. Basic FGF and suppression of BMP signaling sustain undifferentiated proliferation of human ES cells. *Nat Methods*. 2:185-190.

Xu, Y., T. Ashley, E.E. Brainerd, R.T. Bronson, M.S. Meyn, and D. Baltimore. 1996. Targeted disruption of ATM leads to growth retardation, chromosomal fragmentation during meiosis, immune defects, and thymic lymphoma. *Genes Dev*. 10:2411-2422.

Xu, Y., and D. Baltimore. 1996. Dual roles of ATM in the cellular response to radiation and in cell growth control. *Genes Dev*. 10:2401-2410.

Yamashita, M., S. Fukada, M. Yoshikuni, P. Bulet, T. Hirai, A. Yamaguchi, Y.H. Lou, Z. Zhao, and Y. Nagahama. 1992. Purification and characterization of maturation-promoting factor in fish. *Dev Biol*. 149:8-15.

Yang, D., Z.J. Zhang, M. Oldenburg, M. Ayala, and S.C. Zhang. 2008. Human embryonic stem cell-derived dopaminergic neurons reverse functional deficit in parkinsonian rats. *Stem Cells*. 26:55-63.

Yano, K., K. Morotomi-Yano, S.Y. Wang, N. Uematsu, K.J. Lee, A. Asaithamby, E. Weterings, and D.J. Chen. 2008. Ku recruits XLF to DNA double-strand breaks. *EMBO Rep*. 9:91-96.

Yarm, F.R. 2002. Plk phosphorylation regulates the microtubule-stabilizing protein TCTP. *Mol Cell Biol*. 22:6209-6221.

Ying, Q.L., J. Nichols, I. Chambers, and A. Smith. 2003. BMP induction of Id proteins suppresses differentiation and sustains embryonic stem cell self-renewal in collaboration with STAT3. *Cell*. 115:281-292.

Young, B.R., and R.B. Painter. 1989. Radioresistant DNA synthesis and human genetic diseases. *Hum Genet*. 82:113-117.

Yu, J., K. Hu, K. Smuga-Otto, S. Tian, R. Stewart, Slukvin, II, and J.A. Thomson. 2009. Human induced pluripotent stem cells free of vector and transgene sequences. *Science*. 324:797-801.

Yu, J., M.A. Vodyanik, K. Smuga-Otto, J. Antosiewicz-Bourget, J.L. Frane, S. Tian, J. Nie, G.A. Jonsdottir, V. Ruotti, R. Stewart, Slukvin, II, and J.A. Thomson. 2007. Induced pluripotent stem cell lines derived from human somatic cells. *Science*. 318:1917-1920.

Yu, Y., W. Wang, Q. Ding, R. Ye, D. Chen, D. Merkle, D. Schriemer, K. Meek, and S.P. Lees-Miller. 2003. DNA-PK phosphorylation sites in XRCC4 are not required for survival after radiation or for V(D)J recombination. *DNA Repair (Amst)*. 2:1239-1252.

Yuan, H., N. Corbi, C. Basilico, and L. Dailey. 1995. Developmental-specific activity of the FGF-4 enhancer requires the synergistic action of Sox2 and Oct-3. *Genes Dev*. 9:2635-2645.

Zhan, Q., M.J. Antinore, X.W. Wang, F. Carrier, M.L. Smith, C.C. Harris, and A.J. Fornace, Jr. 1999. Association with Cdc2 and inhibition of Cdc2/Cyclin B1 kinase activity by the p53-regulated protein Gadd45. *Oncogene*. 18:2892-2900.

Zhang, S., P. Hemmerich, and F. Grosse. 2007. Centrosomal localization of DNA damage checkpoint proteins. *J Cell Biochem*. 101:451-465.

Zhang, X., I. Neganova, S. Przyborski, C. Yang, M. Cooke, S.P. Atkinson, G. Anyfantis, S. Fenyk, W.N. Keith, S.F. Hoare, O. Hughes, T. Strachan, M. Stojkovic, P.W. Hinds, L. Armstrong, and M. Lako. 2009. A role for NANOG in G1 to S transition in human embryonic stem cells through direct binding of CDK6 and CDC25A. *J Cell Biol*. 184:67-82.

Zhao, S., Y.C. Weng, S.S. Yuan, Y.T. Lin, H.C. Hsu, S.C. Lin, E. Gerbino, M.H. Song, M.Z. Zdzienicka, R.A. Gatti, J.W. Shay, Y. Ziv, Y. Shiloh, and E.Y. Lee. 2000. Functional link between ataxia-telangiectasia and Nijmegen breakage syndrome gene products. *Nature*. 405:473-477.

Zhou, B.B., and S.J. Elledge. 2000. The DNA damage response: putting checkpoints in perspective. *Nature*. 408:433-439.

Zhu, J., S. Petersen, L. Tessarollo, and A. Nussenzweig. 2001. Targeted disruption of the Nijmegen breakage syndrome gene NBS1 leads to early embryonic lethality in mice. *Curr Biol*. 11:105-109.

Ziebold, U., O. Bartsch, R. Marais, S. Ferrari, and K.H. Klempnauer. 1997. Phosphorylation and activation of B-Myb by cyclin A-Cdk2. *Curr Biol*. 7:253-260.